www.reanimatology.com
ISSN 2411-7110 (online)

GENERAL REANIMATOLOGY

SCIENTIFIC-AND-PRACTICAL JOURNAL

ОБЩАЯ РЕАНИМАТОЛОГИЯ

научно-практический журнал

Volume 20 Том 20

№ 1

Moscow
Москва
2024

Поздравление от имени Федерального научно-клинического центра реаниматологии и реабилитологии (ФНКЦ РР) и редакции журнала «Общая реаниматология»

Поздравляем с 40-летием Артема Николаевича Кузовлева, доктора медицинских наук, заместителя директора — руководителя НИИ общей реаниматологии им. В. А. Неговского ФНКЦ РР.

Артем Николаевич окончил в 2007 г. Московскую медицинскую академию им. И. М. Сеченова (в наст. вр. Первый Московский государственный медицинский университет им. И. М. Сеченова).

В 2010 г. связи с защитой диссертации на соискание ученой степени кандидата медицинских наук досрочно закончил аспирантуру по специальности «Анестезиология и реаниматология». В 2015 г. защитил диссертацию на соискание ученой степени доктора медицинских наук по теме «Молекулярные и генетические аспекты диагностики и лечения нозокомиальной пневмонии».

Артем Николаевич является автором 7 монографий, 25 методических рекомендаций и более 460 научных статей, включенных в отечественные и международные наукометрические базы данных, в том числе в WoS и Scopus. По данным Scopus свыше 20% статей опубликовано в журналах первого квартиля; публикации с международным авторским коллективом составляют 21%.

Артем Николаевич подготовил кандидата медицинских наук по специальности «Анестезиология и реаниматология» (3.1.12.), а также доктора медицинских наук по специальности «Патологическая физиология» (3.3.3.)

В качестве заместителя главного редактора научно-практического рецензируемого журнала «Общая реаниматология» Артем Николаевич принимает непосредственное участие в формировании профильного издания, соответствующего международным стандартам. Редакторскую деятельность он совмещает с деятельностью рецензента, как член редколлегий журналов «Вестник интенсивной терапии им. А. И. Салтанова» и «Физическая и реабилитационная медицина, медицинская реабилитация».

За время учебы и работы был неоднократно отмечен государственными поощрениями и наградами:

2006 г. — Стипендия Президента РФ на стажировку за рубежом.

2012, 2014 гг. — Стипендия Президента РФ молодым ученым и аспирантам, осуществляющим перспективные научные исследования и разработки по приоритетным направлениям модернизации российской экономики.

2017 г. — Премия Правительства Москвы молодым ученым за 2016 г. (научный проект «Повышение эффективности диагностики и лечения инфекционных осложнений критических состояний с использованием современных технологий»).

2021 г. — Указом Президента РФ награждение медалью «Луки Крымского».

2023 г. — Премия Правительства Российской Федерации в области науки и техники 2023 г. — «Разработка и внедрение инновационной национальной системы этапной нейрореабилитации реанимационных пациентов с тяжелым повреждением головного мозга на основе индивидуальной маршрутизации».

Желаем здоровья,
продолжения плодотворной работы

ISSN 1813-9779 (print) ISSN 2411-7110 (online)

GENERAL REANIMATOLOGY

OBSHCHAYA REANIMATOLOGIYA

Scientific-and-Practical Peer-Reviewed Journal
Since 2005

• Covers issues of critical care medicine
• Manuscripts in Russian and English are published free-of-charge
• Included in SCOPUS (since 2015), RINTs, RSCI, DOAJ, and other databases, as well as in the Official list of editions recommended for publication of dissertations (PhD, DSci) by the Russian Higher Attestation Commission

Registration certificate of the Journal «Obshchaya reanimatologiya» (General Reanimatology): ПИ № ФС77-18690, November 2, 2004, Federal Service for Supervision of Compliance with Legislation in the Sphere of Mass Communications and Protection of Cultural Heritage
Publication Frequency: 6 numbers per year.
Founder:

ОБЩАЯ РЕАНИМАТОЛОГИЯ

OBŜAÂ REANIMATOLOGIÂ

научно-практический рецензируемый журнал
Выходит с 2005 г.

• охватывает вопросы медицины критических состояний
• публикует рукописи на русском и английском языках бесплатно
• включен в базы данных SCOPUS (с 2015 г.), РИНЦ, RSCI, DOAJ и др. базы данных; Перечень изданий, рекомендованных ВАК для публикации результатов диссертационных работ

Свидетельство о регистрации: ПИ № ФС77-18690 от 02 ноября 2004 г. Печатное издание журнал «Общая реаниматология» зарегистрирован Федеральной службой по надзору за соблюдением законодательства в сфере массовых коммуникаций и охране культурного наследия.
Периодичность: 6 раз в год
Учредитель:

Publisher:
Federal Research and Clinical Center of Intensive Care Medicine and Rehabilitology, Moscow, Russia
Издатель:
Федеральный научно-клинический центр реаниматологии и реабилитологии (ФНКЦ РР), Москва, Россия

Supported by Russian Federation of Anesthesiologists and Reanimatologists
При поддержке Общероссийской общественной организации «Федерация анестезиологов и реаниматологов»

Artwork: Natalia V. Golubeva
Page-proof: Sergey V. Shishkov
Printing House:
Printed at LLC «Advanced Solutions». 19, Leninsky prospekt, build. 1, Moscow, 119071. www.aov.ru
Contacts:
25 Petrovka Str., Bldg. 2, 107031 Moscow, Russia.
Tel. +7-495-694-17-73.
E-mail: **journal_or@mail.ru;**
Web: **www.reanimatology.com**

Subscription:
Index 46338, refer to catalog of «Книга-Сервис»
Signed for printing: 03.03.2024

Оригинал-макет: Н. В. Голубева
Верстка: С. В. Шишков
Типография: отпечатано в ООО «Адвансед солюшнз». 119071, г. Москва, Ленинский пр-т, д. 19, стр. 1. www.aov.ru
Контакты с редакцией:
Россия, 107031, г. Москва, ул. Петровка, д. 25, стр. 2.
Тел.: +7-495-694-17-73.
E-mail: **journal_or@mail.ru;**
сайт: **www.reanimatology.com**

Подписка и распространение: индекс издания по каталогу «Книга-Сервис» — 46338.
Цена свободная
Подписано в печать: 03.03.2024

CONTENTS

CLINICAL STUDIES

FOR PRACTITIONER

EXPERIMENTAL STUDIES

META-ANALYSIS

СОДЕРЖАНИЕ

КЛИНИЧЕСКИЕ ИССЛЕДОВАНИЯ

В ПОМОЩЬ ПРАКТИЧЕСКОМУ ВРАЧУ

ЭКСПЕРИМЕНТАЛЬНЫЕ ИССЛЕДОВАНИЯ

МЕТА-АНАЛИЗ

https://doi.org/10.15360/1813-9779-2024-1-4-14

Linking Immunological Parameters and Recovery of Patient's Motor and Cognitive Functions In The Acute Period of Ischemic Stroke

Anastasia M. Tynterova[1], Natalia N. Shusharina[1], Arkady M. Golubev[2], Ekaterina M. Moiseeva[1], Larisa S. Litvinova[1]

[1] Immanuel Kant Baltic Federal University
14 Alexander Nevsky Str., 236041 Kaliningrad, Russia
[2] V. A. Negovsky Research Institute of General Reanimatology,
Federal Research and Clinical Center of Intensive Care Medicine and Rehabilitology
25 bldg 2 Petrovka Str., 107031 Moscow, Russia

For citation: *Anastasia M. Tynterova, Natalia N. Shusharina, Arkady M. Golubev, Ekaterina M. Moiseeva, Larisa S. Litvinova.* Linking Immunological Parameters and Recovery of Patient's Motor and Cognitive Functions In The Acute Period of Ischemic Stroke. *Obshchaya Reanimatologiya = General Reanimatology.* 2024; 20 (1): 4–14. https://doi.org/10.15360/1813-9779-2024-1-4-14 [In Russ. and Engl.]

*__Correspondence to:__ Anastasia M. Tynterova, antynterova@mail.ru

Summary

Objective. To evaluate the relationship between immunological parameters and functional outcome in patients with varying severity of ischemic stroke based on statistical methodology.

Materials and methods. The prospective study included 78 patients diagnosed with ischemic stroke, who were distributed into two groups: group 1 — 38 mild stroke patients, NIHSS score < 5, group 2 – 40 moderate stroke patients, NIHSS score 5–15. Signs of stroke severity, degree of disability, cognitive decline, and activities of daily living were chosen as criteria to estimate the functional outcome by calculating the difference between the NIHSS, mRS, MoCA, and BI scales at the time of admission and on Day 12 of hospital stay. Lab tests included assessment of plasma concentrations of CXC and CC subfamilies of cytokines, interleukins and TNF-a on Day 2 of hospital stay. Machine learning algorithms, the Python programming language, the Pandas and SciPy libraries, and discriminant analysis were used for statistical processing.

Results. The following parameters were found significant: concentrations of IL-1b and MPIF-1/CCL23 for group 1, and concentrations of IL-16, MPIF-1/CCL23, Eotaxin-2/CCL24, Gro-a/CXCL1 and IL-8/CXCL8 for group 2 patients. Positive correlation was established between NIHSS dynamics and concentrations of TNF-α (R=0.227, P=0.001), MPIF-1/CCL23 (R=0.380, P=0.00061) and Gro-a/CXCL1 (R=0.211, P=0.00001), and between changes in mRS and concentrations of MPIF-1/CCL23 (R=0.277, P=0.00006), Gro-a/CXCL1 (R=0.211, P=0.0075) and IL-16 (R=0, 211, P=0.00001). There was a significant negative correlation between cognitive dysfunction and concentrations of Eotaxin-2/CCL24 (R=–0.378, P=0.00075), Gro-a/CXCL1 (R=–0.313, P=0.0035), and IP-10/CXCL1 (R=–0.214, P=0.00023), and between limited activities of daily living (BI) and concentrations of MPIF-1/CCL23 (R=–0.345, P=0.0024) and Gro-a/CXCL1 (R=–0.210, P=0.00001).

Conclusion. Chemokines form the CC family — MPIF-1/CCL23 and Eotaxin-2/CCL24, and the CXC-Gro-a/CXCL1 and IL-16 clusters are the principal cytokines associated with the dynamics of patient's motor and cognitive functions recovery in the acute period of ischemic stroke. Although obtained results demonstrate negative effect of increased MPIF-1/CCL23, Gro-a/CXCL1, IL-16 and Eotaxin-2/CCL24 concentrations on the improvement of motor and cognitive impairments, further studies are needed to verify the CXC and CC subfamilies chemokines as prognostic markers of patient's functional outcome in the acute period of ischemic stroke.

Keywords: ischemic stroke; functional outcome; severity of stroke; cytokine; biomarker

Conflict of interest. The authors declare no conflict of interest.

Financing. The study was conducted within the framework of the «Priority 2030» project of the I. Kant Baltic Federal University.

Introduction

Ischemic stroke (IS) dominates the structure of cerebrovascular disease, causing disability and death worldwide [1]. In addition to abnormal blood flow and coagulation, inflammatory and neuroimmune processes mediated and regulated by proinflammatory cytokines play important roles in the pathogenesis of ischemic circulatory disorders [2].

Increased levels of cytokines, including chemokines and cell adhesion molecules, which are directly related to the severity and extent of cerebral infarction, exacerbate ischemic brain damage and have an impact on the functional outcome of stroke [3–5]. Currently, there is a large body of evidence describing the role of interleukins in the development of cerebral ischemia [6, 7].

Another promising direction is to investigate the relationship between stroke severity and chemokine production, which influences immune cell activation, differentiation, and migration [8–10]. More than 60 chemokines with different structures and biological properties have been identified in

humans. According to the current classification, they have four subfamilies, two of which are CXC and CC [11].

Results of immunologic studies in patients with IS show a direct correlation between the expression of CC subfamily chemokines, CCL3 (MIP-1α), CCL5 (RANTES), CCL7 (MCP-3), such as CCL13 (MCP-4), CCL14 (HCC-1), CCL15 (LKN-1) and CCL23 (MPIF-1), and stroke severity [12–14]. The CXC subfamily chemokines most associated with ischemic mechanisms are CXCL1 (Gro-a), CXCL-2 (Gro-b), CXCL9 (MIG), CXCL10 (IP-10), CXCL11 (I-TAC), CXCL12 (SDF-1a+b), CXCL16 (SCYB16), and CXCL8 (IL-8) [15]. Understanding the processes of differential expression of cytokines of different subfamilies in patients with acute stroke will help to expand the understanding of the role of the immune response in the pathogenesis of IS, as well as to identify individual cytokines or their combinations as potential biomarkers for assessing the severity of ischemia and risk stratification of adverse outcomes after stroke.

The use of multivariate discriminant analysis based on machine learning (ML) techniques is currently a promising area in basic medicine [16]. Machine learning has been used primarily in clinical settings for diagnosis and prognosis, greatly improving the ability to predict the risk of developing various diseases, their progression, and functional outcome [17].

The aim of the study was to evaluate the influence of immunological parameters on the functional outcome of patients with different severity of ischemic stroke using statistical methods.

Materials and Methods

The prospective cohort study was approved by the Independent Ethical Committee of the Clinical Research Center of the Immanuel Kant Baltic Federal University (Protocol No. 34, dated September 29, 2022) and conducted from October 2022 to February 2023.

The study included 78 primary vascular center patients diagnosed with ischemic stroke. The study sample size was not pre-specified.

To verify the subtype of MI according to TOAST (Trial of Org 10172 in Acute Stroke Treatment) criteria [18], routine clinical and diagnostic examinations were performed.

On admission, patients underwent neurological examination and routine diagnostic tests, including brain CT/MRI, transcranial Doppler study of extra- and intracranial vessels, 12-lead ECG, complete blood count and biochemistry, and pulse oximetry.

Additional tests included MR/CT angiography, echocardiography, ECG Holter monitoring, detailed coagulation studies, evaluation for systemic diseases, blood homocysteine measurement, and lumbar puncture, if indicated. Thrombolytic therapy was not administered due to contraindications or hospitalization beyond the therapeutic window.

Neuroimaging parameters were obtained by computed tomography (CT) and magnetic resonance imaging (MRI). Initial ischemic changes in the middle cerebral artery were assessed using the ASPECTS (Alberta stroke program early CT score) scale.

Functional status of all patients was assessed on admission and at discharge using standard scales [19]. Stroke severity was assessed by the National Institutes of Health Stroke Scale (NIHSS), disability severity by the modified Rankin Scale (mRS), cognitive decline by the Montreal Cognitive Assessment (MoCA) scale, and activities of daily living by the Barthel Index (BI).

Patients were divided into two groups based on the NIHSS score. Group 1 included 38 patients with mild neurological deficit (NIHSS <5 points), while group 2 included 40 patients with moderate neurological impairment (NIHSS 5–15 points). The baseline NIHSS score was 4 [3; 4] points in group 1 and 10 [7; 13] points in group 2. Patients in groups 1 and 2 were comparable in terms of demographic and clinical characteristics (Table 1).

Inclusion criteria were clinical signs and symptoms consistent with a diagnosis of ischemic stroke; age 60 to 80 years; NIHSS score $\leqslant 15$; full consciousness at the time of the study.

Exclusion criteria were pre-existing neurological and psychiatric conditions, hemorrhagic stroke and transient ischemic attack, vertebrobasilar IS, gross motor and/or sensory aphasia.

The criteria for the functional outcome of acute ischemic stroke were the change in the patient's condition, expressed in absolute values by calculating the difference between the NIHSS, mRS, BI, and MoCA parameters at the time of admission and at day 12 of hospitalization (gain/decrease index, delta, $\triangle$) ($\triangle$MoCA, $\triangle$NIHSS, $\triangle$BI, $\triangle$mRS).

The laboratory study included measurement of levels of biologically active molecules (cytokines) in blood plasma. Blood samples were taken on the 2nd day of hospitalization. Interleukins (IL-1b, IL-2, IL-4, IL-6, IL-16), chemokines of CC subfamily (MCP-1/CCL2, MIP-1a/CCL3, MCP-3/CCL7, MCP-4/CCL13, MIP-1d/CCL15, MPIF-1/CCL23, Eotaxin-2/CCL24, Eotaxin/CCL11) and CXC subfamily (Gro-a/CXCL1, Gro-b/CXCL-2, IP-10/CXCL10, SCYB16/CXCL16, IL-8/CXCL8), and TNF-α were measured.

The analysis was performed by flow fluorimetry on an automated dual-beam laser analyzer (Bio-Plex® 200 Systems, Bio-Rad, USA) using a commercial test system (Bio-Plex Human Panel, 40-Plex Assay, Bio-Rad, USA). Results are expressed in pg/mL.

Statistical analysis was performed using the standard SPSS Statistics V23.0 for Windows package, the Python programming language, the Pandas and SciPy libraries, and methods of multivariate analysis using machine learning (ML) algorithms.

The distribution of quantitative variables was assessed using the Shapiro–Wilk test. Variables with normal

distribution were reported as arithmetic mean *(M)* and standard deviation *(SD)*. Data with normal distribution were compared using ANOVA variance test for dependent and independent samples.

For non-normal distribution, quantitative variables were reported as median *(Me)* and lower and upper quartiles *[Q1–Q3]*. For non-normal distribution, the non-parametric Wilcoxon test was used. The Mann–Whitney *U*-criterion was used to compare two groups for a non-normal variable. Differences in frequencies between two independent groups were analyzed using the two-tailed Fisher's exact test, χ^2 test with Yates' correction. The level of statistical significance was set at $P<0.05$. Bonferroni correction ($P<0.0125$) was used for multiple comparisons of variables to eliminate false positives.

The Z-score was not used to calculate the MoCA test and to prevent the occurrence of type II error (false-negative conclusion) due to the lack of control group reference values.

The correlation coefficient *(r)* was calculated to assess the association of functional outcome parameters on the NIHSS, mRS, BI, and MoCA scales with serum cytokine levels on day 2 of hospitalization.

The *r*-value was between –1 and 1, where 1 is a complete inverse correlation, 0 is no correlation, and 1 is a complete direct correlation. The Fechner method was chosen to evaluate the correlation of continuous variables, including those measured in points. The standard *P* value of 0.05 was chosen as the significance level. Correlation coefficients with a *P* value greater than 0.05 were discarded.

Correlation analysis was performed separately for each group, considering four groups of predictors. Grouping according to functional outcome parameters was not performed because the statistical results did not significantly affect the general pattern of correlations.

Discriminant analysis using ML algorithms was performed in two steps. First, the gradient boosting method [20] with interpretable results was used to process continuous variables of serum cytokine levels. Second, the Boruta thresholding and significance identification method [21] was used to determine the significance of a parameter and eliminate spurious correlations.

The significance of a parameter was defined as the total information gain due to its selection. Missing and incomplete values were not present in the original data set.

Results

At the start of the study, all patients were stable after initial treatment. No deaths were observed during hospitalization.

Based on the tests performed, the following clinical and neuroimaging manifestations of ischemic stroke were identified (Table 1).

Group 2 patients had a significant reduction in cognitive function according to the MoCA scale ($P<0.001$), daily activity according to BI ($P<0.001$), and disability severity according to mRS ($P<0.001$) compared to group 1. No significant differences in other parameters were found between the groups ($P>0.05$).

Discriminant analysis using ML showed that the most significant parameters (based on information gain, IG) in group 1 patients were IL-1b and MPIF-1/CCL23 levels. In group 2 patients, the levels of MPIF-1/CCL23, Eotaxin-2/CCL24, Gro-a/CXCL1, IL-8/CXCL8 and IL-16 were found to be relevant (Fig. 1).

In summary, the immunologic parameters directly related to stroke severity were CD4 (IL-16), CXCR2 (Gro-a/CXCL1), CXCR1-2 (IL-8/CXCL8), CCR3 (Eotaxin-2/CCL24), and CCR1 (MPIF-1/CCL23) receptor chemoattractants.

The values of NIHSS, mRS, MoCA, and BI scores at admission and day 12 of hospitalization are shown in Table 2.

Analysis of the changes in the main clinical scores revealed a significant increase in MoCA and BI scores and a decrease in NIHSS and mRS scores after initial therapy and early rehabilitation in patients in both groups (Fig. 2).

Table 1. Demographic and clinical characteristics of patients with carotid ischemic stroke in groups 1 and 2.

Parameter	Values in groups		*P* value
	Group 1 (*N*=38)	Group 2 (*N*=40)	
Demographic feature			
Men, *N* (%)	23 (60.5)	24 (60.0)	0.964
Women, *N* (%)	15 (39.5)	16 (40.0)	0.964
Mean age	68.32±5.62	66.81±4.92	0.212
IS subtype (TOAST), *N* (%)			
IS due to atherosclerosis of large arteries (atherothrombotic)	8 (21.1)	13 (32.5)	0.256
IS due to cardiogenic embolism (cardioembolic)	20 (52.6)	14 (35.0)	0.117
IS due to occlusion of small arteries (lacunar)	7(18.4)	11 (27.5)	0.340
IS of undetermined etiology	3 (7.9)	2 (5.0)	0.601
Clinical stroke scores, *Me [Q1; Q3]*			
Barthel Index, BI	83 [70; 100]	76 [55; 80] *	0.001
Modified Rankin scale, mRS	1.6 [0; 3]	3.5 [1; 5] *	0.008
MoCA	23 [16; 29]	21 [18; 25] *	<0.001
NIHSS	4 [3; 4]	10 [7; 13]*	<0.001
ASPECTS	8 [8; 9]	8 [7; 9]	1.000

Note. * — significant differences between groups.

Analysis of the changes in the parameters of the main clinical scales showed a significant increase in MoCA and BI, and a decrease in NIHSS and mRS after standard therapy and early rehabilitation.

When studying the correlations between the initial cytokine levels and the functional outcome parameters based on MoCA, NIHSS, BI, mRS scores (△MoCA, △NIHSS, △BI, △mRS) in both groups, correlations of different strength and direction were revealed.

In group 1 patients, a significant correlation was found between MPIF-1/CCL23 levels and △mRS (r=0.217, P=0.0004), △BI (r=–0.225, P<0.0001) and △NIHSS (r=0.214, P<0.0001). There was a negative correlation between Gro-a/CXCL1 levels (r=–0.213, P=0.005) and changes in cognitive function (△MoCA). The mRS outcome scores (△mRS) were positively correlated with IL-16 levels (r=0.244, P=0.0007, Fig. 3).

Correlations between functional outcome parameters and levels of CXC subfamily chemokines in group 2 patients are shown in Figure 3.

In group 2 patients, there was a significant negative correlation between the MoCA cognitive deficit score (△MoCA) and the levels of eotaxin-2/CCL24 (r=–0.388, P=0.00075), Gro-a/CXCL1 (r=–0.319, P=0.0035), and IP-10/CXCL1 (r=–0.274, P=0.00023). A significant inverse correlation of △BI values with the levels of MPIF-1/CCL23 (r=–0.345, P=0.0024) and Gro-a/CXCL1 (r=–0.210, P=0.00001) was also observed. We found a significant direct correlation of △mRS with MPIF-1/CCL23 (r=0.294, P=0.00006), Gro-a/CXCL1 (r=0.230, P=0.0075) and IL-16 (r=0.200, P=0.00001) levels. Furthermore, a positive correlation of △NIHSS functional outcome scores with levels of TNF-α (r=0.227, P=0.001), MPIF-1/CCL23 (r=0.288, P=0.00061) and Gro-a/CXCL1 (r=0.214, P=0.00001) was observed.

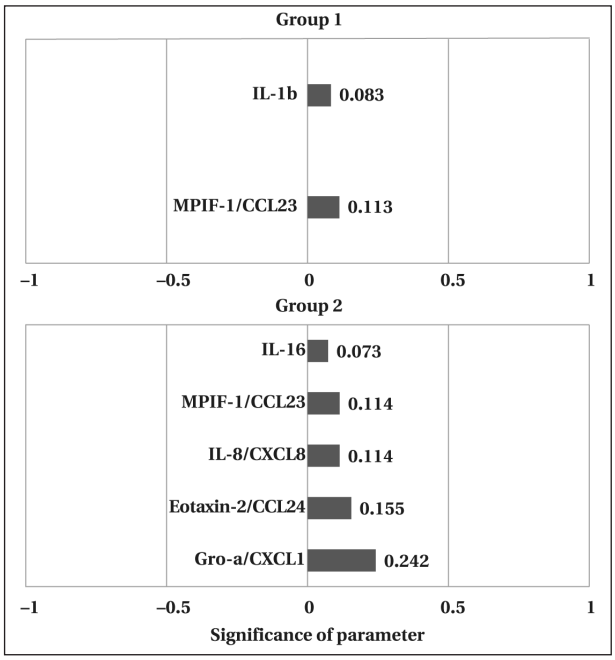

Fig. 1. Relevant cytokine levels in patients with mild and moderate IS on day 2 of hospitalization.

Discussion

Predicting the functional outcome of patients with ischemic stroke is a challenging task for most clinicians due to a poor understanding of the pathogenetic mechanisms of ischemia development and the lack of clear prognostic algorithms [22–24]. The multifaceted nature of factors influencing the functional outcome of the disease necessitates the use of structured and combined techniques for personalized assessment of patient status in early IS [25].

The study of patient status using tools such as mRS, Barthel Index and MoCA showed that in patients with moderate stroke severity, the neurological and cognitive status is characterized by a predomi-

Table 2. Comparative characteristics of clinical parameters at admission and on day 12 of hospital stay

Parameters (points)	Values in groups				*P* value
	Group 1 (*N*=38)		Group 2 (*N*=40)		
	Day 1	Day 12	Day 1	Day 12	
BI	83 [70; 100]	93 [80; 100]	76 [55; 80]	87 [75; 100]	P_1=0.0004* P_2⩽0.0001* P_3=0.163
mRS	1.6 [0; 3]	0.5 [0; 1]	3.5 [1; 5]	2 [0; 4]	P_1⩽0.0001* P_2⩽0.0001* P_3⩽0.001*
MoCA	23 [16; 29]	24 [15; 29]	21 [18; 25]	22.5 [11; 27]	P_1=0.0057* P_2=0.0016* P_3=0.034
NIHSS	4 [3; 4]	2 [0; 4]	10 [7; 13]	5 [0; 9]	P⩽0.0001* P_2⩽0.0001* P_3⩽0.0001*

Note. P_1 – significant difference between the parameters on the 1st and 10th days of of hospital stay in group 1; P_2 — significant difference between the parameters on the 1st and 10th days of hospital stay in group 2; P_3 — significant difference of parameters between groups on the 12th day of hospitalization; * — statistically significant differences between the groups.

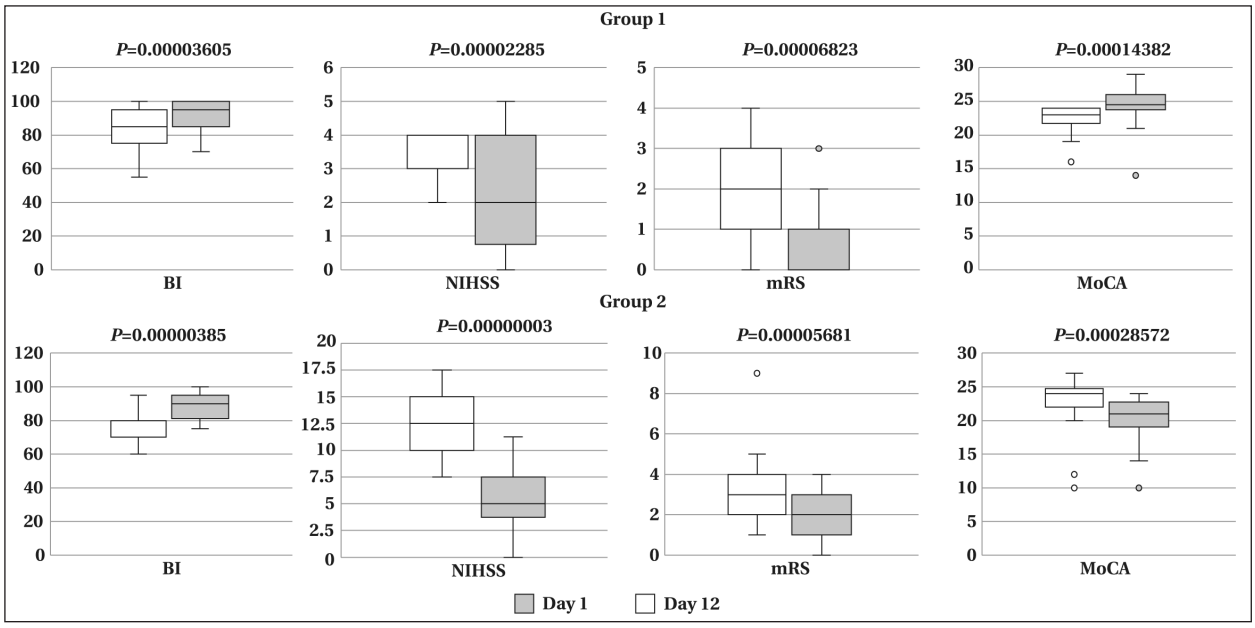

Fig. 2. Changes in the values of the main clinical scales before and after treatment.

nant decrease in daily activity, cognitive function and degree of independence, confirming the association of these parameters with the NIHSS level.

The results obtained are consistent with other studies showing that currently the main predictors of patient recovery are motor and cognitive impairment, age, severe aphasia, and baseline daily activity [26–28]. However, the use of rating scales is not sufficient to develop a rational prognostic model of stroke recovery.

Thus, the NIHSS scale, which is a universal tool for monitoring the effectiveness of therapy, is

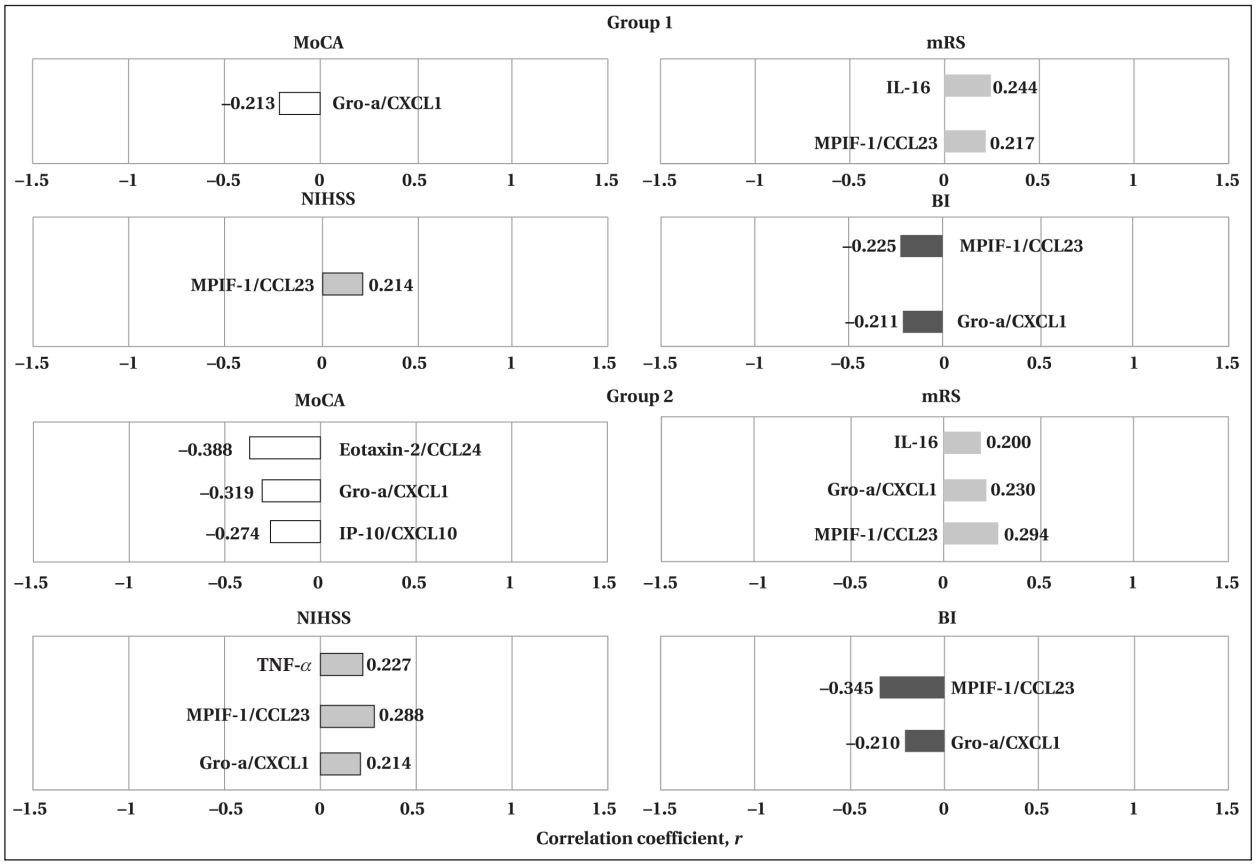

Fig. 3. Correlation between cytokine levels (pg/mL) and main clinical scales (points) in patients with mild *(a)* and moderate *(b)* IS.

of limited value in assessing symptoms of lesions in the anterior and posterior arterial supply territories and the nondominant brain hemisphere [29]. Scales that have demonstrated reliability and validity for various activities of daily living and stroke outcomes (BI and mRS) are not sensitive enough to assess cognitive profile, speech and visual function [30]. The MoCA scale has insufficient specificity for the advanced diagnosis of cognitive dysfunction and is generally used as a screening tool for moderate cognitive impairment.

Therefore, in order to optimize the prediction of functional outcome of IS, it is necessary to expand the range of predictive markers and, in addition to rating scale scores, to consider laboratory parameters as informative criteria of patient recovery in acute IS [31]. To improve the reliability of prognosis, it is reasonable to rely on mathematical modeling algorithms and discrete function construction based on clinical and other data.

Modern trends in the study of immunological and biological mechanisms of ischemia development point to new directions in the identification of biomarkers of functional outcome in patients with various severity of stroke and the role of cytokines in the regulation of pathogenetic mechanisms of ischemia [32, 33].

In the current study, the results of the assessment of interleukin levels using machine learning methods revealed the importance of IL-16 levels in patients with moderate stroke severity. The association of elevated IL-16 levels with neurological deficits has been attributed to its direct effect on the expression of inflammatory cytokines TNF-α, IL-1β, and IL-6, which exacerbate ischemia and brain damage [34, 35].

A study of the expression of CCL cluster chemokines showed that the main members of this group associated with stroke severity were MPIF-1/CCL23 and Eotaxin-2/CCL24. The chemokine ligand CCL23, which has chemotactic activity against T lymphocytes, monocytes and neutrophils and stimulates the production of proinflammatory cytokines and adhesion molecules, is currently considered a new promising biomarker for early diagnosis of brain lesions [36, 37]. The results of the present study demonstrate a direct correlation between the increase in MPIF-1/CCL23 levels and reduced daily activity and independence levels, as measured by mRS and BI scales, in patients with moderate severity of IS. The results obtained are consistent with previous studies showing a positive correlation of MPIF-1/CCL23 expression with NIHSS scores and a negative correlation with BI scores, suggesting the use of this chemokine as a tool for predicting functional outcome in patients with ischemic stroke [38, 39].

Eotaxin-2/CCL24 is a potent chemoattractant for eosinophils, basophils, and lymphocytes in many tissues, including the brain [40]. Despite the lack of convincing data on changes in eotaxin-2 levels during acute IS in the current literature, our results show a clear increase in serum eotaxin-2/CCL24 in patients with moderate ischemia, as well as a correlation between its level and cognitive dysfunction as measured by the MoCA scale.

The most likely explanation for these results is the experimentally demonstrated effect of eotaxin-2 on the mechanisms of atherogenesis by inducing the expression of toll-like receptor 4 (TLR4) with subsequent endothelial dysfunction and atherosclerosis progression [41].

Levels of CXC subfamily chemokines (Gro-a/CXCL1 and IL-8/CXCL8) were important parameters associated with stroke severity. A clear inverse correlation was found between Gro-a/CXCL1 levels and cognitive function score as measured by the MoCA scale and level of daytime activity as measured by the Barthel scale.

Gro-a/CXCL1, acting through CXCR2 receptors, is a potent chemoattractant and activator of neutrophils. Along with macrophages, neutrophils are the predominant immune cells in the ischemic zone and are directly involved in the mechanisms of atherogenesis, aseptic inflammation and thrombosis in acute ischemia [42, 43].

Previously, a number of researchers have identified the role of CXCL1 in the production of reactive oxygen species, which in turn induce and modulate neuroinflammation [44]. Recent studies demonstrate the correlation between CXCL1 expression levels in acute IS and the volume of hypodense brain areas according to neuroimaging data [45]. The increased serum Gro-a/CXCL1 in patients with acute IS reflects early systemic production of CXCL1. No less significant are the results of studies on the involvement of the CXCR1 ligand in the mechanisms of neurogenesis [46, 47].

In experimental animal models, Gro-a/CXCL1 expression has been demonstrated in the hippocampal dentate gyrus and microglia following induced brain injury, including hypoxic-ischemic injury [48]. Several clinical studies have produced similar results, demonstrating an increase in CXCL1 in human hippocampal neural progenitor cells and detecting CXCL1 expression in the cerebrospinal fluid of Alzheimer's patients [49].

Thus, previous experimental and clinical data are consistent with our findings and may explain the association of Gro-a/CXCL1 expression with cognitive dysfunction and lower BI scores in patients with moderate severity of IS.

IL-8 is a chemotactic cytokine similar to Gro-a/CXCL1 that attracts neutrophils. Elevated levels of IL-8/CXCL8 promote chemotaxis of inflammatory

cells, resulting in neutrophil infiltration into the ischemic area, which exacerbates the local inflammatory response and stroke [50]. There is experimental and clinical evidence showing a positive correlation between the severity of clinical impairment and disability and serum IL-8 levels [51]. We found that CXCL8 was associated with stroke severity, but without correlation with other clinical scales.

Limitations. The main limitation was the small number of patients due to limited laboratory diagnostic capacity and the exclusion of patients with severe stroke from the study.

Conclusion

The main cytokines associated with changes in functional and cognitive parameters in patients with acute IS are CC family chemokines such as MPIF-1/CCL23 and Eotaxin-2/CCL24 and CXC cluster chemokines such as Gro-a/CXCL1 and IL-16. The initial increase in MPIF-1/CCL23 and Gro-a/CXCL1 levels negatively affects the recovery of neurological deficits, daily activity and independence of patients regardless of the severity of IS. IL-16 expression is predominantly associated with Modified Rankin Scale disability scores. Elevated eotaxin-2/CCL24 levels were more strongly associated with cognitive performance in patients with moderate IS.

Despite the results demonstrating the negative effect of MPIF-1/CCL23, Gro-a/CXCL1, IL-16 and Eotaxin-2/CCL24 elevation on the improvement of motor and cognitive impairment, further studies are needed to identify chemokines of the CXC and CC subfamilies as prognostic markers for patient functional outcome in acute IS.

The implementation of machine learning methods in neurological practice may result in accurate and accessible predictions of stroke patients' functional outcomes, which is a key goal of contemporary clinical medicine and healthcare. Discriminant analysis of a wide range of disease-related variables will enable clinicians to more accurately predict a stroke patient's potential for recovery without the need for time-consuming diagnostic techniques.

References

1. *Клочихина О. А., Шпрах В. В., Стаховская Л. В., Полунина О. С., Полунина Е. А.* Динамика показателей заболеваемости инсультом и смертности от него за восьмилетний период на территориях, вошедших в федеральную программу реорганизации помощи пациентам с инсультом. *Acta Biomedica Scientifica*. 2021; 6 (1): 75–80. [*Klochikhina O. A., Shprach V. V., Stakhovskaya L. V., Polunina O. S., Polunina E. A.* Dynamics of stroke morbidity and mortality over an eight-year period in the territories included in the Federal program for the reorganization of care for stroke patients. *Acta Biomedica Scientifica*. 2021; 6 (1): 75–80. (in Russ.)]. DOI: 10.29413/ABS.2021–6.1.10.
2. *Song S. H., Kim J. H., Lee J. H., Yun Y. M., Choi D. H., Kim H. Y.* Elevated blood viscosity is associated with cerebral small vessel disease in patients with acute ischemic stroke. *BMC Neurol*. 2017; 17 (1): 20. DOI: 10.1186/s12883-017-0808-3. PMID: 28143595.
3. *Голубев А. М., Гречко А. В., Захарченко В. Е., Канарский М. М., Петрова М. В., Борисов И. В.* Характеристика кандидатных молекулярных маркеров при ишемическом и геморрагическом инсульте. Obshchaya Reanimatologiya = General Reanimatology. 2021; 17 (5): 23–34. [*Golubev A. M., Grechko A. V., Zakharchenko V. E., Kanarsky M. M., Petrova M. V., Borisov I. V.* Comparative characterization of candidate molecular markers in ischemic and hemorrhagic stroke. *General Reanimatilogy/ Obshchaya Reanimatologya*. 2021; 17 (5): 23–34. (in Rus. & Engl.)]. DOI: 10.15360/1813-9779-2021-5-23-34.
4. *Maida C. D., Norrito R. L., Daidone M., Tuttolomondo A., Pinto A.* Neuroinflammatory mechanisms in ischemic stroke: focus on cardioembolic stroke, background, and therapeutic approaches. *Int J Mol Sci*. 2020; 21 (18): 6454. DOI: 10.3390/ijms21186454. PMID: 32899616.
5. *Прилуцкая И. А., Крюк Ю. Я.* Уровни фактора некроза опухолей α у больных ишемическим инсультом. Медицинская иммунология. 2019; 21 (4): 755–764. [*Prilutskaya I. A., Kryuk Yu. Ya.* Levels of tumor necrosis factor alpha in patients with ischemic stroke. *Medical immunology/Meditsinskaya Immunologiya*. 2019; 21 (4): 755–764. (in Russ.]. DOI: 10.15789/1563-0625-2019-4-755-764.
6. *Быкова А. Ю., Кулеш А. А., Кайлева Н. А., Куклина Е. М., Шестаков В. В.* Взаимосвязь динамики сывороточных концентраций интерлейкина-1β, интерлейкина-6 и интерлейкина-10 с клиническими данными в остром периоде ишемического инсульта в зависимости от стратегии реперфузионной терапии. *Бюллетень сибирской медицины*. 2020; 18 (4): 16–25. [*Bykova A. Yu., Kulesh A. A., Kayleva N. A., Kuklina E. M., Shestakov V. V.* Interrelation of the dynamics of serum concentrations of interleukin-1β, interleukin-6 and interleukin-10 with clinical data in acute period of ischemic stroke and the strategy of reperfusion therapy. *Bulletin of Siberian Medicine/ Bulleten Sibirskoy Meditsiny*. 2020; 18 (4): 16–25. (in Russ.)]. DOI: 10.20538/1682-0363-2019-4-16-25.
7. *Вознюк И. А., Ильина О. М., Коломенцев С. В.* Ишемический инсульт как клиническая форма и патогенетическая модель в структуре поражения центральной нервной системы при COVID-19. *Вестник восстановительной медицины*. 2020; 4 (98): 90–98. [*Voznyuk I. A., Ilyina O. M., Kolomentsev S. V.* Ischemic stroke as a clinical form and pathogenetic model in the structure of central nervous system lesions in COVID-19. *Bulletin of Restorative Medicine/ Vestnik Vosstanovitelnoy Meditsiny*. 2020; 4 (98): 90–98. (in Russ.)]. DOI: 10.38025/2078-1962-2020-98-4-90-98.
8. *Ransohoff R. M., Trettel F.* Editorial Research Topic «Chemokines and chemokine receptors in brain homeostasis». *Front Cell Neurosci*. 2015; 9: 132. DOI: 10.3389/fncel.2015. 00132. PMID: 25904848.
9. *Голубев А. М., Петрова М. В., Гречко А. В., Захарченко В. Е., Кузовлев А. Н., Ершов А. В.* Молекулярные маркеры ишемического инсульта. *Obshchaya Reanimatologiya = General Reanimatology*. 2019; 15 (5): 11–22. [*Golubev A. M., Petrova M. V., Grechko A. V., Zakharchenko V. E., Kuzovlev A. N., Ershov A. V.* Molecular markers of ischemic stroke. *General Reanimatology/Obshchaya Reanimatologya*. 2019; 15 (5): 11–22. (in Rus.& Engl.)]. DOI: 10.15360/1813-9779-2019-5-11-22.
10. *Jayaraj R. L., Azimullah S., Beiram R., Jalal F. Y., Rosenberg G. A.* Neuroinflammation: friend and foe for ischemic stroke. *J Neuroinflammation*. 2019; 16 (1): 142. DOI: 10.1186/s12974-019-1516-2. PMID: 31291966.
11. *Hughes C. E., Nibbs, R. J. B.* A guide to chemokines and their receptors. *FEBS J*. 2018; 285 (16): 2944–2971. DOI: 10.1111/febs. 14466. PMID: 29637711.
12. *Feng Y. Q., Xu Z. Z., Wang Y. T., Xiong Y., Xie W., He Y. Y., Chen L., et al.* Targeting C-C chemokine receptor 5: key to opening the neurorehabilitation window after ischemic stroke. *Front Cell Neurosci*. 2022; 16: 876342. DOI: 10.3389/fncel.2022. 876342. PMID: 35573839.
13. *Chen C., Chu S. F., Liu D. D., Zhang Z., Kong L. L., Zhou X., Chen N. H.* Chemokines play complex roles in cerebral ischemia. *Neurochem Int*. 2018;

112: 146–158. DOI: 10.1016/ j.neuint.2017.06.008. PMID: 28629771.
14. *Воробьев С. В., Янишевский С. Н., Кудрявцев И. В., Шубина К. М., Антушева М. С., Кузнецова Р. Н., Серебрякова М. К., с соавт.* Участие иммунного ответа в патогенезе ишемического инсульта. *Медицинский Совет*. 2023; (3): 8–16. [*Vorobyov S. V., Yanishevsky S. N., Kudryavtsev I. V., Shubina K. M., Antusheva M. S., Kuznetsova R. N., Serebryakova M. K., et al.* Involvement immune response in the pathogenesis of ischemic stroke. *Medical Council/ Meditsinskiy Sovet*. 2023; (3): 8–16. (in Russ.)]. DOI: 10.21518/ms2023-024.
15. *Amin M., Vakilian A., Mahmoodi M. H., Hassanshahi G., Falahati-Pour S. K., Dolatabadi M. R., Nadimi A. E.* Circulatory levels of C-X-C motif chemokine ligands 1, 9, and 10 are elevated in patients with ischemic stroke. *Eurasian J Med*. 2017; 49 (2): 92–96. DOI: 10.5152/eurasianjmed. 2017. PMID: 28638249.
16. *Sidey-Gibbons J. A. M., Sidey-Gibbons C. J.* Machine learning in medicine: a practical introduction. *BMC Med Res Methodol*. 2019; 19 (1): 64. DOI: 10.1186/s12874-019-0681-4. PMID: 30890124.
17. *Deo R. C.* Machine learning in medicine. *Circulation*. 2015; 132 (20): 1920–30. DOI: 10.1161/CIRCULATIONAHA.115.001593. PMID: 26572668.
18. *Adams H. P., Jr Bendixen B. H., Kappelle L. J., Biller J., Love B. B., Gordon D. L., Marsh E. E. 3rd*. Classification of subtype of acute ischemic stroke. Definitions for use in a multicenter clinical trial. TOAST. Trial of Org 10172 in Acute Stroke Treatment. *Stroke*. 1993; 24 (1): 35–41. DOI: 10.1161/01.str.24.1.35. PMID: 7678184.
19. *Kasner S. E.* Clinical interpretation and use of stroke scales. *Lancet Neurol*. 2006; 5 (7): 603–612. DOI: 10.1016/S1474-4422 (06)70495–1. PMID: 16781990.
20. *Chen T., Guestrin* C. XGBoost: a scalable tree boosting system. *Proceedings of the 22nd ACM SIGKDD International Conference on knowledge discovery and data mining (KDD '16)*. Association for computing machinery, New York, NY, USA. 2016: 785–794. DOI: 10.1145/2939672.2939785.
21. *Kursa M. B., Jankowski A., Rudnicki W. R.* Boruta — a system for feature selection. *Fundamenta Informaticae*. 2010; 101 (4): 271–285. DOI: 10.3233/FI-2010-288.
22. *Shin S., Lee Y., Chang W. H., Sohn M. K., Lee J., Kim D. Y., Shin Y. I., et al.* Multifaceted assessment of functional outcomes in survivors of first-time stroke. *JAMA Netw Open*. 2022; 5 (9): e2233094. DOI: 10.1001/jamanetworkopen.2022. 33094. PMID: 36149652.
23. *Yeh H. J., Huang N., Chou Y. J., Cheng S. P., Lee W. K., Lai C. C., Cheng C. C.* Older age, low socioeconomic status, and multiple comorbidities lower the probability of receiving inpatient rehabilitation half a year after stroke. *Arch Phys Med Rehabil*. 2017; 98 (4): 707–715. DOI: 10.1016/j.apmr. 2016.08.468. PMID: 27633939.
24. *Alonso A., Ebert A. D., Kern R., Rapp S., Hennerici M. G., Fatar M.* Outcome predictors of acute stroke patients in need of intensive care treatment. *Cerebrovasc Dis*. 2015; 40 (1–2): 10–17. DOI: 10.1159/000430871. PMID: 26022716.
25. *Глущенкова Н. В., Саркисян О. Г., Гончарова З. А.* Злокачественный ишемический инсульт: клинические и биохимические особенности диагностики. *Южно-Российский журнал терапевтической практики*. 2023; 4 (2): 35–45. [*Glushenkova N. V., Sarkisian O. G., Goncharova Z. A.* Malignant ischemic stroke: clinical and biochemical features of diagnosis. *South Russian Journal of Therapeutic Practice/Yuzhno-Rossiyskiy Zhurnal Terapevticheskoy Praktiki*. 2023; 4 (2): 35–45. (in Russ.)]. DOI: 10.21886/2712-8156-2023-4-2-35-45.
26. *Kongsawasdi S., Klaphajone J., Wivatvongvana P., Watcharasaksilp K.* Prognostic factors of functional outcome assessed by using the modified rankin scale in subacute ischemic stroke. *J Clin Med Res*. 2019; 11 (5): 375–382. DOI: 10.14740/jocmr3799. PMID: 31019633.
27. *Harvey R. L.* Predictors of functional outcome following stroke. *Phys Med Rehabil Clin N Am*. 2015; 26 (4): 583–98. DOI: 10.1016/j.pmr. 2015.07.002. PMID: 31019633.
28. *Chen W. C., Hsiao M. Y., Wang T. G.* Prognostic factors of functional outcome in post-acute stroke in the rehabilitation unit. *J Formos Med Assoc*. 2022; 121 (3): 670–678. DOI: 10.1016/ j.jfma.2021.07.009. PMID: 34303583.
29. *Abzhandadze T., Reinholdsson M., Stibrant Sunnerhagen K.* NIHSS is not enough for cognitive screening in acute stroke: a cross-sectional, retrospective study. *Sci Rep*. 2020; 10 (1): 534. DOI: 10.1038/s41598-019-57316-8. PMID: 31953508.
30. *Siniscalchi A.* Use of stroke scales in clinical practice: current concepts. *Turk J Emerg Med*. 2022; 22 (3): 119–124. DOI: 10.4103/2452-2473.348440. PMID: 35936953.
31. *Тынтерова А. М., Моисеева Е. М., Голубев А. М., Шушарина Н. Н.* Роль эндотелинергических и нитроксидергических реакций в прогнозировании функционального исхода пациентов с различной степенью тяжести ишемического инсульта. *Obshchaya Reanimatologiya = General Reanimatology*. 2023; 19 (5). [*Tynterova A. M., Moiseeva E. M., Golubev A. M., Shusharina N. N.* The role of endothelinergic and nitroxydergic reactions in predicting the functional outcome in patients with ischemic stroke of different severity. *General Reanima-*

tology/Obshchaya Reanimatologya. 2023; 19 (5). (in Russ.&Engl.)]. DOI: 10.15360/1813-9779-2023-5-2354.
32. *Pawluk H., Woźniak A., Grześk G., Kołodziejska R., Kozakiewicz M., Kopkowska E., Grzechowiak E., et al.* The role of selected pro-inflammatory cytokines in pathogenesis of ischemic stroke. *Clin Interv Aging*. 2020; 15: 469–484. DOI: 10.2147/CIA.S233909. PMID: 32273689.
33. *Mizum A., Yenari M. A.* Anti-inflammatory targets for the treatment of reperfusion injury in stroke. *Front Neurol*. 2017; 8: 467–487. DOI: 10.3389/fneur.2017.00467. PMID: 28936196.
34. *Ганковская Л. В., Стаховская Л. В., Греченко В. В., Кольцова Е. А., Уварова О. С., Демина М. Д., Громова Т. В., с соавт.* Гиперэкспрессия TLR2 и TLR4 у больных с ишемическим инсультом в остром периоде заболевания. *Медицинская иммунология*. 2020; 22 (4): 665–674. [*Gankovskaya L. V., Stakhovskaya L. V., Grechenko V. V., Koltsova E. A., Uvarova O. S., Demina M. D., Gromova T. V., et al.* Hyperexpression of TLR2 and TLR4 in patients with ischemic stroke in the acute period of the disease. *Medical immunology/Meditsinskaya Immunologiya*. 2020; 22 (4): 665–674. (in Russ.)]. DOI: 10.15789/1563-0625-HOT-1971.
35. *Kleinschnitz C., Kraft P., Dreykluft A., Hagedorn I., Göbel K., Schuhmann M. K., Langhauser F., et al.* Regulatory T cells are strong promoters of acute ischemic stroke in mice by inducing dysfunction of the cerebral microvasculature. *Blood*. 2013; 121: 679–91. DOI: 10.1182/blood-2012-04-426734. PMID: 23160472.
36. *Faura J., Bustamante A., Penalba A., Giralt D., Simats A., Martínez-Sáez E., Alcolea D., et al.* CCL23: a chemokine associated with progression from mild cognitive impairment to Alzheimer's disease. *J Alzheimers Dis*. 2020; 73 (4): 1585–1595. DOI: 10.3233/JAD-190753. PMID: 31958084.
37. *Черных Е. Р., Шевела Е. Я., Морозов С. А., Останин А. А.* Иммунопатогенетические аспекты ишемического инсульта. *Медицинская иммунология*. 2018; 20 (1): 19–34. [*Chernykh E. R., Shevela E. Ya., Morozov S. A., Ostanin A. A.* Immunopathogenetic aspects of ischemic stroke. *Medical immunology/Meditsinskaya Immunologiya*. 2018; 20 (1): 19–34. (in Russ.)]. DOI: 10.15789/1563-0625-2018-1-19-34.
38. *Wang X., Yang Y., Zhao Z., Li P., Ma C., Zhu B.* Diagnostic value of serum MIF and CCL23 in the patients with acute cerebral infarction. *Clin Lab*. 2020; 66 (11). DOI: 10.7754/Clin.Lab.2020.200239. PMID: 33180438.
39. *Li Y. S., Chen W., Liu S., Zhang Y. Y., Li X. H.* Serum macrophage migration inhibitory factor levels are associated with infarct volumes and long-term outcomes in patients with acute ischemic stroke. *Int J Neurosci*. 2017; 127 (6): 539–546. DOI: 10.1080/00207454.2016.1211648. PMID: 27402018.
40. *Furer V., Hazan E., Mor A., Segal M., Katav A., Aloush V., Elkayam O., et al.* Elevated levels of eotaxin-2 in serum of fibromyalgia patients. *Pain Res Manag*. 2018; 2018: 7257681. DOI: 10.1155/2018/7257681. PMID: 29861805.
41. *Tsai C. S., Huang C. Y., Chen C. H., Lin Y. W., Shih C. M., Tsao N. W., Chiang K. H., et al.* Eotaxin-2 increased toll-like receptor 4 expression in endothelial cells in vitro and exacerbates high-cholesterol diet-induced atherogenesis *in vivo*. *Am J Transl Res*. 2016; 8 (12): 5338–5353 PMID: 28078007.
42. *Sreeramkumar V., Adrover J. M., Ballesteros I., Cuartero M. I., Rossaint J., Bilbao I., Nácher M., et al.* Neutrophils scan for activated platelets to initiate inflammation. Science. 2014; 346 (6214): 1234–1238. DOI: 10.1126/science.1256478. PMID: 25477463.
43. *Gill D., Sivakumaran P., Wilding P., Love M., Veltkamp R., Kar A.* Trends in C-reactive protein levels are associated with neurological change twenty-four hours after thrombolysis for acute ischemic stroke. *J Stroke Cerebrovasc Dis*. 2016; 25 (8): 1966–1999. DOI: 10.1016/J.JSTROKECEREBROVASDIS. 2016.05.003. PMID: 27212272.
44. *Boro M., Balaji K. N.* CXCL1 and CXCL2 regulate NLRP3 inflammasome activation via G-Protein-coupled receptor CXCR2. *J Immunol*. 2017; 199 (5): 1660–1671. DOI: 10.4049/jimmunol.1700129. PMID: 28739876.
45. *Zhu W., Nan Y., Wang S., Liu W.* Bioinformatics analysis of gene expression profiles of sex differences in ischemic stroke. *Biomed Res Int*. 2019; 2019: 2478453. DOI: 10.1155/2019/ 2478453. PMID: 31183363.
46. *Huang F., Lan Y., Qin L., Dong H., Shi H., Wu H., Zou Q., et al.* Astragaloside IV promotes adult neurogenesis in hippocampal dentate gyrus of mouse through CXCL1/CXCR2 signaling. *Molecules*. 2018; 23 (9): 2178. DOI: 10.3390/molecules23092178. PMID: 30158469.
47. *Zhang X. F., Zhao Y. F., Zhu S. W., Huang W. J., Luo Y., Chen Q. Y., Ge L. J., et al.* CXCL1 Triggers caspase-3 dependent tau cleavage in long-term neuronal cultures and in the hippocampus of aged mice: implications in Alzheimer's Disease. *J Alzheimers Dis*. 2015; 48 (1): 89–104. DOI: 10.3233/JAD-150041. PMID: 26401931.
48. *Shang Y., Tian L., Chen T., Liu X., Zhang J., Liu D., Wei J., et al.* CXCL1 promotes the proliferation of neural stem cells by stimulating the generation of reactive oxygen species in APP/PS1 mice. *Biochem Biophys Res Commun*. 2019; 515 (1): 201–206. DOI: 10.1016/j.bbrc.2019.05.130. PMID: 31146911.
49. *Korbecki J., Gąssowska-Dobrowolska M., Wójcik J., Szatkowska I., Barczak K., Chlubek M.,*

Baranowska-Bosiacka I. The importance of CXCL1 in physiology and noncancerous diseases of bone, bone marrow, muscle and the nervous system. *Int J Mol Sci*. 2022; 23 (8): 4205. DOI: 10.3390/ijms23084205. PMID: 35457023.

50. *Shaheen H. A., Daker L. I., Abbass M. M., Abd E. l., Fattah A. A.* The relationship between the severity of disability and serum IL-8 in acute ischemic stroke patients. *Egypt J Neurol Psychiatr Neurosurg*. 2018; 54 (1): 26. DOI: 10.1186/s41983-018-0025-z. PMID: 30294205.

51. *Zhang L., Xu D., Zhang T., Hou W., Yixi L.* Correlation between interleukin-6, interleukin-8, and modified early warning score of patients with acute ischemic stroke and their condition and prognosis. *Ann Palliat Med*. 2021; 10 (1): 148–155. DOI: 10.21037/apm-20-2200. PMID: 33440979.

Received 26.10.2023
Accepted 21.12.2023

https://doi.org/10.15360/1813-9779-2024-1-15-23

Immune Cell Response of the Spleen in COVID-19

Svetlana A. Perepelitsa[1,2]*

[1] Immanuel Kant Baltic Federal University,
14A Nevskiy Str., 236041 Kaliningrad, Russia
[2] V. A. Negovsky Research Institute of General Reanimatology,
Federal Scientific and Clinical Center of Reanimatology and Reabilitology,
25 Petrovka Str., Build. 2, Moscow 107031, Russia

For citation: *Svetlana A. Perepelitsa.* Immune Cell Response of the Spleen in COVID-19. *Obshchaya Reanimatologiya = General Reanimatology.* 2024; 20 (1): 15–23. https://doi.org/10.15360/1813-9779-2024-1-15-23 [In Russ. and Engl.]

***Correspondence to:** Svetlana A. Perepelitsa, sveta_perepeliza@mail.ru

Summary

Objective. To study the morphometric characteristics and splenic immune cell response in patients with COVID-19.

Material and methods. A prospective observational study included 70 patients. Of these, 45 patients admitted to the infectious diseases hospital with Coronavirus infection caused by the SARS-CoV-2 virus diagnosis were included in the COVID-19 group, and 25 patients were included in the acute respiratory viral infection (ARVI) comparison group. Spleen linear dimensions, including length, width, and thickness were assessed using ultrasound imaging, and calculations of the spleen weight and spleen weight coefficient (SWC) were obtained. Additionally leukocyte count and formula, erythrocyte sedimentation rate (ESR) were estimated, and the leukocyte index (LI) and neutrophil-to-lymphocyte ratio (NLR) were calculated.

Results. Microsplenia was common in the acute period of COVID-19 with mean SWC value 1.6±0.2. In 17 (37.8%) patients the SWC varied from 1.0 to 1.5, and in 9 (20%) microsplenia was critical with SWC <1.0. Leukocyte count was lower, and ESR — higher in patients with COVID-19, compared to ARVI group (5.4±2.1×10^9/l and 10.8±4.8×10^9/l, respectively $P<0.00001$, and ESR — 36.1±13.8 mm/h and 23.0±5.1 mm/h, respectively $P=0.03$). The course of COVID-19 was characterized by a slight decrease in LI — from 0.29±0.02 to 0.22±0.01 ($P=0.19$), and significant increase in NLR from 3.7±0.1 to 4.3±0.12 ($P=0.002$). Opposite trends were documented in patients with ARVI. On Day 5 since initiation of treatment LI was significantly lower in the COVID-19 vs ARVI group (0.22 [0.16; 0.39] vs. 0.48 [0.29; 0.93], $P=0.003$), and NLR was significantly higher (4.3 [2.5; 6.1] vs. 2.1 [0.9; 2.9], $P=0.002$).

Conclusion. The course of coronavirus infection caused by the SARS-CoV-2 virus is characterized by significant immunological shifts. Microsplenia verified by ultrasonography stays as one of the pathognomonic signs. This phenomenon is explained by rapid «depletion» of the spleen as a secondary immune organ, and is associated with a high risk of developing acute immune deficiency.

Keywords: COVID-19, immune distress, inflammatory markers, spleen, respiratory failure

Conflict of interest. The authors declare no conflict of interest.

Introduction

All aspects of the pathogenesis and clinical course of COVID-19 infection caused by SARS-CoV-2 (Severe Acute Respiratory Syndrome Coronavirus 2) have been intensively studied. During the COVID-19 pandemic, a large body of scientific and clinical data was generated and is being rapidly updated with new information on diagnosis, treatment, and disease progression. Based on these data, risk factors for the development of COVID-19, diagnostic criteria for hyperimmune response («cytokine storm») and disease severity have been identified [1–3], and guidelines for respiratory therapy in acute respiratory failure have been developed [4].

The outcome of any infectious disease depends on the patient's immune status, which includes three important and interrelated aspects: susceptibility, intensity of the protective immune responses, and suggested immune dysregulation.

Previous infections and vaccinations build up an immune memory that provides full or partial immunological protection, manifested as a reduced risk of developing an infectious disease or a milder disease. The SARS-CoV-2 virus is an etiologic factor with no prior immune response. There is no immunologic memory against it, resulting in increased morbidity in the population, immune stress that may result in acute immunodeficiency, and adverse short- and long-term outcomes [5].

Severe COVID-19 is caused by extreme hypoxemia and hyperimmune response, with significant increases in IL-1β, IL-6, TNF-α, CXCL10/CXC, IP-10, MIP-1α, chemokines, and unbalanced levels of type I interferon (IFN-I) at different stages of the disease. IFN-I levels are low during acute COVID-19 but rise later in the disease [2, 6].

The most important receptor for viral entry is angiotensin converting enzyme 2 (ACE 2). A decrease in its production causes hypercytokinemia, which is linked to the severity of inflammation and disease [2, 4, 7]. SARS-CoV-2 RNA is found not only in the blood but also in internal organs like the lungs,

heart, spleen, liver, intestines, kidneys, and brain, indicating that the virus can bind to most cells via the ACE2 receptor [7]. As a result, COVID-19 causes impaired function in these organs [8]. The virus affects several organs and systems, causing changes in both specific and non-specific immune responses [9].

Experiments show that hypoxia and increased glucocorticoid production in critical illness significantly alter myelopoiesis and interfere with the migration of mature leukocytes from the bone marrow into the bloodstream, resulting in cellular changes in the blood and leukocyte infiltration of parenchymal organs [10].

Lymphoid cells, primary and secondary immune organs that actively respond to a variety of negative stimuli, including infection, are useful indicators of immune system function. The spleen is the largest peripheral immune organ and is frequently involved in the immune response which manifests as splenomegaly. However, splenomegaly is not detected in SARS-CoV-2 infection, typically associated with an inflammatory response [3], despite the fact that the virus has been found in the spleens of deceased patients [11].

COVID-19 is distinguished by the rapid onset of multiple organ failure, primarily immunologic, as evidenced by a significant decrease in T lymphocytes, including CD4, CD8, and NK cells, as well as regulatory T cells. Severe lymphopenia is an early warning sign of the disease [11] and is linked to lymph node and splenic atrophy.

The spleen of deceased patients exhibits cell degeneration, focal hemorrhagic necrosis, macrophage proliferation, and intense apoptosis. Immunohistochemical analysis of lymph nodes and spleen reveals a decrease in the number of CD4(+) and CD8(+) T cells [12, 13].

Thus, the spleen plays an active role in the immune response to SARS-CoV-2 coronavirus infection.

The aim of this study was to investigate the morphometric characteristics and the immune cell response in the spleen of patients with COVID-19.

Materials and Methods

The prospective observational study was approved by the Independent Ethical Committee of the Clinical Research Center of the Immanuel Kant Baltic Federal University (protocol of the IEC meeting No. 23 dated April 27, 2021) and was conducted in 2019–2021 at the Infectious Diseases Hospital of the Kaliningrad Region.

Initially, 75 patients were included in the study and divided into 2 groups: COVID-19 and ARVI (acute respiratory viral infection) (Fig. 1).

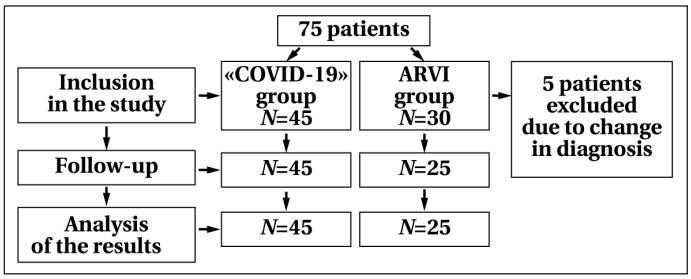

Fig. 1. The flowchart of the prospective clinical study.

Inclusion criteria for the COVID-19 group were clinical signs and laboratory confirmation of coronavirus infection caused by SARS-CoV-2 virus. The diagnosis was confirmed prior to hospitalization by polymerase chain reaction with detection of RNA fragment specific for SARS-CoV-2 coronavirus in the analyzed biological samples. The group was formed in 2021.

Inclusion criteria for the ARVI group were ARVI symptoms and negative viral tests. The group was formed in 2019, before the COVID-19 pandemic.

Medical history data were analyzed during the enrollment phase of the study. Patients with bacterial or fungal complications and decompensated chronic diseases were immediately excluded from the groups.

In all cases, outpatient treatment was ineffective and hospitalization in an infectious disease clinic was required.

The COVID-19 group included 45 patients admitted to an infectious disease clinic with a diagnosis of coronavirus infection caused by SARS CoV-2. All patients had acute onset of illness with fever up to 38–40°C, dry cough or cough with scanty sputum, dyspnea, chest tightness, sore throat, nasal congestion or moderate rhinorrhea, loss of smell, loss of taste, intoxication (fatigue, muscle pain, headache, vomiting, diarrhea). Patients did not receive steroids or anticytokine medications.

The ARVI group consisted of 25 patients with upper respiratory tract infection also characterized by acute onset, fever of 38–40°C, rhinorrhea, sore throat, cough (dry or wet) and fatigue.

The sample size was not predetermined.

Leukocyte count, leukocyte differential, and erythrocyte sedimentation rate were measured on admission (day 1, stage 1) and during treatment (day 5, stage 2). The blood test was performed on the 5diff MEK-8222K analyzer (Italy).

The leukocyte index (LI) was calculated using the formula: LI = lymphocytes/(band neutrophils + segmented neutrophils) [14].

The neutrophil-lymphocyte ratio (NLR) was determined using the formula: NLR = absolute neutrophil count / absolute lymphocyte count [15].

During lung ultrasound (LUS), we additionally performed linear measurements of spleen length, width, and thickness in two perpendicular planes. Based on the obtained morphometric data, we calculated spleen mass (Ms) and spleen weight coefficient (SWC) according to the method of O. Vozgoment et al.

The calculation of Ms was performed according to the formula:

Table 1. Characteristics of the studied groups, *M±SD*.

Parameter, units of measurement	Values in groups		*P* values
	COVID-19, *N*=45	ARVI, *N*=25	
Age, years	57.1±13.2	50.1±19.5	0.074
Body weight, kg	81.5±19.6	77.6±17.8	0.413
Height, cm	170,4±7.9	168.8±9.5	0.427
Duration of disease before hospitalization, days	7.6±3.6	7.1±2.5	0.646
Hypertension, *N* (%)	27 (60)	10 (40)	0.108
Coronary heart disease, *N* (%)	19 (42.2)	11 (44)	0.871
Diabetes mellitus, *N* (%)	5 (11.1)	2 (8)	0.688

Ms =0.34×L×2×h, where *L* is the length of the spleen, *h* is the thickness of the spleen (in cm).

SWC was calculated using the formula: 1000×m/body weight (in grams), where *m* is the mass of the spleen [16].

Statistical analysis was performed using the Statistica 10.0 software package (StatSoft Inc., USA). For normally distributed variables, arithmetic mean *(M)* and standard deviation *(SD)* were reported. The distribution of variables was tested using the Kolmogorov–Smirnov test with Lilliefors correction. For quantitative variables with non-normal distribution, the median *(Me)* and interquartile range *[Q1; Q3]* were calculated. Differences between two quantitative samples with non-Gaussian distribution were determined using the Mann–Whitney test, and the Wilcoxon test was used to compare paired samples. Qualitative data were analyzed by calculating the proportion (percentage) of each value. Qualitative variables were compared across the groups using Pearson's χ^2 test or Fisher's exact test. The two-tailed *P*-value was calculated. Differences were considered significant when $P \leqslant 0.05$. Pearson's parametric correlation test was used to analyze quantitative variables with normal distribution.

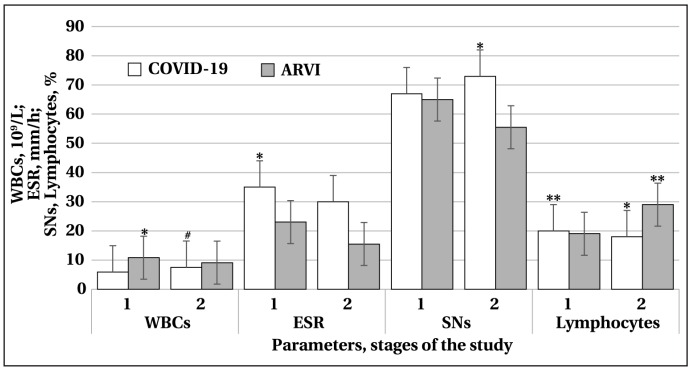

Fig. 2. Results of WBC differential and ESR measurements.
Note. * — $P<0.05$, significant differences between groups; significant differences at the stages of the study: # — $P<0.05$, in the COVID-19 group; ** — $P<0.05$, in the ARVI group. Stages 1,2 correspond to days 1 and 5 of treatment.

Results

The main clinical characteristics of the patients are shown in Table 1.

No significant differences were found between the groups in basic anthropometric parameters, age, duration of illness before hospitalization, and frequency of chronic comorbidities ($P>0.05$). All medical conditions of the participants were compensated.

Parameters of immune cell response are summarized in Fig. 2.

On hospital admission, significant differences between the groups were found in two parameters. The total leukocyte count was lower and the ESR was higher in the COVID-19 group than in the ARVI group ($P<0.001$ and $P=0.03$, respectively). Only in the COVID-19 group 14 (31%) patients had leukopenia on admission. There were no differences in segmented neutrophil and lymphocyte counts between groups ($P>0.05$).

In the COVID-19 group, the total leukocyte count increased significantly from 5.9×10^9/L to 7.5×10^9/L after 5 days of treatment ($P<0.001$), while the other parameters remained practically unchanged. In the ARVI group, the total leukocyte count and the ESR decreased slightly compared to day 1 of the study ($P>0.05$), there was a significant decrease in segmented leukocytes ($P=0.003$) and an increase in lymphocytes ($P=0.009$). In the intergroup analysis, we found that by day 5 of treatment, the percentage of segmented leukocytes was higher in the COVID-19 group and the percentage of lymphocytes was lower than in the ARVI group ($P=0.004$ and $P=0.039$, respectively).

The changes in LI over time are shown in Fig. 3, *a*.

At hospital admission, the median LI was 0.29 [0.18; 0.51] in the COVID-19 group and 0.27 [0.15; 0.48] in the ARVI group, with no significant differences ($P=0.521$). After 5 days of treatment, the leukocyte index showed multidirectional changes. In the COVID-19 group, it started to decrease with a value of 0.22 [0.16; 0.39] ($P=0.19$), while in the ARVI group, it increased 1.8 times compared to day 1, reaching 0.48 [0.29; 0.93] ($P=0.025$). On day 5 of treatment, the COVID-19 group had a significantly lower LI than the ARVI group ($P=0.003$).

At hospital admission, the median NLR was 3.7 [2.1; 6.5] in the COVID-19 group and 3.4 [1.9; 5.4] in the ARVI group (Fig. 3, *b*). There was no significant difference between the groups ($P=0.945$). On day 5 of treatment, the NLR changed in opposite directions. It increased to 4.3 [2.5; 6.1] in the

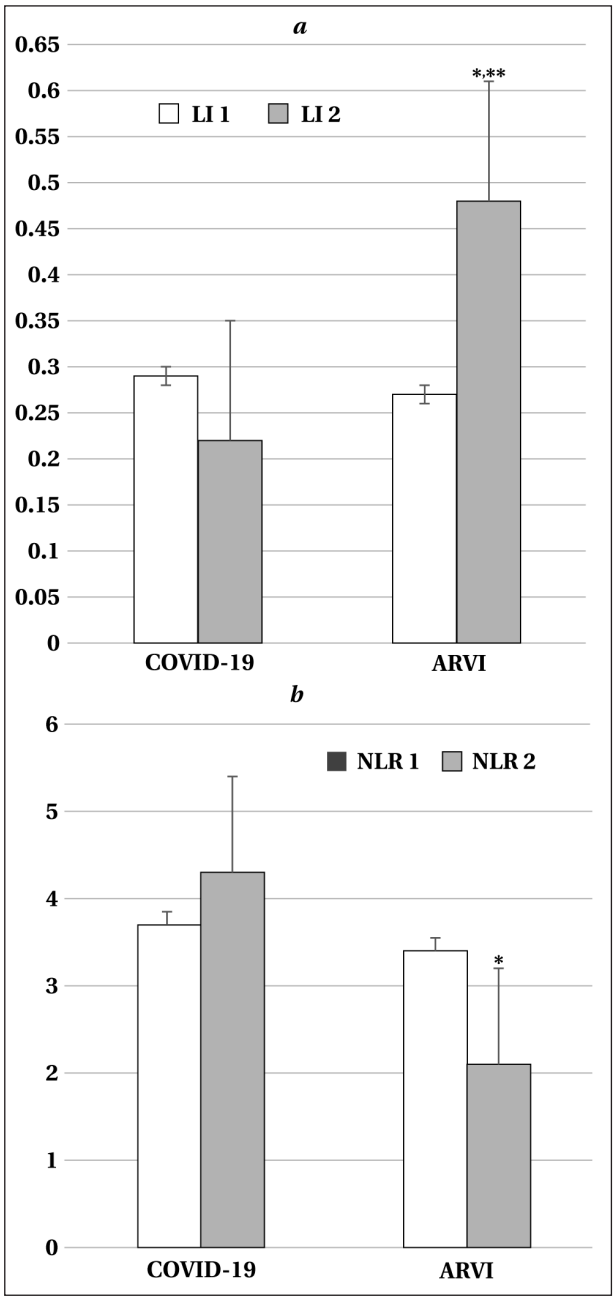

Fig. 3. Changes in leukocyte index (a) and neutrophil-lymphocyte ratio (NLR) (b) during treatment.
Примечание. * — $P<0.05$, significant differences between the groups on day 5; ** — $P<0.05$, significant differences in the ARVI group, compared to day 1. 1, 2 — stages of the study.

COVID-19 group and decreased to 2.1 [0.9; 2.9] in the ARVI group, indicating a significant difference between groups (P=0.002).

Table 2 shows the results of the ultrasonographic morphometric study of the spleen.

In patients in the COVID-19 group, all linear mean spleen dimensions (length, thickness, and width) were significantly smaller compared with the ARVI group ($P<0.001$). Based on the obtained linear dimensions, we calculated the mass and the spleen mass coefficient. The calculated spleen mass ranged from 52 to 138 g in the COVID-19 group and from 166 to 377 g in the ARVI group. The mean values of both spleen mass and SWC were 1.6 times lower in the COVID-19 group than in the ARVI group ($P<0.001$). The scatter plot of the spleen mass coefficient is shown in Fig. 4, *a*. Thus, patients in the COVID-19 group had reduced spleen size.

Previously, the SWC was shown to provide a detailed assessment of changes in spleen size and to allow the ranking of patients based on its value. An SWC value of less than 1.5 corresponds to microsplenia, the range of 1.6 to 3.9 to normal spleen size and more than 4 to splenomegaly [17].

Patients in both groups were ranked according to SWC (Fig. 4, *b*). We found that microsplenia corresponding to SWC less than 1.5 was significantly more frequent in the COVID-19 group compared to the ARVI group ($P<0.001$). Seventeen (37.8%) patients in the COVID-19 group had reduced spleen size with SWC in the range of 1.0 to 1.5, and 9 (20%) patients had critical microsplenia with a coefficient value of less than 1.0. A normal SWC value (1.6–3.9) was found in 18 (40%) patients in the COVID-19 group and 21 (84%) in the ARVI group. These differences were significant ($P<0.001$). Initial splenomegaly was detected in 1 (2.2%) case in the COVID-19 group and in 3 (12%) cases in the ARVI group. The differences were significant ($P<0.001$).

Only in the ARVI group a direct moderate correlation between SWC and WBC count was found (r=0.588; P=0.002).

In the COVID-19 group, 34 (75.6%) patients had moderate disease with bilateral interstitial pneumonia, 10 (22.2%) patients had severe disease and 1 (2.2%) patient had mild «ARVI-like» disease.

All patients in the ARVI group had moderate disease severity.

The distribution of patients by severity of acute respiratory failure (ARF) is shown in Table 3.

In the COVID-19 group, 29 (64.4%) patients had respiratory failure I–III. There was no evidence of ARF in the ARVI group. Significant differences in

Table 2. Measured and calculated morphologic characteristics of the spleen, *M±SD*.

Parameter	Values in groups		*P* value
	COVID-19, *N*=45	ARVI, *N*=25	
Length of the spleen, cm	9.5±1.5*	10.9±1.5	<0.001
Thickness of spleen, cm	3.9±0.9*	4.9±0.8	<0.001
Width of the spleen, cm	4.3±1.6*	5.8±1	<0.001
Weight of spleen, g	127.8±67.7*	204.3±81.6	<0.001
Spleen weight coefficient (SWC)	1.6±0.9*	2.6±1.1	<0.001

Note. Here and in Table 3: * — $P<0.05$, significant differences between groups.

this parameter were found between the groups ($P<0.001$). In all cases, the disease had a favorable course and no fatal outcomes were recorded. Most patients in both groups were discharged home. In the COVID-19 group, 6 (13.3%) patients required further treatment and were transferred to other hospitals.

Discussion

Hematologic parameters such as leukocyte count, segmented neutrophils, and ESR generally reflect the performance of the immune system in response to infection. In coronavirus infection caused by SARS-CoV-2 virus, leukopenia and elevated ESR are most prominent [18, 19]. Lymphopenia, elevated ferritin, fibrinogen, D-dimer, and troponin levels detected during hospitalization are considered predictors of mortality [18, 20, 21].

Integral markers can provide a more detailed assessment of immunologic changes and serve as predictors of disease progression [22, 23]. The LI reflects the balance between the cellular and humoral components of the immune system [24]. In the acute phase, LI decreased in both groups, indicating immunosuppression. This parameter changed differently in the two groups. While in patients with acute respiratory infections it returned to normal, i. e., an active inflammatory response occurred, in patients with COVID-19 the LI decreased only slightly, indicating further suppression of the immune system.

Lymphopenia and elevated NLR can predict a severe course of viral infection [18, 20, 24]. Both patients with COVID-19 and patients with ARVI had an increase in NLR in the acute phase, but its further changes differed between the two groups. While it decreased and then returned to normal in patients with acute respiratory viral infection, NLR grew further in COVID-19, indicating a persistent immune imbalance, as evidenced by low phagocytic activity and the dominance of specific immunological defense system.

Ultrasound revealed that the reduced spleen size is a pathognomonic sign of coronavirus infection caused by SARS-CoV-2 virus, which is consistent with previous research [25]. Pathologic and histologic studies have shown that coronavirus infection reduces the volume and cellular structure of the spleen and causes white pulp atrophy, resulting in an abnormal red/white pulp ratio [26, 27]. The number of lymphoid follicles is also significantly reduced or absent, although neutrophil infiltration or scattered plasma cells are occasionally seen. In some cases, macrophage proliferation and hemophagocytosis are observed. Lymphocyte necrosis and apoptosis, arteriolar thrombosis, and splenic

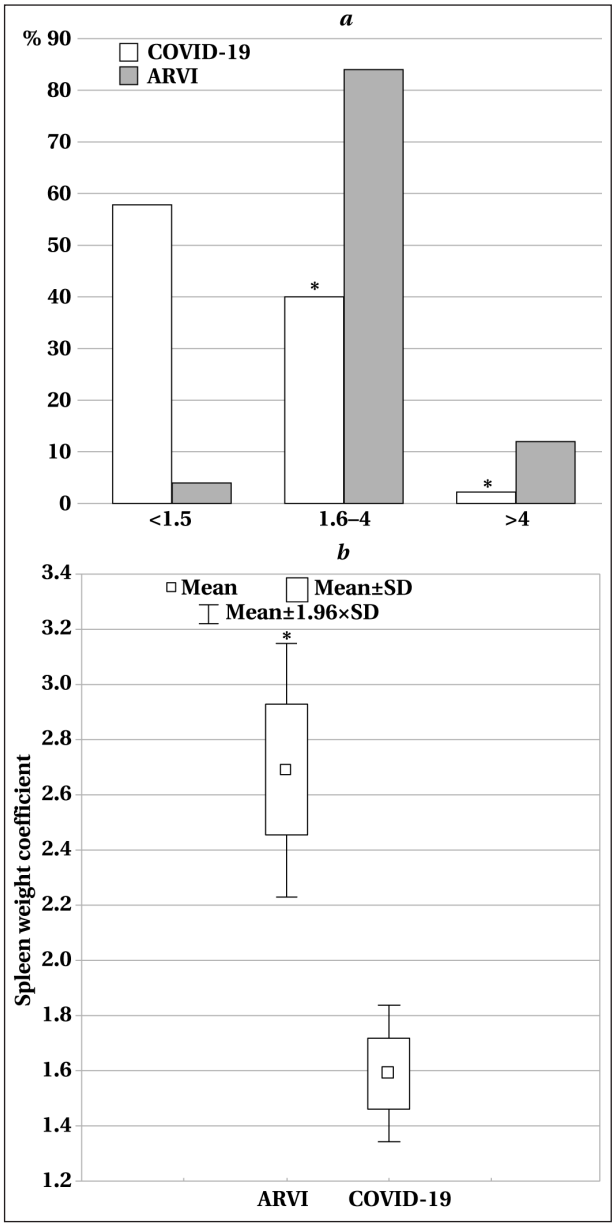

Fig. 4. Scatter diagram of the mean spleen weight coefficient *(a)* and ranking of patients according to its values *(b)*.

Table 3. Severity of respiratory failure and outcomes in patients with COVID-19 and ARVI.

Parameter, *N* (%)	Values in groups		*P* value
	COVID-19, *N*=45	ARVI, *N*=25	
ARF 0	17 (37.7)*	25 (100)	<0.001
ARF I	24 (53.3)*	0 (0)	<0.001
ARF II–III	5 (11.1)	0 (0)	0.085
Total ARF	29 (64.4)*	0 (0)	<0.001
Discharged	39 (86.7)	25 (100)	0.06
Transferred to other hospital	6 (13.3)	0 (0)	0.06

infarction are all characteristic. Immunohistochemical study [22] showed that the T and B lymphocyte counts decrease to varying degrees, and CD20 (+) B cells accumulate in the lymphoid tissue surrounding the splenic artery. The number of CD3(+), CD4(+) and CD8(+) T lymphocytes decreases, while the number of CD68(+) cells increases. J. Guet al. presented the results of a histological study of tissues from patients with ARDS caused by SARS-CoV-2 virus. In all cases, the virus was found in circulating lymphocytes and lymphoid organs, with atrophy of the spleen and lymph nodes [28]. Post-mortem, high viral loads were found in the lungs, followed by the liver and spleen, resulting in a significant reduction of the latter.

The SARS-CoV-2 virus targets several organs, including the spleen. Direct effect of the virus on all the structures of spleen causes active changes with a significant decrease in the lymphocyte population and the development of an acute immunodeficiency. Immunosuppression in the early stages can result in hyperacute disease [26, 28, 29]. In this regard, there is a need for early evaluation of splenic morphometric parameters using various radiologic techniques. A. Batur et al. demonstrated by computed tomography that in addition to lung damage, the spleen is also involved in the pathologic response. During the disease, it undergoes structural changes and shrinks, but the extent of this transformation is not related to the severity of lung damage. The spleen shrinks the most during the first two weeks of coronavirus infection [30], while the Hounsfield number (densitometric index) remains stable, indicating heterogeneous changes in the organ parenchyma. The observed changes could be attributed to the resulting cellular imbalance, proliferation, and response to hypoxia and necrosis [31]. L. Xie et al. using ultrasound imaging found that COVID-19 reduced the linear dimensions of the spleen. Patients with coronavirus infection had a mean spleen length of 89.57±11.49 mm, while healthy controls had a mean spleen length of 103.82±11.29 mm. This difference was significant ($P<0.001$). The study and control groups had a mean spleen thickness of 29.97±4.04 mm and 32.45±4.49 mm, respectively ($P<0.001$), indicating that the disease resulted in a reduced spleen size. Microsplenia is associated with a reduction in the T lymphocyte count [25].

In the acute period of COVID-19 against the background of systemic coagulation disorder, thrombosis of splenic arteries and veins may develop, leading to total ischemia of spleen [32]. The ultrasonographic morphology of splenic infarcts is highly variable. They can be both classic, wedge-shaped, or rounded, or irregularly shaped. In the recovery phase, new infarcts do not occur, but fibrosis and scarring appear in place of the existing ones, and the size of the organ remains reduced, which is manifested by changes in the ultrasound image of the spleen [33]. The formation of cysts is possible [34].

COVID-19, unlike ARVI, is characterized by a high frequency of bilateral interstitial pneumonia and acute respiratory failure, which is associated not only with direct viral damage to respiratory structures, but also with the development of immune distress as an early manifestation of multiple organ failure.

Study limitations. A representative sample was not pre-calculated during the planning of the study.

Conclusion

COVID-19 infection is characterized by significant immunological disturbances. This phenomenon is associated with a rapid «depletion» of the spleen as a secondary immune organ and a high risk of acute immune failure. One of the specific signs of the disease is microsplenia, which is diagnosed by ultrasound.

References

1. *Garibaldi B. T., Fiksel J., Muschelli J., Robinson M. L., Rouhizadeh M., Perin J., Schumock G., et al.* Patient trajectories among persons hospitalized for COVID-19: a cohort study. *Ann Intern Med.* 2021; 174 (1): 33–41. DOI: 10.7326/M20-3905. PMID: 32960645.
2. *Ramasamy S., Subbian S.* Critical determinants of cytokine storm and type I interferon response in COVID-19 pathogenesis. *Clin Microbiol Rev.* 2021; 34 (3): e00299–20. DOI: 10.1128/CMR.00299-20. PMID: 33980688.
3. *Caricchio R., Gallucci M., Dass C., Zhang X., Gallucci S., Fleece D., Bromberg M., Criner G. J.* Preliminary predictive criteria for COVID-19 cytokine storm. *Ann Rheum Dis.* 2021; 80 (1): 88–95. DOI: 10.1136/annrheumdis-2020-218323. PMID: 32978237.
4. *Fan E., Beitler J. R., Brochard L., Calfee CS., Ferguson N. D., Slutsky A. S., Brodie D.* COVID-19-associated acute respiratory distress syndrome: is a different approach to management warranted? *Lancet Respir Med.* 2020; 8 (8): 816–821. DOI: 10.1016/S2213-2600 (20)30304–0. PMID: 32645311.
5. *Chen Y., Klein S. L., Garibaldi B. T., Li H., Wu C., Osevala N. M., Li T., et al.* Aging in COVID-19: Vulnerability, immunity and intervention. *Ageing Res Rev.* 2021; 65: 101205. DOI: 10.1016/j.arr.2020.101205. PMID: 33137510.
6. *Lagunas-Rangel F. A., Chavez-Valencia V.* High IL-6/IFN-gamma ratio could be associated with severe disease in COVID-19 patients. *J. Med. Virol.* 2020; 92 (10): 1789–1790. DOI: 10.1002/jmv.25900. PMID: 32297995.
7. *Remmelink M., De Mendonça R., D'Haene N., De Clercq S., Verocq C., Lebrun L., Lavis P., et al.* Unspecific post-mortem findings despite multiorgan viral spread in COVID-19 patients. *Crit Care.* 2020; 24: 495. DOI: 10.1186/s13054-020-03218-5. PMID: 32787909.
8. *Wölfel R., Corman V. M., Guggemos W., Seilmaier M., Zange S., Müller M. A., Niemeyer D., et al.* Virological assessment of hospitalized patients with COVID-2019. *Nature.* 2020; 581: 465–469. DOI: 10.1038/s41586-020-2196-x. PMID: 32235945.
9. *Sette A., Crotty S.* Adaptive immunity to SARS-CoV-2 and COVID-19. *Cell.* 2021; 184 (4): 861–880. DOI: 10.1016/j.cell.2021.01.007. PMID: 33497610.
10. *Волчегорский И. А., Цейликман В. Э., Цейликман О. Б., Бубнов Н. В., Синицкий А. И.* Влияние триамцинолона ацетонида на распределение лейкоцитов в системе крови, мононуклеарную инфильтрацию печени и иммунореактивность при стрессовой сенсибилизации к гипоксии у крыс. *Экспериментальная и клиническая фармакология.* 2005; 68 (1): 61–66. [*Volchegorskiy I. A., Tseilikman V. E., Tseilikman O. B., Bubnov N. V., Sinickiy A. I.* Effect of triamcinolone acetonide on leukocyte distribution in the blood system, hepatic mononuclear infiltration and immunoreactivity during stress sensitization to hypoxia in rats. *Experimental and Clinical Pharmacology/Eksperimentalnaya i Klinicheskaya Farmakologiya.* 2005; 68 (1): 61–66. (In Russ.)]. DOI: 10.30906/0869-2092-2005-68-1-61-66.
11. *Zhang W., Zhao Y., Zhang F., Wang Q., Li T., Liu Z., Wang J., et al.* The use of anti-inflammatory drugs in the treatment of people with severe coronavirus disease 2019 (COVID-19): the experience of clinical immunologists from China. *Clin Immunol.* 2020; 214: 108393. DOI: 10.1016/J.CLIM.2020. 108393. PMID: 32222466.
12. *Xu Z., Shi L., Wang Y., Zhang J., Huang L., Zhang C., Liu S., et al.* Pathological findings of COVID-19 associated with acute respiratory distress syndrome. *Lancet Respir Med.* 2020; 8 (4): 420–422. DOI: 10.1016/S2213-2600 (20)30076-X. PMID: 32085846.
13. *Yao X., Li T., He Z., Ping Y., Liu H., Yu S., Mou H., et al.* A pathological report of three COVID-19 cases. *Zhonghua Bing Li Xue Za Zhi.* 2020; 49 (5): 411–417. DOI: 10.3760/cma.j. cn112151-20200312-00193. PMID: 32172546.
14. *Коваленко Л. А., Суходолова Г. Н.* Интегральные гематологические индексы и иммунологические показатели при острых отравлениях у детей. *Obshchaya Reanimatologiya = General Reanimatology.* 2013; 9 (5): 24–28. [*Kovalenko L. A., Sukhodolova G. N.* Integral Hematological indices and immunological parameters in acute poisoning in children. *General Reanimatology/Obshchaya Reanimatologya.* 2013; 9 (5): 24–28. (In Russ. and Eng.)]. DOI: 10.15360/1813-9779-2013-5-24.
15. *Carpio-Orantes L. D., García-Méndez S., Hernández-Hernández S. N.* Neutrophil-to-lymphocyte ratio, platelet-to-lymphocyte ratio and systemic immune-inflammation index in patients with COVID-19-associated pneumonia. *Gac Med Mex.* 2020; 156 (6): 527–531. DOI: 10.24875/GMM.M21000480. PMID: 33877106.
16. *Возгомент О. В.,* Пыков М. И., Зайцева Н. В. Новые подходы к ультразвуковой оценке размеров селезенки у детей. *Ультразв. и функц. диагностика.* 2013; 6: 56–62. [*Vozgoment O. V., Pykov M. I., Zaitseva N. V.* Ultrasound assessment of spleen size in children. New approaches. *Ultrasound and Functional Diagnostics/Ultrazvukovaya i Funkcionalnaya Diagnostika.* 2013; 6: 56–62. (In Russ.)]. eLIBRARY ID: 21482839.
17. *Перепелица С. А., Перминова Л. А., Степанян И. А., Захар Е. В.* Морфометрическая харак-

теристика селезенки при инфекционном мононуклеозе (ультразвуковое исследование). *Инфекция и иммунитет*. 2021; 11 (3): 556–564. [*Perepelitsa S. A., Perminova L. A., Stepanyan I. A., Zakhar E. V.* Splenic morphometric characteristics in infectious mononucleosis (ultrasonic study). *Russian Journal of Infection and Immunity/Infektsiya I Immunitet*. 2021; 11 (3): 556–564. (In Russ.)]. DOI: 10.15789/2220-7619-MCO-1481.

18. *Bohn M. K., Lippi G., Horvath A., Sethi S., Koch D., Ferrari M., Wang C-B., et al.* Molecular, serological, and biochemical diagnosis and monitoring of COVID-19: IFCC taskforce evaluation of the latest evidence. *Clin Chem Lab Med*. 2020; 58 (7): 1037–1052. DOI: 10.1515/cclm-2020-0722. PMID: 32459192.
19. *Xie J., Wang Q., Xu Y., Zhang T., Chen L., Zuo X., Liu J., et al.* Clinical characteristics, laboratory abnormalities and CT findings of COVID-19 patients and risk factors of severe disease: a systematic review and meta-analysis. *Ann Palliat Med*. 2021; 10 (2): 1928–1949. DOI: 10.21037/apm-20-1863. PMID: 33548996.
20. *Onur S. T., Altýn S., Sokucu S. N., Fikri B. Ý., Barça T., Bolat E., Toptaş M.* Could ferritin level be an indicator of COVID-19 disease mortality? *J Med Virol*. 2021; 93 (3): 1672–1677. DOI: 10.1002/jmv.26543. PMID: 32965712.
21. *Бычинин М. В., Клыпа Т. В., Мандель И. А., Коршунов Д. И., Колышкина Н. А., Джелиев Р. А.* Сравнительная клинико-лабораторная характеристика пациентов реанимационного профиля первой и второй волн пандемии COVID-19. *Анестезиология и реаниматология*. 2022; (4): 5765. [*Bychinin M. V., Klypa T. V., Mandel I. A., Korshunov D. I., Kolyshkina N. A., Dzheliev R. A.* Clinical and laboratory characteristics of intensive care patients of the first and second waves of the COVID-19 pandemic. *Russian Journal of Anaesthesiology and Reanimatology/Anesteziologiya i Reanimatologiya*. 2022; (4): 5765. (In Russ.)]. DOI: 10.17116/ anaesthesiology202204157.
22. *Carpio-Orantes L. D., García-Méndez S., Hernández-Hernández S. N.* Neutrophil-to-lymphocyte ratio, platelet-to-lymphocyte ratio and systemic immune-inflammation index in patients with COVID-19-associated pneumonia. *Gac Med Mex*. 2020; 156 (6): 527–531. DOI: 10.24875/GMM.M21000480. PMID: 33877106.
23. *Хаджиева М. Б., Грачева А. С., Ершов А. В., Чурсинова Ю. В., Степанов В. А., Авдейкина Л. С., Гребенчиков О. А., Бабкина А. С., Шабанов А. К., Тутельян А. В., Петриков С. С., Кузовлев А. Н.* Биомаркеры повреждения структур аэрогематического барьера при COVID-19. *Obshchaya Reanimatologiya = General Reanimatology*. 2021; 17 (3): 16–31. [*Khadzhieva M. B., Gracheva A. S., Ershov A. V., Chursinova Y. V., Stepanov V. A., Avdeikina L. S., Grebenchikov O. A., Babkina A. S., Shabanov A. K., Tutelyan A. V., Petrikov S. S., Kuzovlev A. N.* Biomarkers of air-blood barrier damage in COVID-19. *General Reanimatology/Obshchaya Reanimatologya*. 2021; 17 (3): 16–31. (In Russ. and Eng.)]. DOI: 10.15360/1813-9779-2021-3-2-0.
24. *Зайченко А. В., Мищенко О. Я., Шарифов Х. Ш., Кошевая Е. Ю., Халеева Е. Л.* Влияние экстракта из листьев персика обыкновенного на состояние иммунологической реактивности крыс при хроническом иммобилизационном стрессе. *Вестник фармации*. 2019; 85 (3): 102–108. [*Zajchenko A. V., Mishchenko O. Ya., Sharifov H. Sh., Koshevaya E. Yu., Haleeva E. L.* Effect of ordinary peach leaves extract on the immunological reactivity of rats under chronic immobilization stress. *Bulletin of Pharmacy/Vestnik Farmacii*. 2019; 85 (3): 102–108. (In Russ.)].
25. *Xie L., Lin Y., Deng Y., Lei B.* The effect of SARS-CoV-2 on the spleen and T lymphocytes. *Viral Immunol*. 2021; 34 (6): 416–420. DOI: 10.1089/vim.2020.0320. PMID: 33902347.
26. *Xu X., Chang X. N.,. Pan H. X., Su H., Huang B., Yang M., Luo D. J., et al.* Pathological changes of the spleen in ten patients with coronavirus disease 2019 (COVID-19) by postmortem needle autopsy. *Zhonghua Bing Li Xue Za Zhi*. 2020; 49 (96): 576–582. DOI: 10.3760/cma.j.cn112151-20200401-00278. PMID: 32340089.
27. *Brook O. R., Piper K. G., Mercado N. B., Gebre M. S., Barouch D. H., Busman-Sahay K., Starke C. E., et al.* Feasibility and safety of ultrasound-guided minimally invasive autopsy in COVID-19 patients. *Abdom Radiol (NY)*. 2021; 46 (93): 1263–1271. DOI: 10.1007/s00261-020-02753-7. PMID: 32939636.
28. *Gu J., Gong E., Zhang B., Zheng J., Gao Z., Zhong Y., Zou W., et al.* Multiple organ infection and the pathogenesis of SARS. *J Exp Med*. 2005; 202 (3): 415–424. DOI: 10.1084/jem.20050828. PMID: 16043521.
29. *Матюшков Н. С., Тюрин И. Н., Авдейкин С. Н., Бояркова А. В., Казаков Д. Н., Костин Д. М., Средняков А. В., с соавт.* Респираторная поддержка у пациентов с COVID-19. Опыт инфекционного госпиталя в Коммунарке: одноцентровое ретроспективное исследование. *Вестник интенсивной терапии им. А. И. Салтанова*. 2021; 3: 47–60. [*Matiushkov N. S., Tyurin I. N., Avdeikin S. N., Boyarkov A. V., Kazakov D. N., Kostin D. M., Srednyakov A. V., et al.* Respiratory support in COVID-19 patients in Kommunarka hospital: a single-centered, retrospective study. *Ann Crit Care/Vestnik Intensivnoy Terapii im AI Saltanova*. 2021; 3: 47–60. (In Russ.)]. DOI: 10.21320/1818-474X-2021-3-47-60.

30. *Batur A., Kýlýnçer A., Ateş F., Demir N. A., Ergün R.* Evaluation of systemic involvement of Coronavirus disease 2019 through spleen; size and texture analysis. *Turk J Med Sci.* 2021; 51 (3): 972–980. DOI: 10.3906/sag-2009-270. PMID: 33421971.
31. *Ganeshan B., Goh V., Mandeville H. C., Ng Q. S., Hoskin P. J., Miles K. A.* CT of non-small cell lung cancer: histopathological correlates for texture parameters. *Radiology*. 2013; 266: 326–336. DOI: 10.1148/radiol.12112428. PMID: 23169792.
32. *Vidali S., Morosetti D., Granai A. V., Legramante J. M., Buonomo O. C., Argirò R.* Splenoportal-mesenteric axis thrombosis and splenic artery occlusion as initial presentations of COVID-19 disease. *Eur Rev Med Pharmacol Sci.* 2021; 25 (3): 1680–1683. DOI: 10.26355/eurrev_202102_24879. PMID: 33629338.
33. *Boraschi P., Giugliano L., Mercogliano G., Donati F., Romano S., Neri E.* Abdominal and gastrointestinal manifestations in COVID-19 patients: is imaging useful? *World J Gastroenterol.* 2021; 27 (26): 4143–4159. DOI: 10.3748/wjg.v27.i26.4143. PMID: 34326615.
34. *Balcar I., Seltzer S. E., Davis S., Geller S.* CT patterns of splenic infarction: a clinical and experimental study. *Radiology*. 1984; 151 (3): 723–729. DOI: 10.1148/radiology.151.3. 671873. PMID: 6718733.

Received 14.05.2023
Accepted 28.11.2023

https://doi.org/10.15360/1813-9779-2024-1-24-30

Preemptive Analgesia with Nonsteroidal Anti-Inflammatory Drugs in the Perioperative Period

Mark S. Danilov[1,2]*, Ionas S. Simutis[1,2], Daria S. Salygina[1], Evgeny G. Polovtsev[1], Alexey A. Syrovatsky[1], Vyacheslav A. Ratnikov[1,3], Alexander A. Bogatikov[1], Alexey E. Karelov[2]

[1] Sokolov Northwestern District Research and Clinical Center, Federal Medico-Biological Agency of Russia, 4 Ave. Culture, 194291 Saint Petersburg, Russia
[2] I. I. Mechnikov North-West State Medical University, Ministry of Health of Russia 41 Kirochnaya Str., 191015 Str. Petersburg, Russia
[3] Scientific, Clinical and Educational Center for Radiation Diagnostics and Nuclear Medicine, Faculty of Medicine, St. Petersburg State University, 7–9 Universitetskaya nab., 199034 Saint Petersburg, Russia

For citation: *Mark S. Danilov, Ionas S. Simutis, Daria S. Salygina, Evgeny G. Polovtsev, Alexey A. Syrovatsky, Vyacheslav A. Ratnikov, Alexander A. Bogatikov, Alexey E. Karelov*. Preemptive Analgesia with Nonsteroidal Anti-Inflammatory Drugs in the Perioperative Period. *Obshchaya Reanimatologiya = General Reanimatology*. 2024; 20 (1): 24–30. https://doi.org/10.15360/ 1813-9779-2024-1-24-30 [In Russ. and Engl.]

***Correspondence to:** Mark S. Danilov, markdani@yandex.ru

Summary

Objective. A comparative assessment of the efficacy and safety of the preemptive use of ibuprofen and ketoprofen in patients undergoing elective surgery under general anesthesia.

Material and methods. A multicenter randomized prospective study included 58 patients grouped into 2 arms. Ibuprofen 800 mg in Group 1 (*N*=32), and ketoprofen 100 mg in Group 2 (*N*=26) were administered intravenously 30 minutes prior to surgical procedure, and afterwards every 12 hours during patient's stay in the intensive care unit. Efficacy and safety were assessed using a visual analog scale (VAS), patient's need in opioid analgesics, laboratory parameters (serum levels of cortisol, cystatin C, CBC, coagulogram, TEG) and instrumental methods (algesimetry — qNOX).

Results. VAS values were 32.4% lower in Group 1 vs Group 2 in the immediate postoperative period, *P*=0.003. By the end of Day 1 this difference was no longer visible following the use of promedol. There was a correlation between qNOX values at the end of surgery and VAS values at patient's waking up from anesthesia (*P*=0.0007). Cortisol plasma concentrations in groups 1 and 2 did not differ significantly, *P*=0.105. The average daily promedol consumption in Groups 1 and 2 was 42±17.5 mg/day and 50±19.7 mg/day, respectively, *P*=0.022. Cystatin C concentrations in the first morning after surgery was 0.95±0.29 mg/l in the ibuprofen group, and 1.19±0.43 mg/l — in the ketoprofen group, *P*=0.027. Signs of renal dysfunction were documented in 4 out of 32 patients (12, 5%) from Group 1, and in 10 of 26 (38.5%) patients from Group 2 since the end of surgery and up to the first postop morning, the Chi-squared value was 0.031. Hemostasis was not affected by NSAIDs use in both groups.

Conclusion. Ibuprofen provided more powerful analgesia, than ketoprofen in the postoperative period, while during surgical procedure both drugs showed similar anlgesic efficacy. Patients on ibuprofen required significantly fewer additional boluses of opioid analgesics. Both drugs showed no clinically significant effect on hemostasis and hematopoiesis. More rare occurrence of renal dysfunction in Group 1 patients is indicative of lower nephrotoxicity of ibuprofen.

Keywords: preemptive analgesia; anesthesia; nonsteroidal anti-inflammatory drugs; NSAIDs; ibuprofen; ketoprofen; perioperative period; automated monitoring of sedation; ICU

Conflict of interest. The authors declare no conflict of interest.

Introduction

Surgical intervention is a source of more or less persistent pain syndrome, and its control is one of the main tasks of the anesthesiologist. According to various data, more than 80% of patients suffer from post-operative pain, regardless of the type of surgery, and less than 50% consider the pain relief to be adequate [1–6]. This is a priority issue, as pain significantly affects patients' quality of life, activities of daily living, psychosocial functioning [6–11], and increases the need for medical care [12], including in the context of health insurance [13].

Importantly, despite similarities in the causes of pain, each patient experiences pain differently and therefore requires a personalized approach to pain management [14]. Pain assessment systems such as the CONOX method (using qNOX as a modifiable index of anesthesia) can be used to personalize pain management. However, the method is applicable intraoperatively under general anesthesia and it remains unclear how such personalization will affect analgesia in the postoperative period.

The concept of multimodal analgesia, including the use of non-steroidal anti-inflammatory drugs

(NSAIDs), opioids, local anesthetics and, in some cases, adjuvants such as gabapentin, is the cornerstone of quality analgesia [15]. The prophylactic administration of analgesics, mainly NSAIDs, in the preoperative period plays an important role in this approach [16–19]. However, intensive use of analgesics, including in the immediate postoperative period, is considered necessary for good-quality pain relief [20]. This approach has been shown to reduce postoperative pain intensity and the need for additional opioid analgesia [12, 21–26]. On the other hand, there are still questions about the safety of NSAIDs as part of pain management. It is well known that their use is limited by their safety profile due to possible renal damage, impaired blood coagulation, etc. [27–29]. Meanwhile, a Cochrane 2021 meta-analysis [21] suggests that the results of the perioperative use of NSAIDs are mixed and further research is needed. Finally, the paucity of publications on preemptive analgesia with intravenous ibuprofen is an important point.

We believe that our work will contribute to the development of preemptive analgesia strategies as a basis for multimodal analgesia in the perioperative period.

The aim of the study was to compare the efficacy and safety of the preemptive use of ibuprofen and ketoprofen in elective surgery under general anesthesia.

Materials and Methods

A multicenter randomized prospective study was conducted on the basis of the L. G. Sokolov North-Western District Scientific and Clinical Center and the I. I. Mechnikov North-West State Medical University in 2023, after approval by the local ethics committee (Protocol No. 4 of the meeting of the Local Ethics Committee of the L. G. Sokolov North-Western District Scientific and Clinical Center, dated March 27, 2023).

Patients were selected for inclusion in the study according to the criteria listed in Table 1. There was no preliminary calculation of the sample size and no blinding of the study participants; randomization was performed using the envelope method.

A total of 58 patients undergoing surgery for diseases of the thoracic (thoracoscopic) and urinary organs were studied; the mean age was 59.6±17.6 years (Tables 2, 3).

The patients were divided into 2 groups. In group 1 (*N*=32), patients received ibuprofen 800 mg as an intravenous drip 30 min before surgery and then every 12 h in the intensive care unit (ICU). Patients in group 2 (*N*=26) received ketoprofen 100 mg as an intravenous drip at the same time.

The study groups were comparable in terms of patient characteristics (Table 2). Three patients supposed to be included in group 2 were excluded due to the exclusion criteria (Table 1), resulting in different group sizes despite randomization.

The mean duration of surgery was 194.3±37.6 minutes. Average doses of drugs used for induction of anesthesia were 1.9±0.6 mg/kg propofol, 151.1±50.6 μg fentanyl; for maintenance of anesthesia were 1–3 vol% sevoflurane, 2–3 μg/kg/h fentanyl, 101.2±33.7 mg rocuronium bromide.

Table 1. Patient selection criteria for the study.

Inclusion criteria	1. Signed consent form 2. Males and females at least 18 years of age 3. Elective thoracic/urologic surgery
Non-inclusion criteria	1. Hypersensitivity to NSAIDs 2. Bronchial asthma 3. Erosive and ulcerative diseases of gastrointestinal tract 4. Liver failure 10–15 points on the Child-Pugh scale 5. Severe renal failure (creatinine clearance <50 mL/min) 6. Decompensated heart failure 7. Cerebrovascular or other hemorrhage (including intracranial hemorrhage) 8. Hemophilia and other blood coagulation disorders (including hypocoagulation) 9. Pregnancy or lactation 10. Children under 18 years of age
Postrandomization exclusion criteria	1. Withdrawal of informed consent 2. Refusal to follow up as per study protocol

Table 2. Patient characteristics.

Parameters	Values in groups		*P* value
	Ibuprofen	Ketoprofen	
Number	32	26	
Male, %	66.7	62.5	0.73
Age, years, median [min; max]	57 [38; 70]	61 [40; 73]	0.89
CHF (NYHA), median [min; max]	3 [1; 5]	3 [1; 5]	0.89
Rhythm disturbances, %	32.4	20.0	0.82
Type 2 diabetes mellitus, %	44.4	42.7	0.70
COPD, %	14.8	20.0	0.87
Body mass index >30, %	44.4	40.0	0.74

Note. CHF — chronic heart failure; COPD — chronic obstructive pulmonary disease

Patients underwent the same type of anesthesia: induction of anesthesia was performed with propofol and fentanyl, sevoflurane and microjet injection of fentanyl were used to maintain anesthesia, depending on the stage of surgery. Relaxation was maintained with rocuronium bromide using TOF monitoring.

Harvard standard monitoring was used during surgery. In addition, the CONOX Fresenius Kabi (Germany) monitor, which evaluates the level of anesthesia and depth of hypnosis during general anesthesia, was used to assess the nociceptive response based on changes in the qNOX index. Simultaneous monitoring of qCON and qNOX indices allows clinical assessment of the level of anesthesia and measurement of the analgesic component as a predictor of response to various stimuli, which enables reduction of risks associated with anesthesia and optimization of hypnotic and analgesic doses. The latter value was recorded at the end of surgery. Otherwise, intensive postoperative therapy did not differ between the groups.

Table 3. Types of operations performed.

Type of surgery	Groups, *N* (%)	
	Ibuprofen	Ketoprofen
Upper lobectomy	7 (21.9)	8 (30.8)
Middle lobectomy	3 (9.4)	1 (3.8)
Lower lobectomy	6 (18.8)	2 (7.7)
Thymectomy	3 (9.4)	2 (7.7)
Bullae resection, pleurectomy	8 (25.0)	11 (42.3)
Kidney resection	5 (15.6)	2 (7.7)
Total	32 (100)	26 (100)

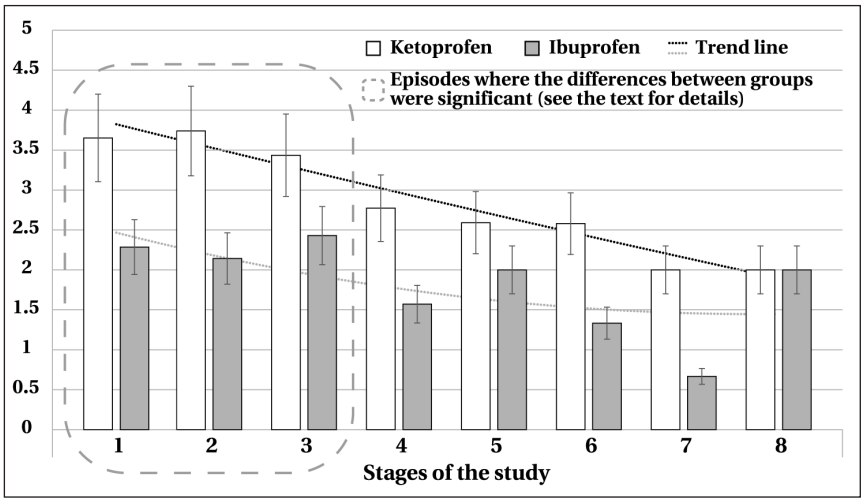

Fig. 1. Pain severity assessed using VAS in the post-op period.
Note. Horizontal axis shows 3-hour episodes of the postoperative period, vertical axis shows VAS score (cm) as mean value and standard deviation.

The postoperative period was divided into 8 stages. Efficacy and safety of analgesia were assessed by VAS every 3 hours from the moment of admission of the patient to the intensive care unit, as well as by the need for opioid analgesics and laboratory criteria (cortisol, cystatin C, CBC with reticulocytes, thromboelastogram). Opioid analgesics (boluses of Promedol (trimeperidine), Moscow Endocrine Factory, Russia) were administered when the VAS score was > 4 with routine analgesic therapy.

Statistical analysis was performed using Jamovi software (version 2.3.18). The 95% confidence interval (CI) and two-tailed significance level of $P<0.05$ were selected. The Shapiro–Wilk test was chosen to test the normality of the distribution. Pearson's *t*-test and correlation coefficient and nonparametric chi-square test without continuity correction were used to compare the data obtained. For all comparisons described below, except for the VAS score, the Shapiro–Wilk test for normality yielded a value of $P>0.05$, indicating a normal distribution.

Results and Discussion

The first step was to evaluate the effect of preventive use of NSAIDs on the quality of pain relief during surgery. The induction of anesthesia provided a sufficient level of pain relief in both groups, but at the same time the values of the pain measuring device increased until the end of anesthesia. Thus, the qNOX index in the ibuprofen group was 37.5±7.3 at the beginning of surgery and 61.8±8.4 at the end of surgery, while in the ketoprofen group it was 40.6±4.8 and 57.2±9.0, respectively. The difference in values between the stages within each group was significant ($P<0.05$), but no significant difference was found when comparing the groups.

It can be assumed that the prophylactic use of the studied NSAIDs has a similar effect on intraoperative pain severity.

The groups were also compared in terms of postoperative pain intensity. Throughout the follow-up period, VAS scores were lower in the ibuprofen group than in the ketoprofen group.

In the first stage of the postoperative period, the VAS in the ibuprofen group was 2.93±1.53 cm and in the ketoprofen group 4±2.30 cm, $P=0.04$; in the second stage, 2.25±0.86 cm (ibuprofen) and 3.67±1.79 cm (ketoprofen), $P=0.036$; in the third stage, 2.31±1.08 cm and 3.38±1.86 cm, $P=0.044$ (chi-squared test), i.e., the maximum difference was observed in the first hours and averaged 32.4% (Fig. 1). After 9 hours post-surgery, the VAS difference between the groups decreased significantly, with no differences observed only at the end of the first day after surgery.

Correlation analysis was performed to determine the relationship between the VAS score after

the patient awakening and the qNOX score at the end of surgery. The Pearson correlation coefficient was 0.43 (P=0.0007), indicating that the patient's perception of pain in the postoperative period corresponded to the instrumental assessment intraoperatively (Fig. 2).

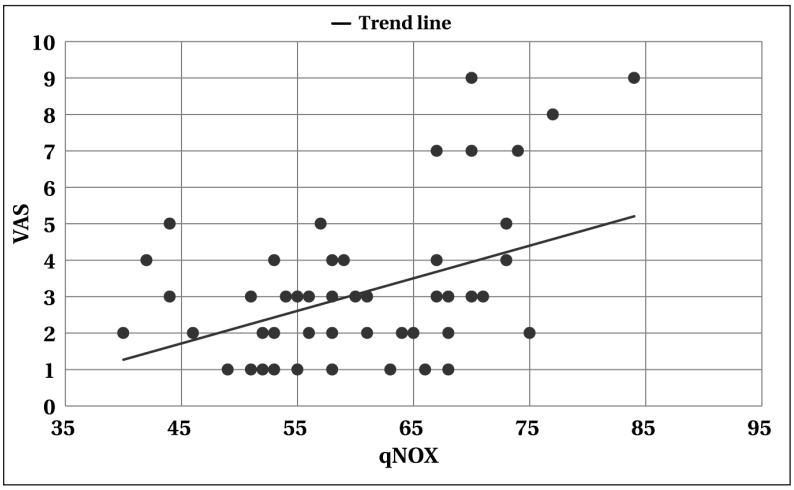

Fig. 2. Pearson's correlation of VAS values after patient awakening and qNOX at the end of surgery.

Ibuprofen and ketoprofen had similar intraoperative analgesic effect, but on admission to the ICU, patients in the ibuprofen group reported a lower intensity of pain syndrome. It seems unlikely that the effect of ketoprofen stops at the moment of anesthesia termination, so the reason for the differences in pain assessment between the groups, most likely, was the individual patient's perception of pain sensation. In other words, ibuprofen probably influences not only the focus of pain, but also its conscious perception by brain.

When assessing the changes in plasma cortisol, no significant intergroup difference was observed: in group 1 its concentration at the end of observation was 571.3±336.8 nmol/L, and in group 2, 402.2±265.0 nmol/L (P=0.105), while the need for opioid analgesics occurred significantly less frequently in the ibuprofen group. Thus, in this group the need for Promedol boluses was observed in 10 out of 32 patients (31%), while in the ketoprofen group, in 17 out of 26 patients (65%). Mean daily drug consumption was assessed only among those patients who received the drug. In group 1, the mean daily requirement for Promedol was 42±17.5 mg versus 50±19.7 mg in group 2; the differences were significant (P=0.022).

The data obtained suggests that while patients' self-rated pain levels appeared to level off by the end of the first day, this was likely due to higher doses of opioid analgesics administered in the second group.

A comparative assessment of the effect of the drugs on the kidneys, based on urea and creatinine levels, showed no statistically significant differences between the groups. The level of cystatin C immediately following surgery was 0.92±0.24 mg/L in the ibuprofen group and 1.17±0.42 mg/L in the ketoprofen group, though the differences between the groups were not significant (P=0.05). However, this parameter exceeded the upper limit of the reference interval in 10 patients (31.3%) in group 1 and 5 patients (19.2%) in group 2.

The level of cystatin C the following morning was 0.95±0.29 mg/L in the ibuprofen group and 1.19±0.43 mg/L in the ketoprofen group (P=0.027). Furthermore, values exceeding the upper reference limit were observed in 14 cases (43.8%) of group 1 and 15 cases (57.8%) of group 2.

An increase in cystatin C levels above normal indicates kidney function impairment. Renal dysfunction was observed in 4 of 32 patients (12.5%) in group 1 and 10 of 26 patients (38.5%) in group 2 from postoperative day to the next morning. The chi-squared value of 0.031 confirmed significant differences between the two groups (P=0.05). The immediate increase in the renal dysfunction marker after surgery reflects the combined negative effects of surgical stress and medication. Despite similar surgical procedures in both groups, the lower incidence of renal dysfunction in the ibuprofen group suggests a safer profile for this drug compared to ketoprofen.

To evaluate blood coagulation, we compared coagulation parameters (fibrinogen, APTT, D-dimer, INR) and thromboelastographic results. We found no significant intergroup differences in both static and dynamic tests, which allows us to assume the absence of any significant effect of the studied drugs on the function of the blood coagulation system with the current regimen of their administration. We also found no effect of both NSAIDs on hematopoiesis (the reticulocyte count did not fall below the reference interval in any patient).

In general, the use of ibuprofen in the perioperative period provided better anesthesia than the use of ketoprofen. However, the authors acknowledge that the lack of a predetermined sample size is a limitation of the study.

Conclusion

Preventive administration of ibuprofen and ketoprofen resulted in a similar analgesic effect during elective surgery under general anesthesia.

We found a statistically significant reduction in the need for additional boluses of opioid analgesics in the group of patients receiving ibuprofen in the postoperative period.

Neither drug had a clinically significant effect on coagulation and hematopoiesis. However, renal dysfunction was less frequent in the ibuprofen group.

Thus, the use of ibuprofen for preemptive analgesia in the perioperative period offers several advantages for pain management.

References

1. *Taylor K. O.* Morbidity associated with axillary surgery for breast cancer. *ANZ J Surg.* 2004; 74 (5): 314–317. DOI: 10.1111/j.1445-1433.2004.02992.x. PMID: 15144248.
2. *Bradley N., Davis L., Chow E.* Symptom distress in patients attending an outpatient palliative radiotherapy clinic. *J Pain Symptom Manage.* 2005; 30 (2): 123–131. DOI: 10.1016/ j.jpainsymman.2005.02.015. PMID: 16125027.
3. *Di Maio M., Gridelli C., Gallo C., Manzione L., Brancaccio L., Barbera S., Robbiati S. F., et al.* Prevalence and management of pain in Italian patients with advanced non-small-cell lung cancer. *Br J Cancer.* 2004; 90 (12): 2288–2296. DOI: 10.1038/sj.bjc.6601810. PMID: 15162156.
4. *Hwang S. S., Chang V. T., Cogswell J., Morales M., Srinivas S., Kasimis B.* Study of unmet needs in symptomatic veterans with advanced cancer: incidence, independent predictors and unmet needs outcome model. *J Pain Symptom Manage.* 2004; 28 (5): 421–432. DOI: 10.1016/j.jpainsymman.2004. 02.023.
5. *van den Beuken-van Everdingen M. H. J., Hochstenbach L. M. J., Joosten E. A. J., Tjan-Heijnen V. C. G., Janssen D. J. A.* Update on prevalence of pain in patients with cancer: systematic review and meta-analysis. *J Pain Symptom Manage.* 2016; 51 (6): 1070–1090.e9. DOI: 10.1016/j.jpainsymman.2015.12.340. PMID: 27112310.
6. *Kroenke K., Theobald D., Wu J., Loza J. K., Carpenter J. S., Tu W.* The association of depression and pain with health-related quality of life, disability, and health care use in cancer patients. *J Pain Symptom Manage.* 2010; 40 (3): 327–341. DOI: 10.1016/j.jpainsymman.2009.12.023. PMID: 20580201.
7. *Porter L. S., Keeffe F. J.* Psychosocial issues in cancer pain. *Curr Pain Headache Rep.* 2011; 15 (4): 263–270. DOI: 10.1007/s11916-011-0190-6. PMID: 21400251.
8. *Rief W., Bardwell W. A., Dimsdale J. E., Natarajan L., Flatt S. W., Pierce J. P.* Long-term course of pain in breast cancer survivors: a 4-year longitudinal study. *Breast Cancer Res Treat.* 2011; 130 (2): 579–586. DOI: 10.1007/s10549-011-1614-z. PMID: 21656272.
9. *He Q.-H., Liu Q.-L., Li Z., Li K.-Z., Xie Y.-G.* Impact of epidural analgesia on quality of life and pain in advanced cancer patients. *Pain Manag Nurs.* 2015; 16 (3): 307–313. DOI: 10.1016/j.pmn.2014.08.003. PMID: 25439118.
10. *Ovayolu N., Ovayolu Ö., Serçe S., Tuna D., Çöçelli L. P., Sevinç A.* Pain and quality of life in Turkish cancer patients. *Nurs Health Sci.* 2013; 15 (4): 437–443. DOI: 10.1111/nhs.12047. PMID: 23480371.
11. *Oliveira K. G. von Zeidler S. V., Podestá J. R., Sena A., Souza E. D., Lenzi J., Bissoli N. S., et al.* Influence of pain severity on the quality of life in patients with head and neck cancer before antineoplastic therapy. *BMC Cancer.* 2014; 14: 39. DOI: 10.1186/1471-2407-14-39. PMID: 24460780
12. *Bona L. G., Geleta D., Dulla D., Deribe B., Ayalew M., Ababi G., Bogale N., et al.* Economic burden of cancer on cancer patients treated at Hawassa university comprehensive specialized hospital. *Cancer Control.* 2021; 28: 107327482110092. DOI: 10.1177/10732748211009252. PMID: 33858225.
13. Хронический болевой синдром (ХБС) у взрослых пациентов, нуждающихся в паллиативной медицинской помощи. Клнические рекомендации. 2016. [Chronic pain syndrome (CPS) in adult patients in need of palliative care. Clinical recommendations. 2016. (in Russ.)]. Hronicheskij-bolevoj-sindrom-HBS-u-vzroslyh-1.pdf (pro-palliativ.ru)
14. *Попов А. С., Экстрем А. В., Казанцев Д. А.* Персонализированная терапия послеоперационной боли: Монография. Волгоградский государственный медицинский университет. 2019. [*Popov A. S., Ekstrem A. V., Kazantsev D. A.* Personalized therapy of postoperative pain: Monograph. Volgograd State Medical University. 2019. (in Russ.)]. ISBN 978-5-9652-0554-7.
15. *Aurilio C., Pace M. C., Sansone P., Giaccari L. G., Coppolino F., Pota V., Barbarisi M.* Multimodal analgesia in neurosurgery: a narrative review. *Postgrad Med.* 2022; 134 (3): 267–276. DOI: 10.1080/00325481.2021.2015221. PMID: 34872428.
16. *Ochroch E. A., Mardini I. A., Gottschalk A.* What is the role of NSAIDs in pre-emptive analgesia? *Drugs.* 2003; 63 (24): 2709–2723. DOI: 10.2165/00003495-200363240-00002. PMID: 14664651.
17. *Silva P. U. J., Meneses-Santos D., de Andrade Vieira W., Ramacciato J., da Silva R. P., Silva M. C.P., Rode S. M., et al.* Preemptive use of intravenous ibuprofen to reduce postoperative pain after lower third molar surgery: a systematic review of randomized controlled trials. *Clinics.* 2021; 76 (1): e2780. DOI: 10.6061/clinics/2021/e2780.
18. *Кислицын А. А.* Упреждающая анальгезия в эндодонтической практике. *Устойчивое Развитие Науки И Образования.* 2019; 4: 452–455. [*Kislitsyn A. A.* Pre-emptive analgesia in endodontic practice. *Sustainable Development of Science and Education/Ustoichivoe Razvitie Nauki i Obrazovaniya.* 2019; 4: 452–455. (in Russ.)]. eLIBRARY ID: 38564758
19. *Болобошко К. Б., Ходьков Е. К., Кубраков К. М., Абдулина З. Н.* Эффективность комплексного подхода к периоперационному обеспечению эндопротезирования коленного сустава. *Новости хирургии.* 2020; 28 (1):

53–61.[*Balaboshka K. B., Khadzkou Y. K., Kubrakov K. M., Abdulin Z. N.* Efficacy of integrated approach to total knee replacement perioperative management. *Novosti Khirurgii*. 2020; 28 (1): 53–61. (in Russ.)]. DOI: 10.18484/2305-0047.2020.1.53.
20. *Burkey D. R.* Regional anesthesia and pain management. Philadelphia: Saunders/Elsevier; 2009: 403–414. ISBN13-9781416033448.
21. *Doleman B., Leonardi-Bee J., Heinink T. P., Boyd-Carson H., Carrick L., Mandalia R., Lund J. N., et al.* Pre-emptive and preventive NSAIDs for postoperative pain in adults undergoing all types of surgery. *Cochrane Database Syst Rev*. 2021; 6 (6): CD012978. DOI: 10.1002/14651858.CD012978.pub2. PMID: 34125958
22. *Helander E. M., Menard B. L., Harmon C. M., Homra B. K., Allain A. V., Bordelon G. J., Wyche M. Q., et al.* Multimodal analgesia, current concepts, and acute pain considerations. *Curr Pain Headache Rep*. 2017; 21 (1): 3. DOI: 10.1007/s11916-017-0607-y. PMID: 28132136.
23. *Ozlem S., Banu C., Saracoglu K. T.* The effect of single-dose preemptive intravenous ibuprofen on the intraoperative hemodynamic parameters, recovery characteristics, and acute pain after laparoscopic cholecystectomy: a randomized double-blind, placebo-controlled clinical trial. *International Journal of Anesthetics and Anesthesiology*. 2020; 7 (4). Open access. DOI: 10.23937/2377-4630/1410118
24. *Pýnar H. U., Karaca* Ö, *Karakoç F., Doða R.* Effects of addition of preoperative intravenous ibuprofen to pregabalin on postoperative pain in posterior lumbar interbody fusion surgery. *Pain Research and Management*. 2017. Open access. DOI: 10.1155/2017/1030491.
25. *Selçuk I., Selçuk N., Can M. F., Yilmaz A. T.* Karotis arter stenozunda cerrahi endarterektomi ile endovasküler stent implantasyonunun orta ve geç dönemde morbidite ve mortalite sonuçlarının karşılaştırılması. *Göğüs Kalp Damar Anestezi ve Yoğun Bakım Derneği Dergisi*. 2021; 27 (2): 155–160. (in Turk.). Comparison of mid-, and late-term morbidity and mortality results of surgical endarterectomy versus endovascular stent implantation in carotid artery stenosis. *Journal of Cardio-Vascular-Thoracic Anaesthesia and Intensive Care Society*. 2021; 27 (2): 155–160. DOI: 10.5222/GKDAD.2021. 63496.
26. *Садыкова Т. Т., Жалгасбаев С. К.* Упреждающее влияние внутривенной формы ибупрофена на снижение потребности в опиоидах в онкогинекологии. Личный опыт. *Инновации. Наука. Образование*. 2021; 43: 846–852. [*Sadykova T. T., Zhalgasbaev S. K.* The pre-emptive effect of intravenous ibuprofen on reducing the need for opioids in oncogynecology. Personal experience. *Innovation. Science. Education.* / *Innovatsii. Nauka. Obrazovaniye*. 2021; 43: 846–852. (in Russ.)]. eLIBRARY ID: 47235514.
27. *Drożdżal S., Lechowicz K, Szostak B., Rosik J., Kotfis K., Machoy-Mokrzyńska A., Białecka M., et al.* Kidney damage from nonsteroidal anti-inflammatory drugs — myth or truth? Review of selected literature. *Pharmacol Res Perspect*. 2021; 9 (4): e00817. DOI: 10.1002/prp2.817. PMID: 34310861.
28. NSAIDs and acute kidney injury. URL: https://www.medsafe.govt.nz/profs/PUArticles/June2013NSAIDS.htm (дата обращения/accessed: 10.07.2023).
29. *Schafer A. I.* Effects of nonsteroidal antiinflammatory drugs on platelet function and systemic hemostasis. *J Clin Pharmacol*. 1995; 35 (3): 209–219. DOI: 10.1002/j.1552-4604.1995. tb04050.x. PMID: 7608308

Received 13.07.2023
Accepted 12.01.2024

https://doi.org/10.15360/1813-9779-2024-20-X

Effect of Different Methods of Anesthesia on Surgically Created Arteriovenous Fistula

Richard Koyš[1], Beata Sániová Drobná[1]*, Eva Drobná[2]

[1] Clinic of Anesthesiology and Intensive Medicine, Jessenius Faculty of Medicine in Martin, Comenius University in Bratislava, Martin University Hospital
2 Kollarova Str., 03601 Martin, Slovak Republic
[2] Department of Informatics, Academy of the Armed Forces of General M. R. Štefánik, L. Mikuláš
393 Demanovska cesta, 03101 Liptovsky Mikulas, Slovak Republic

For citation: *Richard Koyš, Beata Sániová Drobná, Eva Drobná.* Effect of Different Methods of Anesthesia on Surgically Created Arteriovenous Fistula. *Obshchaya Reanimatologiya=General Reanimatology.* 2024; 20 (1): 31–36. https://doi.org/10.15360/1813-9779-2024-20-X [In Engl.]

***Correspondence to:** Beata Sániová Drobná, beata.saniova @uniba.sk

Summary

Aim of the study was to determine the advantages of peripheral nerve blocks (PNB) versus local infiltration anesthesia (LIA) in the formation of arteriovenous fistula (AVF) surgically created for hemodialysis treatment

Type of study: prospective non-randomized study. Approved by the ethics committee of JLF UK in Martin.

Type of workplace: clinical workplace of a university hospital.

Material and method. The cohort of patients (*N*=40) who required arteriovenous fistula (AVF) creation was divided into 2 groups, 20 patients each: patients operated under peripheral nerve blockade and patients operated under local infiltration anesthesia. The preserved function of the fistula was monitored 24 hours, 6 weeks and one year after the operation, without revision. Patient inclusion criteria included: age 19–75 years, ASA 3–4, weight 40–120 kg, BMI up to 40. Statistical treatment of data included Mann-Whitney exact test, Fisher's test, *t*-test, Shapiro–Wilk normality test.

Results. After 24 hours, all fistulas created with peripheral nerve blockade were functional whereas only 90% developed under local infiltration anesthesia remained functional ($P>0.05$ between groups). However, after 6 weeks, 80% of fistulas created under peripheral nerve block were functional, compared to 50% of functional fistulas created in patients under local infiltration anesthesia ($P=0.048$). One year after surgery, the difference remained as a trend since 55% of fistulas created under peripheral nerve block remained functional while only 35% of fistulas created in patients receiving local infiltration anesthesia were functional without complications ($P=0.097$).

Conclusion. In our study, the peripheral nerve block anestesia seem superior in term of improved survival of created fistula compared to local infiltration anesthesia.

Keywords: brachial plexus block; local infiltration anesthesia; peripheral nerve block; arteriovenous fistula

Conflict of interest. The authors declare no conflict of interest.

Introduction

Supraclavicular block of the brachial plexus is a relatively new form of anesthesia used in the surgical creation of arteriovenous fistulas (AVF) on the distal forearm [1]. These are currently the gold standard of vascular access for patients who require chronic hemodialysis treatment. In Europe, local infiltration anesthesia (LIA) is still the most common type of anesthesia for AVF formation. There are several reasons. It is simple to perform, safe, does not require the presence of an anesthesiology team, is not time-consuming and is cheap. However, early or late AVF failure is common, most often due to stenosis, poor maturation or thrombosis of the fistula. In the USA, general anesthesia (GA) is often used, but it does not have the advantages of local infiltration anesthesia and poses an increased risk in this group of patients with numerous comorbidities [2, 3]. Therefore, in recent years, peripheral nerve blocks (PNBs) that represent supraclavicular brachial plexus block with ultrasound navigation have also been promoted, which seem to have certain advantages over GA or LIA [4]. Several studies have recently been conducted that support this view. They compared LIA and PNB or LIA and GA [5, 6]. Comparison of all three types of anesthesia is rare [7]. A large multicenter randomized trial ACCess comparing PNB and LIA is currently underway in the UK. The results should be published in 2025 [8]. In our study, the LIA and PNB were compared. The study took place between January 2020 and May 2022.

The aim of the study was to determine the advantages of peripheral nerve blocks (PNB) versus local infiltration anesthesia (LIA) in the formation of arteriovenous fistula (AVF) surgically created for hemodialysis treatment.

Material and Methods

The set of patients was in ASA category 3 or 4, comorbidities were similar with respect to chronic kidney damage, comorbidities were more significant in older patients. After informed consent, the patients chose the method of anesthesia (PNB or LIA) by themselves. A total of 40 patients were included in the study. Twenty patients were operated under PNB and 20 patients received LIA.

PNB was performed as a supraclavicular block of the brachial plexus under dual navigation by ultrasound and neurostimulation. 20 mL of 0.5% levobupivacaine and 10 mL of 1% trimecaine were administered. We have chosen this PNB method because of relatively simple execution and high efficiency even with a less experienced anesthesiologist to decrease the risk of failure. A higher dose of local anesthetic was supposed to ensure a longer duration of PNB and an expected increased and long lasting effect on the sympathetic system and dilation of the vessels of the operated limb [8]. Neurostimulation was used mainly for educational reasons [9]. LIA was administered by the surgeon in a total dose of 20 mL of 1% trimecaine. Inclusion criteria for the study were age 19–75 years, ASA 3–4, weight 40–120 kg, BMI up to 40. Standard anesthesia monitoring was used for LIA and PNB and included ECG, NIBP, SpO_2 monitoring. The primary AVF was created in the area of the distal forearm above the wrist of the non-dominant hand, the skin incision was also more or less identical, the operators were three experienced vascular surgeons.

The primary monitored indicators were: AVF functionality 24 hours after the operation (pulsation of the draining vein and auscultation murmur above the fistula) and after 6 weeks after the operation (the flow and parameters of the supply and draining vessels were monitored sonographically), when the AVF was considered mature. We also monitored the functionality of the fistula one year after the operation without the need for intervention.

Another important monitored parameter was the change in diameter of a. radialis after the administration of anesthesia compared to the initial value and the change in diameter of v. cephalica after administration of anesthesia compared to the initial value. Measurement of blood vessels in the location of planned AVF creation was performed sonographically at an accuracy of 0.1 mm.

We also monitored the following parameters: 1) the time required to perform the operation and the length of anesthetic care for individual groups, 2) the occurrence of serious adverse events requiring medical intervention during the operation for individual types of anesthesia (cardiovascular, respiratory, neurological), 3) the visual analog scale (VAS) of pain value at the end of anesthesia and the highest value of VAS during the first 24 hours after the operation, and 4) the necessity of administration of analgesics during the first 24 hours after the surgery. Statistical methods used in study: Mann–Whitney exact test, Fisher's test, *t*-test, Shapiro–Wilk normality test. Even in a small cohort with a sample size of N=20, after testing for the normal distribution, the Student's *t*-test exhibited sufficient validity and reliability.

Results

No final conclusions can be drawn due to the small cohort of 40 patients in the study. There were 15 men and 5 women in the LIA group, aged from 36 to 75 years, the average age was 64.2 years. There were 16 men and 4 women in the PNB group, in a range of 28–75 years old, the average age was 57.7 years.

When comparing the effect of methods of anesthesia on the diameter a. radialis in the distal forearm of the operated limb, we found that in PNB, there was an average dilation of 0.45 mm (average +20.4%), In patients under LIA, dilation occurred by an average of 0.09 mm (an average of +4.8%). Compared to LIA, there was a statistically significant dilation of artery diameter in patients under PNB (P=0.0003, *t*-test). When comparing the change of diameter of v. basilicae in the distal forearm of the operated hand after administration of individual types of anesthesia, we found that in patients under PNB there was an average dilation of 0.93 mm (average 51.6%), whereas patients under LIA exhibited the average change in the lumen of the vein by 0.13 mm in terms of vasoconstriction (average –1%). When comparing PNB versus LIA, there was a statistically significant change in a vessel diameter in terms of dilation in PNB group compared to LIA group (P=0.000025, *t*-test).

When monitoring AVF functionality 24 hours after surgery, we found that there was no early failure of function in fistulas created in PNB and early failure in 10% of fistulas in LIA. No significant differences in AVF functionality after 24 hours were revealed between the PNB and LIA groups (P=0.487, Fisher test).

When monitoring the functionality of the AVF after 6 weeks from the operation in individual groups of anesthesia, we found that 80% of the fistulas created in the PNB were functional. For fistulas created in LIA, only 50% of fistulas were functional after 6 weeks. When comparing PNB versus LIA, a significant difference in fistula survival was found in favor of PNB (P=0.048, Fisher test).

When monitoring the functionality of the fistula without complications one year after the operation, 55% of fistulas created under PNB and 35% created under LIA were functional without complication or any intervention. There was, however, a marginal trend toward difference in fistula survival in favor of PNB (P=0.097, Fisher test).

We also compared the length of anesthesia care in the operating room for individual types of anesthesia. PNB anesthetic care was significantly longer than LIA care (P=0.017, *t*-test). Another monitored parameter was the duration of surgery for individual types of anesthesia. The duration of the operation under PNB compared to LIA differed significantly, with PNB the performance was shorter (P=0.012, *t*-test).

The incidence of adverse events and effects on methods of anesthesia was as follows: in PNB patients it was 5% and in LIA patients there were no such events. The occurrence of adverse effects during surgery between RA and LA was statistically

Table. Values of monitored parameters, valid cases *N*=20.

Parameters	95% CI	Mean	Median	Standard deviation	Quartil		Interquartile range
					Lower	Upper	
Change of diameter of a. radialis in PNB, mm	0.3–0.6	0.46	0.45	0.2542	0.3	0.6	0.3
Change of diameter of a. radialis in LIA, mm	0–0.3	0.13	0.15	0.2975	0	0.3	0.3
Change of diameter of v. cephalica in PNB, mm	0.5–1.5	1.03	1	0.882	0.5	1.65	1.15
Change of diameter v. cephalica in LIA, mm	–0.7–0.4	–0.115	0.1	0.691	–0.75	0.4	1.15
PNB — length of anesthesia care, min	130–165	148	142.5	28.81	127.5	170	42.5
LIA — length of anesthesia care, min	100–155	125.75	117.5	37.14	95	157.5	62.5
Duration of surgery in PNB patients, min	60–80	77.75	75	25.26	60	85	25
Duration of surgery in LIA patients, min	65–120	94.25	90	35.88	65	120	55
Maximal VAS 24 h after surgery in PNB patients	0–4	1.7	0.5	2.13	0	4	4
Maximal VAS 24 h after surgery in LIA patients	0–3	1.35	0.5	1.4965	0	3	3

insignificant (*P*=1, Fisher test). There were no critical incidents during the study.

We investigated further, whether there was a difference in VAS when the patients left the operating room. There was no significant difference between PNB patients and LIA patients (*P*=1, Fisher's test).

When monitoring the maximum VAS during the first 24 hours after surgery, no significant difference between PNB patients and LIA patients found (*P*=0.7, Mann–Whitney exact test). The average maximum of VAS value was 1.7 in PNB group and 1.35 in LIA group.

The last monitored parameter was the need to administer analgesics during the first 24 hours after the procedure. The need for administration of analgesics had been revealed in 40% of patients receiving PNB and in 65% of patients receiving LIA. The association between the groups during the first 24 hours after the procedure, however, was insignificant (*P*=0.63, Fisher's test). Descriptive statistical results are presented in a table.

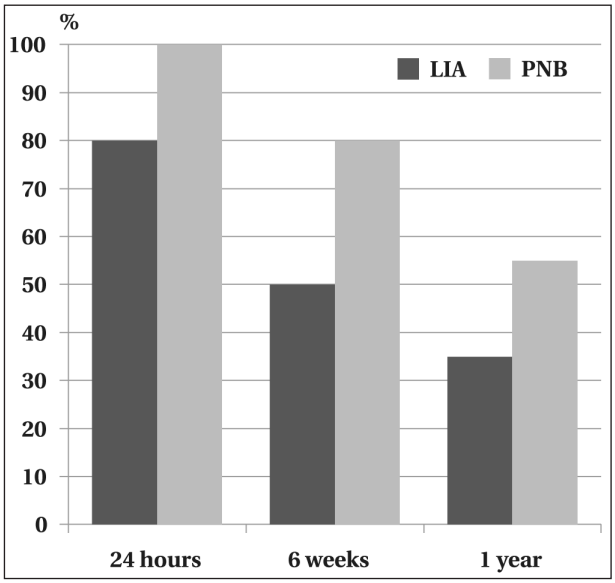

Fig. 1. Functionality of fistulas after operation.

Discussion

Our study was focused on comparing several parameters when using different types of anesthesia. The main monitored parameter was the preserved functionality of the fistula 24 hours after the operation, 6 weeks after the operation, when the fistula is already considered mature, and after 1 year. Twenty-four hours after surgery, all AVFs created under PNB were functional, and 10% of AVFs failed in LIA. Significant difference between PNB and LIA in term of AVF functionality was absent at this time point. Primary failure of AVF had been further compared depending on a method of anesthesia. Six weeks post-surgery, when AVF maturation should have occurred, 80% of AVFs formed under PNB anesthesia were functional. At the same time point, only 50% of the AVFs created in the LIA remained functional with significant differtence in fistula survival in favor of PNB. One year after the operation, 55% of fistulas created by PNB and only 35% of fistula created under LIA were functional without complications (Fig. 1). the results suggest that it might be more advantageous to use PNB because of better AVF functionality.

Another important monitored parameter was the effect of individual types of anesthesia on a lumen of *a. radialis* and *v. cephalica* in the distal forearm, i.e. at the site of creation of the primary fistula. Local anesthetic administered by infiltration at the site of surgery generally has a vasodilating effect depending on its concentration. Higher concentrations of anesthetic provided incerased vasodilating effect, whereas lower concentrations remained neutral or even slightly vasoconstrictive [10]. Under PNB, the local anesthetic by blocking sympathetic nerve fibers causes significant vasodilatation in the innervated area [11].

We found that arterial dilatation occurred in all types of anesthesia, with average dilatation of 20.4% in PNB group and only 4.8% in LIA patients. When comparing PNB versus LIA, there was a statistically significant dilatation in PNB patients. When comparing the change in lumen diameter of *v. basilicae* after administration of individual types of anesthesia, we found that in

patients recceiving PNB the dilation occurred by an average of 51.6%, whereas in LIA patients the lumen of the vessel even decreased by an average of 1% (Fig. 2). When comparing the vasodilation effect in PNB and LIA groups, there was a statistically significant change in a vessel diameter in terms of dilation in PNB patients compared to LIA patients. These changes in the lumen of the vessels in the area of the distal forearm, i. e. in the place where the AVF was subsequently created, seem to have had a significant impact on the duration of the surgical procedure and the functionality of the AVF itself after 24 hours, 6 weeks and 1 year. Vasodilation of both vessels used in AVF creation had an impact on operative technique, when the operator could work more easily on wider vessels, and a few hours after the operation, the persistent vasodilation improved primary functionality of the AVF.

The length of anesthesia care in the operating room was statistically significantly longer with PNB than with LIA, it is related to the time needed to perform the block and its onset. It can be reduced by performing a blockade outside the OR by another team.

When monitoring the time needed to perform the operation, we found that when comparing PNB and LIA, the operation time was statistically significantly shorter with PNB. From this it can be concluded that PNB, if performed outside the operating room, can speed up the operation in the operating room.

When monitoring adverse events and effects in individual types of anesthesia (we monitored the occurrence of severe hypertension, hypotension, arrhythmia, cardiovascular and neurological complications with the need for therapeutic intervention), the incidence was only 5% in PNB group (1 patient with symptomatic arterial hypertension). No such events occurred under LIA. The incidence of adverse events during the procedure was not significant when PNB and LIA were compared. There were no critical incidents. If we consider the administration of PNB, it is necessary to take into account anticoagulant or antiplatelet treatment, which may represent a relative contraindication for the administration of PNB [12].

There was no statistically significant difference between PNB and LIA when monitoring the VAS when leaving the operating room or the maximum VAS during the first 24 hours after the operation.

The last monitored parameter was the need to administer analgesics in individual anesthesia groups during the first 24 hours after the procedure. Administration of analgesics required in 40% of PNB patients and in 65% of LIA patients. The association between the PNB and LIA groups was only statistically insignificant (P>0.05 between groups).

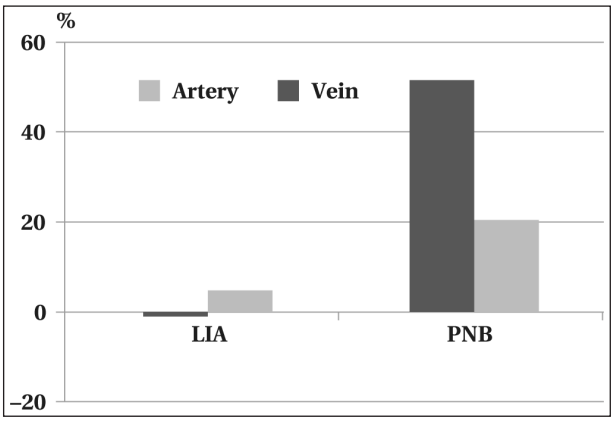

Fig. 2. Change in vein and artery diameter after administration of different types of anesthesia.

Our data confirm previously published results of other studies [13–16].

Patients with chronic renal failure who are being prepared for hemodialysis treatment or have an acute dialysis catheter in place and are indicated for the AVF creation in the forearm for hemodialysis represent a serious medical problem for a relatively broad group of patients. This group may include patients from young adults to elderly patients who are varying in diagnosis that causekidney failure. They usually have developed a wide spectrum of diseases associated with renal failure and fall into the ASA classification of anesthetic risk 3 or more (commonly, risk 4). General anesthesia itself can represent a relatively high risk for them [17, 18]. The operation is performed on the vessels of the forearm (*a. radialis* and *v. cephalica*), and the non-dominant hand is preferred. Vascular conditions are often limited by a narrow lumen or sclerotic changes in the vessels. This complicates the operative technique during the operation itself and often causes early or late failure of the AVF function and necessitates reoperations, radiointervention procedures, or formation of a new fistula proximally, or using the other upper extremity. Sometimes it is necessary to insert an acute or permanent hemodialysis catheter until a new fistula is formed. This entails the risk of various serious medical complications, exposes the patient to repeated invasive procedures and significantly worsens the patient's quality of life. In addition, increased demands for the provided health care and financial costs negatively impact the complications.

Conclusion

In our study, we sought to determine the potential advantages of PNB over LIA in AVF formation. The results of our small cohort suggest that the use of PNB could improve fistula functionality at 6 weeks and 1 year postoperatively versus LIA. It seems that

the use of this method also shortens the duration of the operation due to the improved conditions for the operator. This is probably due to the vasodilatation of the vessels used to create the AVF, which persists for some time even in the postoperative period and improves the flow in the newly created AVF in the first critical hours after the operation. No major conclusions can be drawn from our small sample. Large randomized trials are needed for definitive conclusions, some of which are currently underway and their results may influence future clinical practice.

References

1. *Armstrong R. A., Wilson C., Elliott L., Fielding C. A., Rogers C. A., Caskey F. J., Hinchliffe R. J., et al.* Regional anaesthesia practice for arteriovenous fistula formation surgery. *Anaesthesia*. 2020; 75 (5): 626–633. DOI: 10.1111/anae.14983. PMID: 32030735.
2. *Macfarlane A. J. R., Neuman M. D., Aitken E.* Could anaesthetic technique be blocking successful outcomes in arteriovenous fistula surgery? *Br J Anaesth*. 2021; 126 (2): 349–352. DOI: 10.1016/ j.bja.2020.10.014. PMID: 33187637.
3. *Gao C., Weng C., He C., Xu J., Yu L.* Comparison of regional and local anesthesia for arteriovenous fistula creation in end-stage renal disease: a systematic review and meta-analysis. *BMC Anesthesiol*. 2020; 20 (1): 219. DOI: 10.1186/s12871-020-01136-1. PMID: 32867692.
4. *Kearns R. J., Womack J., Macfarlane A. J.* Regional anaesthesia research — where to now? *Br J Pain*. 2022; 16 (2): 132–135. DOI: 10.1177/20494637221 091139. PMID: 35419194.
5. *Aitken E., Jackson A., Kearns R., Steven M., Kinsella J., Clancy M., Macfarlane A.* Effect of regional versus local anaesthesia on outcome after arteriovenous fistula creation: a randomised controlled trial. *Lancet*. 2016; 388 (10049): 1067–1074. DOI: 10.1016/S0140-6736 (16)30948-5. PMID: 27492881.
6. *Cerneviciute R., Sahebally S. M., Ahmed K., Murphy M., Mahmood W., Walsh S. R.* Regional versus local anaesthesia for haemodialysis arteriovenous fistula formation: a systematic review and meta-analysis. *Eur J Vasc Endovasc Surg*. 2017; 53 (5): 734–742. DOI: 10.1016/j.ejvs.2017.01.025. PMID: 28285956.
7. *Shemesh D., Raikhinstein Y., Goldin I., Olsha O.* General, regional or local anesthesia for successful radial cephalic arteriovenous fistula. *J Vasc Access*. 2017; 18 (Suppl. 1): 24–28. DOI: 10.5301/jva.5000676. PMID: 28297053.
8. *Macfarlane A. Jr., Kearns R. J., Clancy M. J., Kingsmore D., Stevenson K., Jackson A., Mark P., et al.* Access collaborative group; ACCess collaborative group. Anaesthesia Choice for Creation of Arteriovenous Fistula (ACCess) study protocol: a randomised controlled trial comparing primary unassisted patency at 1 year of primary arteriovenous fistulae created under regional compared to local anaesthesia. *BMJ Open*. 2021; 11 (12): e052188. DOI: 10.1136/bmjopen-2021-052188. PMID: 34937718.
9. *Hadzic A.* Hadzic´s textbook of Regional anesthesia and acute pain management. McGraw-Hill Education. 2017: 568–573. ISBN 978-0-07-1717595. LCCN 2016008484
10. *Sung H.-J., Ok S.-H., Sohn J.-Y., Son Y. H., Kim J. K., Lee S. H., Han J. Y., et al.* Vasoconstriction potency induced by amidoamide local anaesthetics correlates with lipid solubility. *J Biomed Biotechnol*. 2012; 2012: 170958. DOI: 10.1155/ 2012/ 170958. PMID: 22778542.
11. *Flood P., Rathmell J. P., Shafer S.* (eds). Stoelting´s pharmacology & physiology in anesthetic practice — 5th edition. Wolters Kluwer, Philadelphia, USA. 2015: 301. ISBN-13: 978-1-60547-550-9.
12. *Horlocker T. T., Vandermeuelen E., Kopp S. L., Gogarten W., Leffert L. R., Benzon H. T.* Regional anesthesia in the patient receiving antithrombotic or thrombolytic therapy: American Society of Regional Anesthesia and Pain Medicine Evidence-Based Guidelines (Fourth Edition). *Reg Anesth Pain Med*. 2018; 43 (3): 263–309. DOI: 10.1097/ AAP.0000000000000763. PMID: 29561531.
13. *Metogo M. J., Halle M. P., Mvondo C. M.V.E., Toua M. M., Sango J., Massom A., Yakana L., et al.* Comparison between ultrasound guided regional anaesthesia and general anaesthesia in arteriovenous fistula creation at the Douala General Hospital. *African Annals of Thoracic and Cardiovascular Surgery*, 2021; 13 (2): 13–19. DOI: 10.5897/AATCVS2021.0026
14. *Stolić R., Markovic-Jovanovic S., Peric V., Mitrović V., Relic G., Bulatović K., Sovtic S., et al.* The importance of anesthesiological methods in the creation of arteriovenous fistulas. *Int Surg J*. 2021; 8 (3): 1068. DOI: 10.18203/2349-2902. isj20210954.
15. *Aitken E., Kearns R., Gaianu L., Jackson A., Steven M., Kinsella J., Clancy M., et al.* Long-term functional patency and cost-effectiveness of arteriovenous fistula creation under regional anesthesia: a randomized controlled trial. *J Am Soc Nephrol*. 2020; 31 (8): 1871–1882. DOI: 10.1681/ASN.2019111209. PMID: 32709710.
16. *Jorgensen M. S., Farres H., James B. L.W., Li Z., Almerey T., Sheikh-Ali R., Clendenen S., et al.* The role of regional versus general anesthesia on arteriovenous fistula and graft outcomes: a single-institution experience and literature review. *Ann Vasc Surg*. 2020; 62: 287–294. DOI: 0.1016/j.avsg.2019.05.016. PMID: 31382001.
17. *Ismail A., Abushouk A. I., Bekhet A. H., Abunar O., Hassan O., Khamis A. A., Al-Sayed M., et al.* Regional versus local anesthesia for arteriovenous fistula creation in end-stage renal disease: a systematic review and meta-analysis. *J Vasc Access*. 2017; 18 (3): 177–184. DOI: 10.5301/jva. 5000683. PMID: 28478618.
18. *Palaniappan S., Subbiah V., Gopalan V. R., Kumar P. V., Vinothan R. J. S.* Observational study of the efficacy of supraclavicular brachial plexus block for arteriovenous fistula creation. *Indian J Anaesth*. 2018; 62 (8): 616–620. DOI: 10.4103/ija. IJA_293_18. PMID: 30166657.

Received 09.08.2023
Accepted 30.11.2023
Online first 29.12.2023

https://doi.org/10.15360/1813-9779-2024-1-2350

The Effect of Transfusion and Hypoxia on Cells in an *in vitro* Model of the Neurovascular Unit

Artem A. Ivkin[1]*, Evgeny V. Grigoriev[1], Elena D. Khilazheva[2], Andrey V. Morgun[2]

[1] Research Institute of Complex Problems of Cardiovascular Disease
6 Sosnovy bulvar, 650002 Kemerovo, Russia
[2] Prof. V. F. Voino-Yasenetsky Krasnoyarsk State Medical University, Ministry of Health of Russia,
1 Partizana Zheleznyaka Str., 660022 Krasnoyarsk, Krasnoyarsk region, Russia

For citation: *Artem A. Ivkin, Evgeny V. Grigoriev, Elena D. Khilazheva, Andrey V. Morgun.* The Effect of Transfusion and Hypoxia on Cells in an *in vitro. Obshchaya Reanimatologiya = General Reanimatology.* 2024; 20 (1): 37–42. https://doi.org/10.15360/1813-9779-2024-1-2350 [In Russ. and Engl.]

***Correspondence to:** Artem A. Ivkin, ivkiaa@kemcardio.ru

Summary

Up to 57% of patients develop postoperative delirium after surgery for congenital heart defects (CHD). To reduce cerebral damage in pediatric patients during CHD surgery it is important to find out what inflicts the worse damage: would it be a systemic inflammatory response (SIR) triggered by transfusion, or hypoxia developed in non-transfused patients? *In vitro* evaluation of hypoxia and SIR effects on the neurovascular unit (NVU) cells might contribute to finding the answer.

The aim of the study was to compare the effect of varying severity hypoxia and SIR on the functional activity of NUV cells *in vitro*.

Materials and methods. An *in vitro* NVU model was designed including neurons, astrocytes and endotheliocytes. The effect of hypoxia on NVU was evaluated in the control (C) and 4 study groups (H 1–4), formed based on O_2 content in the medium. The C group NVU were cultivated in standard conditions: N_2 — 75%, O_2 — 20%, CO_2 — 5%; H1: N_2 — 99%, O_2 — 1%; H2: N_2 — 98%, O_2 — 2%; H3: N_2 — 97%, O_2 — 3%; H4: N_2 — 96%, O_2 — 4%. The significance of the differences was 0.0125. The effect of interleukin-6 (IL-6) content on NVU was measured by adding to culture medium pediatric patients' serum with known minimal or maximal SIRS-response. The assessment was made in the Control — an intact NVU model, and 2 study groups — «Minimum» and «Maximum», i. e. samples with minimum or maximum IL-6 content in culture, respectively. The significance of the differences was 0.017. The cells were incubated at a normothermia regimen for 30 minutes. Then, the functional activity of NVU cells was evaluated by measuring transendothelial resistance (TER) for 24 hours and Lucifer Yellow (LY) permeability test at 60 and 90 minutes after the start of the experiment.

Results. After incubation under hypoxic conditions, TER changes occurred in all studied groups. However, they were statistically significant only in the group with 1% oxygen content in the medium. TER decrease in this group was observed after 2, 4 and 24 hours. LY permeability also changed at 60 and 90 minutes, similarly — in NVU cultivated with 1% oxygen in the medium. Minimal TER values were documented at 4 hours after patients' serum was added to NVU cells culture medium, and TER increased at 24 hours in both study groups. Cellular permeability to LY changed significantly after 1 hour exposure in both groups — with minimum and maximum IL-6 content in the medium. Although at 90 minutes, there was no difference between the 3 groups in LY permeability tests.

Conclusion. Intensive SIR demonstrated short-term but more deleterious than hypoxia, effect on cells in the NVU model. Hypoxia disrupted functional activity of NUV cells only at 1% O_2 concentration in the medium.

Keywords: transfusion; hypoxia; neurovascular unit; systemic inflammatory response; interleukin-6; cerebral damage; cardiopulmonary bypass; children; cardiac surgery

Conflict of interest. The authors declare no conflict of interest.

Funding. The research was supported by No. 22-15-00258; https://rscf.ru/project/22-15-00258/ grant from the Russian Science Foundation.

Introduction

Contemporary cardiac surgery and anesthesiology are rapidly evolving, with an increasing number of procedures being performed using minimally invasive or endovascular techniques. However, correction of congenital heart disease (CHD) in children often requires an extensive surgical intervention and the use of cardiopulmonary bypass (CPB). These surgical procedures carry the risk of potential brain damage in children due to various pathological factors, mainly associated with CPB. The effects of CPB can be both direct (embolism, hypoxia, hemodynamic changes) and indirect, through the initiation of a systemic inflammatory response (SIR) as a result of blood contact with the extracorporeal circuit, hemolysis, and disturbances in thermoregulation [1–4]. Furthermore, the infant brain, especially in the first year of life, exhibits various specific patterns, such as active neuronal differentiation and synaptogenesis, rapid glial cell growth and myelination, high hydrophilicity and metabolic rate [5, 6]. All these patterns make the brain vulnerable to

any pathological factors, which explains high incidence of postoperative cognitive disorders. For instance, postoperative delirium occurs in up to 57% of patients following congenital heart disease correction [7]. Importantly, the impact of any brain damage and dysfunction in childhood on a child's further development has received little attention. Meanwhile, studies in children who have undergone cardiac surgery show reduced cognitive performance one year later [8].

Therefore, it is important to explore ways to prevent brain injury during the correction of congenital heart disease in children. One promising approach is to minimize the perioperative use of transfusions. This strategy is based on the understanding that components of donor blood can induce a systemic inflammatory response that manifests in the brain as neuroinflammation, ultimately leading to damage of the entire neurovascular unit (NVU) which includes neurons, astrocytes, and endothelial cells [2, 9].

However, it is important to understand that by refusing transfusions of RBC-rich donor blood components, we increase chances of hemic hypoxia as a result of the hemodilution that occurs during CPB. Thus, a critical question is: what poses a greater risk to the NVU — the increased SIR following transfusion administration, or the hypoxia resulting from refusal of transfusion? Due to patient risk, this question cannot be answered in a clinical trial. However, there is a way to study the effect of different levels of hypoxia and systemic inflammatory response on the functional activity of NVU cells. The aim of the study was to compare the effect of different degrees of hypoxia and SIR on the functional activity of NVU cells using an in vitro cell model [10].

Materials and Methods

Serum samples were available from 78 pediatric patients, aged 1 month to 6.5 years (13 [9–23] months) and weighing between 3.3 and 21.5 kg (8.7 [6.9–11.0] kg), who underwent surgery for correction of congenital septal heart defects under CPB at the Research Institute for Complex Problems of Cardiovascular Diseases. The level of interleukin-6 (IL-6), an important SIR marker, was measured in each sample [11]. Three blood samples from this pool with the highest and lowest IL-6 levels were selected for the in vitro phase of the study. The frozen serum was delivered to the V. F. Voino-Yasenetsky Krasnoyarsk State Medical University (KSMU) in accordance with the temperature control protocol.

The KSMU laboratory has developed a method to assess brain damage during cardiac surgery based on a cellular model of the neurovascular unit that can be cultured under various conditions that mimic the intraoperative period.

Developing primary cultures of brain cells *in vitro*. Primary cultures of brain endothelial cells, astrocytes, and neurons obtained from Wistar rats were used. The animals were housed in cages with free access to food and water. A constant temperature of 21±1°C was maintained. The light cycle was 12 h day/12 h night. Animal studies were conducted in accordance with the principles of humane care as set forth in the European Community Directive (2010/63/EC). The total number of animals used was 10.

Several steps were required to obtain an in vitro cell model of the NVU:

1. Isolation of brain endothelial cells.
2. Isolation and culture of neurospheres.
3. Obtaining astrocytes and neurons from the obtained neurospheres by targeted differentiation into astrocytes and neurons.
4. Establishing an in vitro model of NVU. For this purpose, a mixture of endothelial cells and neurons was placed at the bottom of the wells of the culture plate, then culture inserts (Corning-Costar, USA) were installed on which astrocytes were placed. The cell mixture was cultured in a medium consisting of DMEM with PBS, glutamine, antibiotic mixture at 37°C with 5% CO_2 [12].

After establishing a cell model of NVU, the main experiment was performed.

Experimental design. To determine the effects of IL-6 on the NVU cell model in vitro, blood serum samples with minimal and maximal concentrations of IL-6 were added to the culture medium.

Groups were formed according to the level of IL-6 in the sample:

1. «Control» —intact model of NVU.
2. «Minimum» — samples with minimal level of IL-6 in the culture.
3. «Maximum» — samples with maximum level of IL-6 in culture.

The number of replicates in serum incubation groups was 10.

According to the conditions of hypoxic incubation of NVU, the following groups were formed:

1. Control (C), standard culture conditions: N_2 — 75%, O_2 — 20%, CO_2 — 5%.
2. Hypoxia 1 (H1): N_2 — 99%, O_2 — 1%, CO_2 — 0%.
3. Hypoxia 2 (H2): N_2 — 98%, O_2 — 2%, CO_2 — 0%.
4. Hypoxia 3 (H3): N_2 — 97%, O_2 — 3%, CO_2 — 0%.
5. Hypoxia 4 (H4): N_2 — 96%, O_2 — 4%, CO_2 — 0%.

The number of replicates in the hypoxic incubation groups was 5.

The incubation time was 30 minutes. The temperature conditions were normothermic (37.0°C).

Evaluation of NVU performance. To evaluate the effect of hypoxia and blood serum with different levels of IL-6 on cell culture, transendothelial resistance and endothelial layer permeability were measured in the model of NVU as indicators of blood-brain barrier function.

Transendothelial resistance (TER) in the in vitro cell model was measured after 1, 2, 4, and 24 hours of culture. Direct measurement of transendothelial electrical resistance (TEER) was performed with an EVOM2 epithelial voltmeter using a STX2 electrode (World Precision Instruments, USA).

Table 1. TER parameters during incubation of cells in hypoxia.

Stage	Values of TER in groups				
	C	H1	H2	H3	H4
0 h	199.5 [197.25–201.5]	197.0 [196.75–199.25] *P*=0.1533	197.5 [196.25–199.25] *P*=0.3316	192.5 [190.75–195.0] *P*=0.0407	195.0 [194.75–196.5] *P*=0.1169
1 h	204.25 [202.75–206.0]	191.0 [189.75–193.0] *P*=0.03	191.0 [189.5–192.5] *P*=0.031	191.0 [189.75–193.25] *P*=0.033	193.0 [191.5–195] *P*=0.034
2 h	200.0 [196.75–203.5]	185.0 [182.25–187.25] *P*=0.0105	191.5 [188.75–194.75] *P*=0.0407	192.0 [187.5–195.0] *P*=0.066	193.0 [190.75–194.5] *P*=0.0408
4 h	194.5 [193–195.75]	175.5 [174.5–176.75] *P*=0.0105	177.0 [175.75–178.25] *P*=0.0151	183.5 [182.0–185.5] *P*=0.0329	189.0 [187.5–191.25] *P*=0.1441
24 h	203.0 [200.75–205.5]	141.0 [138.75–143.0] *P*=0.0105	162.0 [160.0–164.0] *P*=0.021	179.5 [175.0–183.25] *P*=0.0152	192.0 [191.0–192.75] *P*=0.0531

Note. For Tables 1, 3, Fig.1, *a*: C — control group; H — Hypoxia group 1–4.

The fluorescent dye Lucifer Yellow (LY) was added to the culture medium at a final concentration of 50 μM to measure permeability. The medium was removed from the lower compartment of the wells after 60 and 90 minutes, and the optical density of the mixture was measured using a spectrofluorometer SM 2203 (SOLAR, Belarus). Relative permeability was calculated based on the variation of LY concentration between experimental and control groups.

Statistical analysis of data was performed using BioStat Pro 5.9.8 software. Data in the text, tables, and figures were reported as median *(Me)*, upper *(Q1)* and lower quartile *(Q3)* because most variables had non-normal distribution (Shapiro–Wilk test, $P<0.05$). The Mann–Whitney test was used for one-way comparisons of quantitative variables. Differences were considered significant when $P<0.05$. Bonferroni correction was used to compare more than one group.

The effect of hypoxia on NVU was evaluated in 4 study groups and one control group, and the differences were significant at $P=0.0125$.

The effect of IL-6 on NVU was evaluated in two study groups and one control group, and the difference was significant at $P=0.017$.

Results and Discussion

When assessing the effect of hypoxia on NVU (Table 1, Fig. 1, *a*), transendothelial resistance (TER) decreased insignificantly in all groups after 1 hour of hypoxia exposure, by 7% on average.

After 2, 4, and 24 hours, there was a decrease in TER in all groups, but it was significant only in the group with 1% oxygen in the medium. In this group, the TER decreased by 7.5% after 2 hours, by 9.8% after 4 hours, and by 30.5% after 24 hours. In general, this confirms the fact that even short-term hypoxia has an effect on TES values, but it also shows that the effect of hypoxia on NVU varies depending on the percentage of oxygen in

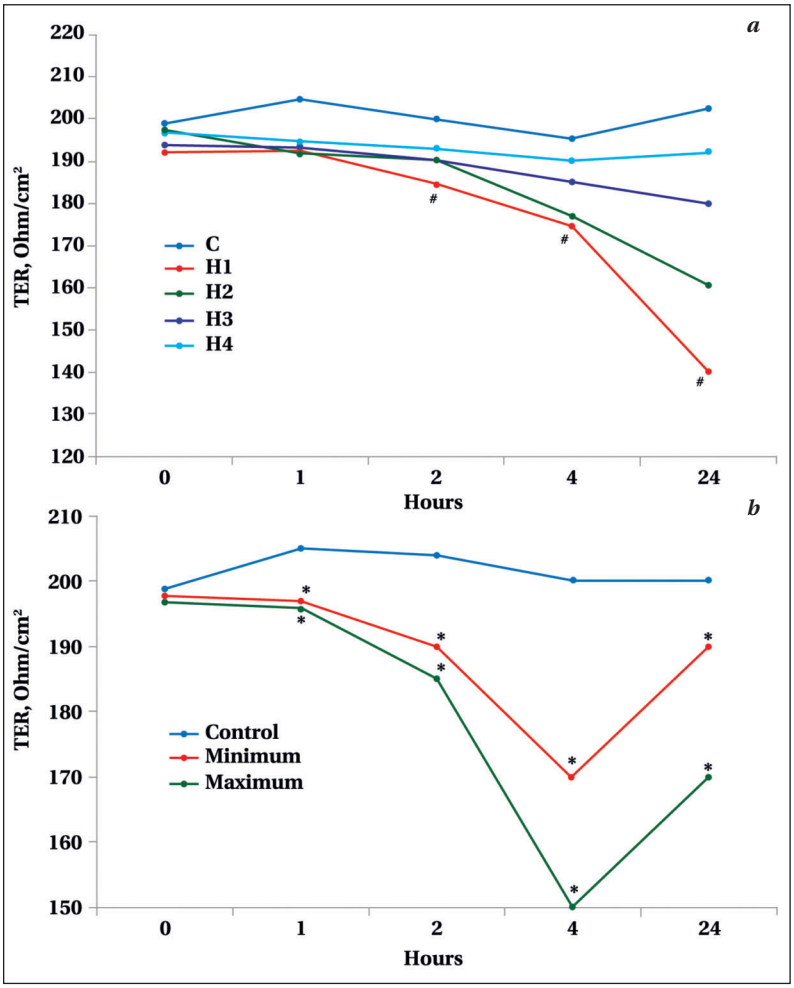

Fig. Effect of hypoxia *(a)* and serum from patients with different levels of IL-6 *(b)* on the transendothelial resistance index.
Note. # — $P<0.0125$, * — $P<0.017$, Mann–Whitney test with Bonferroni correction.

the medium. Furthermore, the absence of significant changes in TER in the 2, 3, and 4% oxygen groups suggests that moderate short-term hypoxia did not affect the functional activity of the NVU.

When evaluating the effect of IL-6 on TER (Fig. 1, *b*, Table 2), we found that at 2 hours, TER was significantly decreased by 5% in the minimum group and by 7.5% in the maximum group compared to the control (Fig. 1, *b*). At 4 hours after IL-6 exposure, the TER decreased by 15% in the minimum group and by 25% in the maximum group compared with the control. After 24 hours, the TER values increased but still remained significantly lower than in the control, maximum and minimum groups. Therefore, the presence of IL-6 in blood serum resulted in a decrease in TER, which was reversible and had a stronger and faster impact than hypoxia, albeit for a shorter period of time. Meanwhile, a significant difference in TER values between the minimum and maximum groups was observed at the following time points: 2 hours (P=0.00640), 4 hours (P=0.00017), and 24 hours (P=0.00016), indicating varying levels of NVU damage based on the concentration of IL-6 in the medium and, thus, the severity of systemic inflammation.

Table 2. TER during incubation of cells with serum.

Stage	Values in groups		
	Control	Minimum	Maximum
0 h	198.0 [197.0–200.0]	199.0 [197.0–199.0] P=0.25	197.0 [195.0–198.0] P=0.073
1 h	206.0 [205.0–207.0]	197.0 [196.0–198.0] P=0.00027	196.0 [196.0–197.0] P=0.00016
2 h	203.0 [202.0–204.0]	190.0 [188.0–192.0] P=0.00017	185.0 [185.0–188.0] P=0.00016
4 h	200.0 [196.0–203.0]	168.0 [168.0–170.0] P=0.00016	151.0 [148.0–152.0] P=0.00017
24 h	199.0 [198.0–202.0]	190.0 [188.0–192.0] P=0.00020	169.0 [169.0–172.0] P=0.00031

Table 3. Relative permeability of cells during incubation in hypoxia.

Stage	Values in groups				
	C	H1	H2	H3	H4
60 min	99.5 [98.0–101.5]	121.0 [117.5–124.25] *P=0.01008	119.5 [118.5–120.75] P=0.0140	100.5 [99.5–101.25] P=0.44084	101.0 [100.75–102.5] P=0.37185
90 min	99.5 [99.0–100.0]	146.0 [143.75–148.0] *P=0.00971	139.0 [137.5–141.0] P=0.01942	110.0 [107.75–112.0] P=0.03228	107.0 [106.0–109.0] P=0.05095

Note. * — P<0.0125, Mann–Whitney test with Bonferroni correction.

Table 4. Relative permeability of cells during incubation with serum.

Stage	Values in groups		
	Control	Minimum	Maximum
60 min	99.5 [98.75–100.5]	119.5 [118.75–121.0] *P=0.01046	114.5 [114.0–115.25] *P=0.01470
90 min	99.5.0 [99.0–100.5]	106.5 [105.75–107.25] P=0.05314	109.5 [108.75–110.5] P=0.03291

Note. * — P<0.017, Mann–Whitney test with Bonferroni correction.

Cell permeability to LY after exposure to short-term hypoxia increased by 21.6% after 60 minutes of incubation and by 46.7% after 90 minutes only in the Hypoxia 1 group (Table 3).

The results of the cell permeability assay correlated with the changes in TER, generally indicating the effect of only the extremely low (1%) concentration of oxygen in the medium on NVU.

The effect of patient serum on cell permeability is shown in Table 4. After 60 minutes of exposure, a 15–20% increase in relative permeability was observed in both experimental groups. Interestingly, after 90 minutes, the permeability in the control and experimental groups did not differ, confirming the assumption of a rapid but short-term and possibly reversible effect of serum with IL-6. Meanwhile, cell permeability to LY was significantly higher (P=0.01470) in the group with maximal IL-6 in the medium than in the group with minimal IL-6 in the medium, which may confirm the relationship between the severity of blood-brain barrier damage and systemic inflammation.

Conclusion

The study using the NVU cell model showed that 30 min of hypoxia had no significant effect on rat brain cells. Changes in TER and cell permeability to LY were observed only at 1% oxygen concentration in the medium. Exposure to patient serum containing IL-6 caused more severe but transient damage to NVU. The severity of the damage was determined by the concentration of IL-6 in the medium, which indicated the strength of the inflammatory response. Thus, withholding intraoperative transfusion to limit SIR and resulting hemic hypoxia may be less damaging to the patient's brain than the transfusion-induced increase in systemic inflammatory activity.

The study of TER and permeability to LY allowed us to identify trends in the effects of hypoxia and SIR in an NVU model.

Further studies using functional activity markers of the neurovascular unit (NVU), such as s100β protein, neuron-specific enolase, glial fibrillary acidic protein, occludin, claudin, and others, will offer a detailed understanding of NVU performance in response to pathological factors.

References

1. *Guenther U., Theuerkauf N., Frommann I., Brimmers K., Malik R., Stori S., Scheidemann M., et al.* Predisposing and precipitating factors of delirium after cardiac surgery: a prospective observational cohort study. *Ann Surg.* 2013; 257 (6): 1160–1167. DOI: 10.1097/sla.0b013e318281b01c. PMID: 23426334.
2. *Hirata Y.* Cardiopulmonary bypass for pediatric cardiac surgery. *Gen Thorac Cardiovasc Surg.* 2018; 66 (2): 65–70. DOI: 10.1007/s11748-017-0870-1. PMID: 29185163.
3. *Engelman R., Baker R. A., Likosky D. S., Grigore A., Dickinson T. A., Shore-Lesserson L., Hammon J. W.* The Society of Thoracic Surgeons, The Society of Cardiovascular Anesthesiologists, and The American Society of ExtraCorporeal Technology: Clinical practice guidelines for cardiopulmonary bypass — temperature management during cardiopulmonary bypass. *J Cardiothorac Vasc Anesth.* 2015; 29 (4): 1104–1113. DOI: 10.1053/j.jvca.2015.07.011. PMID: 26279227.
4. *Борисенко Д. В., Ивкин А. А., Шукевич Д. Л., Корнелюк Р. А.* Значение эритроцитсодержащих компонентов донорской крови в объеме первичного заполнения контура искусственного кровообращения в развитии системного воспаления при коррекции врожденных пороков сердца у детей. *Obshchaya Reanimatologiya = General Reanimatology.* 2022; 18 (3): 30–37. [*Borisenko D., Ivkin A., Shukevich D., Kornelyuk R.* The effect of erythrocyte — containing donor blood components in the priming of the cardiopulmonary bypass circuit on the development of systemic inflammation during correction of congenital heart defects in children. *General Reanimatology/ Obshchaya Reanimatologiya.* 2022; 18 (3): 30–37. (in Russ&Eng.)]. DOI: 10.15360/1813-9779-2022-3-30-37.
5. *Hansen T. G.* Anesthesia-related neurotoxicity and the developing animal brain is not a significant problem in children. *Paediatr Anaesth.* 2015; 25 (1): 65–72. DOI: 10.1111/pan.12548. PMID: 25266176.
6. *Jevtovic-Todorovic V.* General anesthetics and neurotoxicity: how much do we know? *Anesthesiol Clin.* 2016; 34 (3): 439–451. DOI: 10.1016/j.anclin.2016.04.001. PMID: 27521190.
7. *Alvarez R.V., Palmer C., Czaja A. S., Peyton C., Silver G., Traube C., Mourani P. M., et al.* Delirium is a common and early finding in patients in the pediatric cardiac intensive care unit. *J Pediatr.* 2018; 195: 206–212. DOI: 10.1016/j.jpeds.2017. 11.064. PMID: 29395177.
8. *Gunn J. K., Beca J., Hunt R. W., Goldsworthy M., Brizard C. P., Finucane K., Donath S., et al.* Perioperative risk factors for impaired neurodevelopment after cardiac surgery in early infancy. *Arch Dis Child.* 2016; 101 (11): 1010–1016. DOI: 10.1136/archdischild-2015-309449. PMID: 27272973.
9. *Ferraris V. A., Ballert E. Q., Mahan A.* The relationship between intraoperative blood transfusion and postoperative systemic inflammatory response syndrome. *Am J Surg.* 2013; 205 (4): 457–465. DOI: 10.1016/j.amjsurg.2012.07.042. PMID: 23414633.
10. *Ивкин А. А., Григорьев Е. В., Моргун А. В.* Обоснование защиты нейроваскулярной единицы на клинической модели искусственного кровообращения. *Комплексные проблемы сердечно-сосудистых заболеваний.* 2022; 11 (4): 177–183. [*Ivkin A. A., Grigoriev E. V., Morgun A. V.* Substantiation of protection of a neurovascular unit in the clinical model of cardiopulmonary bypass. *Complex Issues of Cardiovascular Diseases/Kompleksnye Problemy Serdechno-Sosudistykh Zabolevany.* 2022; 11 (4): 177–183. (in Russ.)]. DOI: 10.17802/2306-1278-2022-11-4-177-183.
11. *Jekarl D. W., Lee S.-Y., Lee J., Park Y.-J., Kim Y., Park J. H., Wee J. H., et al.* Procalcitonin as a diagnostic marker and IL-6 as a prognostic marker for sepsis. *Diagn Microbiol Infect Dis.* 2013; 75 (4): 342–347. DOI: 10.1016/j.diagmicrobio.2012.12.011. PMID: 23391607
12. *Khilazheva E. D., Boytsova E. B., Pozhilenkova E. A., Solonchuk Yu.R., Salmina A. B.* Obtaining a three-cell model of a neurovascular unit *in vitro*. *Cell Tiss Biol.* 2015; 9 (6): 447–451. DOI: 10.1134/ S1990519X15060048

Received 07.06.2023
Accepted 11.12.2023
Online first 14.12.2023

https://doi.org/10.15360/1813-9779-2024-1-2366

Autophagy Activity in Epicardial Cells in Acute Pericarditis

Konstantin V. Dergilev[1]*, Zoya I. Tsokolaeva[1,2],
Alexander D. Gureenkov[1], Mohidil T. Rasulova[3], Elena V. Parfenova[1]

[1] Experimental Cardiology Institute,
Acad. Chazov National Medical Research Center for Cardiology, Ministry of Health of Russia,
15a Cherepkovskaya 3rd Str., 121552 Moscow, Russia
[2] V. A. Negovsky Research Institute of General Reanimatology,
Federal Research and Clinical Center of Intensive Care Medicine and Rehabilitology,
25 Petrovka Str., Bldg. 2, 107031 Moscow, Russia
[3] Fergana Medical Institute for Public Health,
2A Yangi Turon Str., 150100 Fergana, Fergana region, Uzbekistan

For citation: *Konstantin V. Dergilev, Zoya I. Tsokolaeva, Alexander D. Gureenkov, Mohidil T. Rasulova, Elena V. Parfenova.* Autophagy Activity in Epicardial Cells in Acute Pericarditis. *Obshchaya Reanimatologiya = General Reanimatology.* 2024; 20 (1): 43–49. https://doi.org/10.15360/1813-9779-2024-1-2366 [In Russ. and Engl.]

***Correspondence to:** Konstantin V. Dergilev, kvdergilev@cardio.ru

Summary

Pericarditis is a group of polyetiological diseases often associated with emergence of life–threatening conditions. Poor knowledge of underlying cellular mechanisms and lack of relevant approaches to investigation of pericarditis result in major challenges in diagnosis and treatment.

The aim of this work was to identify changes in the activity of autophagy in epicardial cells in acute pericarditis.

Materials and methods. Acute pericarditis in mice was induced by intrapericardial injection of Freund's adjuvant in the study group (*N*=15). The control group included animals receiving either intrapericardial injection of phosphate-buffered saline (PBS) (*N*=15), or sham surgery without injections (*N*=7). On Days 3 or 5 after surgery the animals were euthanized under isoflurane anesthesia. Immunofluorescence staining of cardiac tissue cryo-sections and immunoblotting were used to assess the intensity of inflammation and autophagy in the epicardium.

Results. Inflammation and other signs of acute pericarditis resulting in thickening of some epicardial areas were found: 68±9% in the control (after PBS injection) and 124±22% after Freund's adjuvant injection (*P*=0.009); other signs included cellular infiltration of epicardium and multiple adhesions. The epicardial layer exhibited signs of mesothelial cells reorganization with 11-fold increase of autophagy markers LC3 II/LC3 I ratio: 0.07±0.02 in the control group (after PBS injection) and 0.84±0.07 — in acute pericarditis (*P*=0.04), and accumulation of collagen fibers.

Conclusion. Development of acute pericarditis is accompanied by activation of epicardial mesothelial cells, intensified autophagy and development of fibrous changes in epicacardial/ subepicardial areas.

Keywords: autophagy; acute pericarditis; epicardium

Conflict of interest. The authors declare no conflict of interest.

Financing. The work was financially supported by RSF grants: 19-15-00384 (modeling of acute pericarditis) and 23-15-00540 (investigation of autophagy).

Introduction

Pericarditis is an inflammatory condition of the serous membranes of the heart characterized by thickening, fusion, and fibrotic transformation of the pericardial layers, which can lead to heart chamber compression and their abnormal diastolic filling [1–3]. It is a fairly common clinical finding during the evaluation of hospitalized patients with chest pain, dyspnea, and other signs of heart failure. According to the literature, pericarditis is found in 0.1–0.2% of hospitalized patients with nonischemic chest pain, and acute pericarditis is diagnosed in 5–7% of emergency department admissions [3, 4].

According to biopsy data, fibrotic changes of the visceral pericardial layer (epicardium) are found in most cases, regardless of the etiology. These changes are often accompanied by fibrosis in the underlying myocardial layers and subsequent heart failure [5, 6]. The progression of fibrosis to the underlying myocardium associates with a poor prognosis [7–9]. The therapy for these patients is often chosen based on the nature of the disease, with treatment limited to prescribing non-steroidal anti-inflammatory drugs and colchicine [10]. This is largely due to the fact that many aspects of the pathogenesis of pericarditis remain poorly understood, as do the cellular mechanisms of its development.

According to recent research, one of the mechanisms of cellular response to the inflammatory microenvironment is an alteration in autophagy activity [11, 12]. Autophagy is an evolutionarily conserved mechanism that, at a basic level, helps to maintain cellular homeostasis by utilizing macromolecules and organelles via the lysosomal degradation pathway [13, 14]. Under stress, autophagy

can help cells survive by providing a temporary cellular adaptation to unfavorable conditions, but excessive activation has the opposite effect, resulting in cell death and the development of abnormalities such as fibrosis.

The aim of the study was to identify changes in autophagy activity in epicardial cells during acute pericarditis.

Materials and Methods

Modeling of acute pericarditis. Acute pericarditis was modeled *in vivo* in male C57BL/6 mice (*N*=37, age 8 weeks, weight 28–30 g). Animal experiments were performed in accordance with the European Convention for the Protection of Vertebrate Animals used for Experimental and other Scientific Purposes (Strasbourg, March 18, 1986, ETS 123), International Guiding Principles (Code of Ethics) for Biomedical Research Involving Animals, developed and published in 1985 by the Council for International Organizations of Medical Sciences (CIOMS), Rules for Conducting Research Using Experimental Animals, approved by the Appendix to the Order of the Ministry of Health of the USSR No. 755 dated August 12, 1977. Animals were maintained on a standard diet and had free access to water. Surgery was performed under aseptic conditions under general anesthesia (Avertin, intraperitoneal injection). Mice were intubated and placed on a ventilator (MiniVent, Hugo Sachs Elektronik/Harvard Apparatus, Germany). After preparation of the surgical field, a longitudinal skin incision was made along the anterior midline from the angle of the sternum to the base of the xiphoid process. The underlying tissues were separated by blunt dissection. After exposing the outer surface of the intercostal muscles, a horizontal incision was made in the 9th intercostal space from the sternocostal joint to the mid-axillary line to enter the thoracic cavity and provide access to the heart. Study group animals (*N*=15) were injected intrapericardially with 50 µL complete Freund's adjuvant under visual guidance using a Leica M620 surgical microscope. The control animals were injected intrapericardially with 50 µL phosphate-buffered saline (*N*=15) or underwent surgery without intrapericardial injection of any drug (sham-operated animals, *N*=7). The wound was then sutured layer by layer. On day 3 or 5 after surgery, animals were euthanized by cervical dislocation after inhalational anesthesia with isoflurane.

Analysis of myocardial cryosections after modeling of acute pericarditis in mice. To evaluate the manifestations of acute pericarditis, murine hearts were extracted, washed with physiological solution, embedded in Tissue-Tek O.C.T. Compound Medium (Sakura Finetek), frozen in liquid nitrogen vapor, and used to prepare cryosections. Cryosections (7 µm thick) were placed on slides and stored at –70°C Heart sections were stained with hematoxylin-eosin and Mallory's method according to previously described protocols [15–18]. The following solutions were used for Mallory staining: solution A (1% acid fuchsin), B (1% phosphomolybdic acid), and C (2% orange G, 0.5% methyl blue, 2% oxalic acid). Fixed cryosections were sequentially incubated in solution A (2 min), solution B (4 min), and solution C (15 min). Between each staining, the slides were washed with distilled water, dehydrated, and mounted with xylene-based medium.

Immunofluorescence staining was performed using antibodies against markers of activated epicardium Wt1 (Abcam, USA), CD68 macrophages (Abcam, USA), autophagy LC3B (Abclonal, China; Millipore, Germany), and secondary antibodies conjugated to the fluorescent dyes Alexa Fluor 488, Alexa Fluor 594.

Morphometry was performed by manual counting using Image J software (National Institutes of Health, USA).

Evaluation of LC3 expression by immunoblotting. For the analysis of autophagy activity, we used samples of epicardial scrapings from the hearts of control animals and mice after modeling acute pericarditis. Proteins were separated by DSN electrophoresis in 10% polyacrylamide gel on a Mini-PROTEAN 2 device (Bio-rad, USA) and electrotransferred to PVDF membrane (Millipore, USA) on a Trans-blot Turbo device (Bio-rad, USA). After electrotransfer, the membrane was incubated in a blocking buffer (phosphate-buffered saline containing 5% skim milk powder (AppliChem, USA)). The membrane was then incubated with antibodies against LC3 I/II (Abclonal, USA) for 12 hours at +4°C with constant stirring. The membrane was then washed three times in PBS containing 0.05% Tween-20 (each wash for 10 minutes with continuous agitation). After the washes, the membrane was incubated with secondary antibodies against rabbit immunoglobulins conjugated to AffiniPure (H+L) horseradish peroxidase (HRP) (Jackson ImmunoResearch, USA). The membranes were then washed 3 times for 10 minutes each in phosphate-buffered saline containing 0.05% Tween-20. Proteins were detected using SuperSignal West Pico chemiluminescent substrate (Thermo Scientific, USA). The signal was captured using a Fusion-SL 3500.WL gel documentation system (Vilber Lourmat, France). Morphometry was performed using Image J software (National Institutes of Health, USA).

Microscopy and image analysis. Myocardial cell structures and cryosections were analyzed using an Axiovert 200 M fluorescence microscope (Carl Zeiss, USA) and AxioVision 4.8 software (Carl Zeiss, USA).

Statistical significance of differences between samples was evaluated using the non-parametric Mann–Whitney test. Data were analyzed using Statistica 8.0 software (StatSoft, Inc.).

Results

Intrapericardial injection of Freund's adjuvant resulted in the development of signs of acute pericarditis. Intrapericardial injection of Freund's adjuvant into the pericardial cavity induced an inflammatory response in the pericardial leaflets. On day 3 of observation, the acute inflammatory response was manifested by exudation and infiltration with polymorphic cells, including lymphocytes, monocytes, and plasmocytes.

Macroscopically, thickening of pericardial leaflets with loss of transparency and development of adhesions with pleura, diaphragm and lungs was observed on day 5 after inducer administration. Hematoxylin and eosin staining results showed that sham-operated animals showed no signs of morphological changes in the epicardial layer of the heart and did not express Wt1 marker in the epicardial zone. Meanwhile, the visceral pericardium (epicardium) of the experimental group mice was significantly thicker (Fig. 1, *a*, *b*) than the epicardium of the control group animals injected with PBS.

The percentage of thickened epicardial zone in control (after PBS administration) and after Freund's adjuvant administration was 68±9% and 124±22%, respectively (N=6, P=0.009). Wt1+ cells of activated epicardial mesothelium, reorganization of the epicardial/subepicardial area and collagen accumulation were detected (Fig. 2, *c*, *d*), which was practically absent in the control group.

The development of fibrotic transformation of the pericardial leaflet is accompanied by the activation of autophagy in epicardial cells.

Numerous studies show that inflammatory and fibrotic changes in various body tissues are associated with autophagy dysregulation.

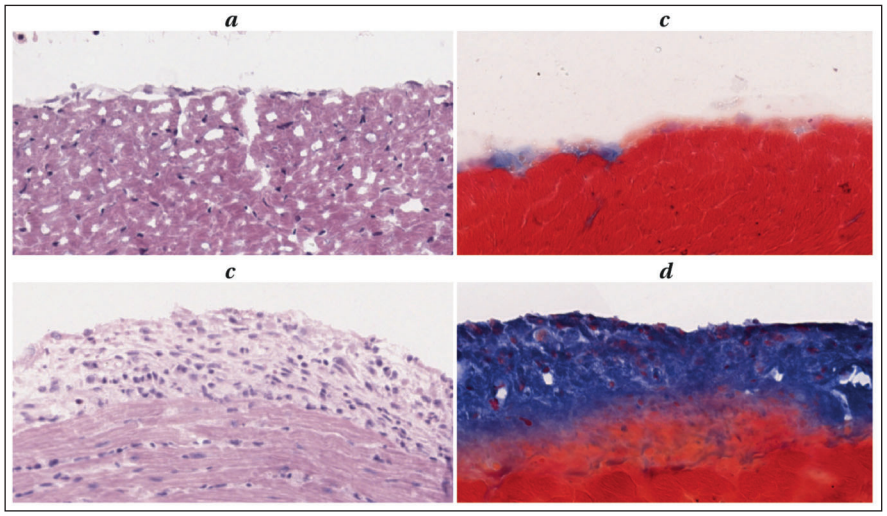

Fig. 1. Morphological changes in the epicardial/subepicardial area after modeling of acute pericarditis (day 5).
Notes. Sections of murine hearts stained: *a, b* — with hematoxylin-eosin; *c, d* — by Mallory method. *a, c* — control group; *b, d* — after acute pericarditis modeling. Blue staining indicates the presence of collagen.

Considering these data, we analyzed autophagy activity after modeling acute pericarditis. LC3 II expression was found to be significantly increased in cells of the activated epicardial layer after adjuvant administration (Fig. 2, *b*) compared to that in control group mice (after PBS administration) (Fig. 2, *a*).

Immunoblotting results showed (Fig. 2, *c*) that during the development of pericarditis, epicardial cells exhibited an 11-fold increase in the ratio of LC3 II / LC3 I (0.07±0.02 in controls and 0.84±0.07 in acute pericarditis groups, P=0.04), indicating increased autophagosome formation and autophagy activity.

Discussion

Currently, pericarditis remains a rather rare disease, which causes significant diagnostic difficulties for primary care physicians [19, 20]. At the same time, even in the case of successful diagnosis, medical treatment has limited efficacy, is often prescribed without considering the etiology, has no effect on the progression of fibrosis in the pericardial leaflets and long-term prognosis. This is largely due to the limited understanding of the cellular mechanisms of pericarditis development and the lack of relevant animal models in the study of the disease [21].

For the first time, our modeling of acute pericarditis in mice showed the following.

1) Intrapericardial Freund's adjuvant injection resulted in an acute inflammatory reaction in the pericardium with thickening and fibrous transformation of the visceral pericardial leaflet, as well as the formation of adhesions.

2) The development of acute pericarditis manifestations was accompanied by autophagy activation in epicardial and subepicardial cells.

The injection of Freund's adjuvant into the pericardial cavity resulted in chaotic redistribution of epicardial cells and significant thickening of the visceral pericardial leaflet. These changes are most likely caused by epicardial cells' ability to initiate epithelial-mesenchymal transition (EMT) in response to proinflammatory microenvironment factors, resulting in their cell cycle entry, enhanced migration ability, differentiation into fibroblasts/myofibroblasts, and matrix accumulation [22]. Furthermore, activated epicardium cells accumulated LC3 II protein involved in autophagosome assembly, indicating autophagy

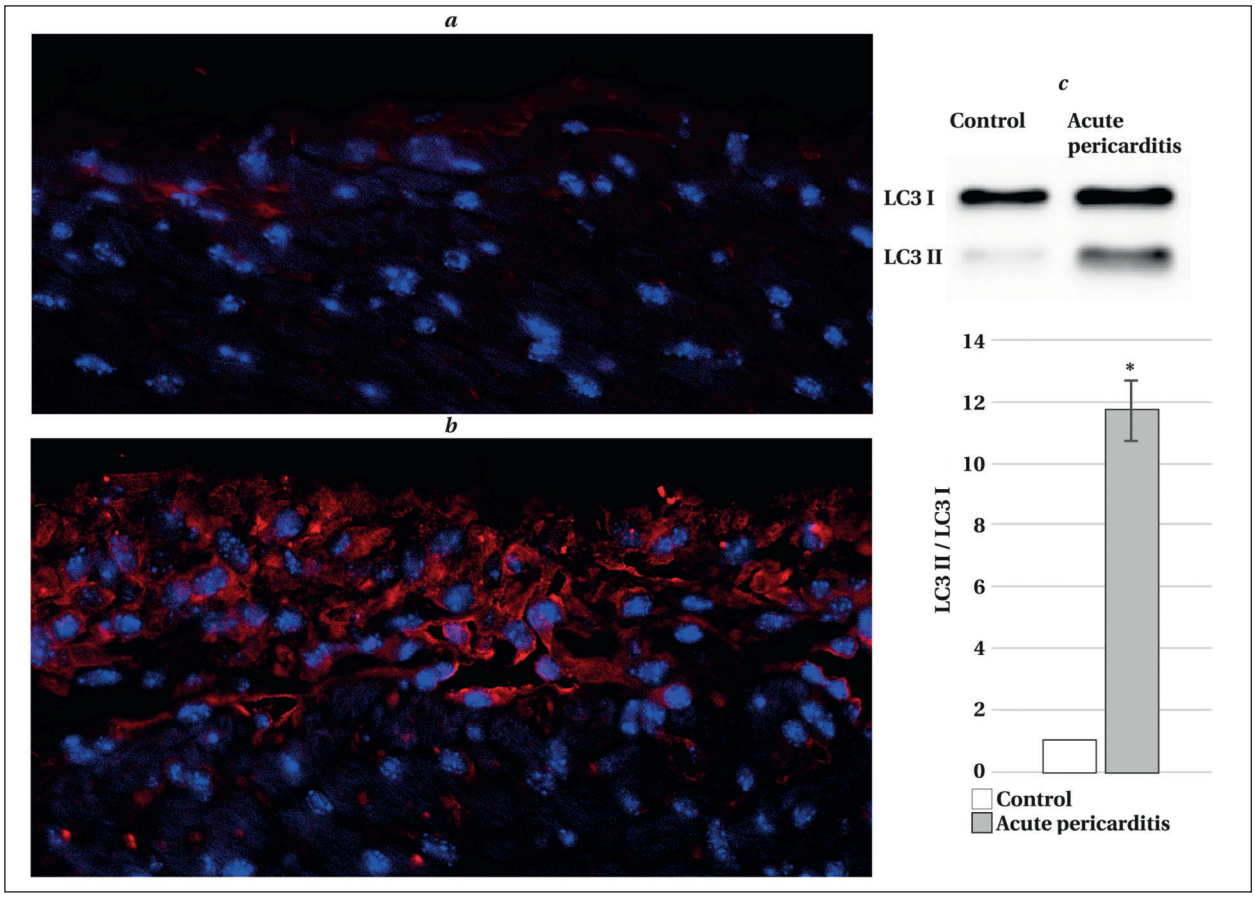

Fig. 2. Development of acute pericarditis induces increased expression of the autophagy marker LC3 in epicardial cells of the murine heart.

Note. Red color *(a, b)* indicates staining of autophagy marker LC3 II. *a* — control group (after FSB injection); *b* — after induction of acute pericarditis. *c* — evaluation of autophagy marker LC3 I and LC3 II expression by immunoblotting and graph. The ratio of LC3 II/LC3 I in the control was taken as 1. * *P*=0.04. Data are shown on day 5 after surgery.

activation, which is a highly conserved process aimed at cell development, differentiation, and adaptation to specialized microenvironmental conditions [23, 24]. These findings are consistent with previous research indicating that autophagy plays an important role in the regulation of the inflammatory response associated with fibrosis [25–27]. High autophagy activity has been linked to the development and maintenance of a proinflammatory microenvironment. Autophagy can regulate the secretion of cytokines like IL-1, IL-18, TNF-α, and IFNγ [28, 29]. Macrophages secrete the mature form of IL-1β in an unconventional manner, relying on chaperone-mediated autophagy that inhibits its secretion in the «baseline» state [30]. The IL-1β secreted by macrophages suppresses the transformation of fibroblasts into myofibroblasts. However, it also stimulates the synthesis of proinflammatory cytokines and matrix metalloproteinases (MMP), promoting inflammation and matrix remodeling [31].

According to the results of recent studies, there is still a strong scientific interest in studying the mechanisms of autophagy involvement in the development of fibrosis in various tissues [32, 33]. However, there is no information on the role of autophagy in the pathogenesis of acute pericarditis or the development of cardiac fibrosis. Meanwhile, the role of autophagy in the formation of myofibroblast pools, which are key players in progressive fibrosis, deserves attention. Suppression of autophagy prevents cardiac fibroblasts from transforming into myofibroblasts, resulting in decreased expression of αSMA and ED-A fibronectin, as well as decreased contractile and migratory activity [34]. In a recent study, autophagy was found to increase collagen I secretion by dermal fibroblasts [35].

Thus, autophagy activation observed during acute pericarditis may be linked to the development of fibrosis in the epicardial zone by promoting a proinflammatory microenvironment, fibroblast/myofibroblast formation, and collagen accumulation. Investigating the possibility of interfering with the progression of epicardial fibrosis by modulating autophagy levels may be a promising area of research for the development of new, highly effective treatments for pericarditis. New Zealand researchers have already taken the first steps in this direction by demonstrating the efficacy of the autophagy in-

hibitor hydroxychloroquine in the treatment of rheumatic pericarditis [36]. Russian researchers [37] confirmed the potential usefulness of hydroxychloroquine by showing that it reduces the severity of inflammation and effusion development in subacute and chronic pericarditis, both alone and in combination with low-dose steroids. According to these findings, autophagy may be a promising therapeutic target for pericardial inflammation.

Conclusion

Acute pericarditis is characterized by activation of epicardial mesothelial cells, increased autophagy activity, and fibrotic changes in the epicardial/subepicardial area.

More research is needed to determine if modulating autophagy can affect the development of acute pericarditis.

References

1. *Лутай Ю. А., Крючкова О. Н., Ицкова Е. А., Турна Э. Ю.* Современные подходы к диагностике и лечению перикардитов. Крымский терапевтический журнал. 2015; 4: 41–45. [*Lutay U. A., Kryuchkova O. N., Itskova E. A., Turna E. U.* Modern approaches to diagnosis and treatment of pericarditis. *Crimean Therapeutic Journal / Krymskiy Terapevticheskiy Zhurnal. 2015*; 4: 41–45. (in Russ.)].
2. *Демин А. А., Дробышева В. П.* Болезни перикарда. Российский кардиологический журнал. 2016; (1): 90–98. [*Dyomin A. A., Drobysheva V. P.* Pericardium diseases. *Russian Journal of Cardiology/ Rossiysky Kardiologichesky Zhurnal.* 2016; (1): 90–98. (in Russ.)]. DOI: 10.15829/1560-4071-2016-1-90-98.
3. *Adler Y., Charron P., Imazio M., Badano L., Barón-Esquivias G., Bogaert J., Brucato A., et al.* 2015 ESC Guidelines for the diagnosis and management of pericardial diseases: The Task Force for the diagnosis and management of pericardial diseases of the European Society of Cardiology (ESC) endorsed by: The European Association for Cardio-Thoracic Surgery (EACTS). *Eur Heart J.* 2015; 36 (42): 2921–2964. DOI: 10.1093/eurheartj/ehv318. PMID: 26320112.
4. *Косоногов А. Я., Немирова С. В., Поздышев В. И., Никольский А. В., Косоногов К. А., Рыбинский А. Д., Сидоров М. А., с соавт.* Жизнеугрожающие состояния при перикардитах различной этиологии: диагностика и лечение. *Медицинский альманах.* 2019; 2 (59): 40–45. [*Kosonogov A. Ya., Nemirova S. V., Pozdishev V. I., Nikolskiy A. B., Kosonogov K. A., Rybincky A. D., Sidorov M. A., et al.* Life-threatening conditions in pericarditis of different etiologies: diagnosis and treatment. *Medical Almanac/ Meditsinsky Almanah.* 2019; 2 (59): 40–45. (in Russ.)]. DOI: 10.21145/2499-9954-2019-2-40-45.
5. *He Y., Sawalha A. H.* Drug-induced lupus erythematosus: an update on drugs and mechanisms. *Curr Opin Rheumatol.* 2018; 30 (5): 490–497. DOI: 10.1097/BOR. 0000000000000522. PMID: 29870500.
6. *Zipes D. P., Libby P., Bonow R. O., Mann D. L., Braunwald E., Tomaselli G. F.* Braunwald's Heart disease: a textbook of cardiovascular medicine. Elsevier; 2019. https://books. google.ru/books?id=CJyjzQEACAAJ.
7. *Imazio M., Gaita F.* Diagnosis and treatment of pericarditis. *Heart.* 2015; 101 (14): 1159–1168. DOI: 10.1136/HEARTJNL-2014-306362. PMID: 25855795.
8. *Козлов И. А., Овезов А. М., Петровская Э. Л.* Периоперационные повреждение миокарда и сердечная недостаточность в некардиальной хирургии (обзор). Часть 1. Этиопатогенез и прогнозирование периоперационных кардиальных осложнений. *Obshchaya Reanimatologiya = General Reanimatology.* 2019; 15 (2): 53–78.[*Kozlov I. A., Ovezov A. M., Petrovskaya E. L.* Perioperative myocardial damage and heart failure in non-cardiac surgery. Part 1. Etiopathogenesis and prognosis of perioperative cardiac complications (review). *General Reanimatology/Obshchaya Reanimatologya.* 2019; 15 (2): 53–78. (in Russ&Eng.)]. DOI: 10.15360/1813-9779-2019-2-53-78.
9. *Козлов И. А., Овезов А. М., Петровская Э. Л.* Периоперационное повреждение миокарда и сердечная недостаточностьв некардиальной хирургии (обзор). Часть 2. Снижение риска периоперационных кардиальных осложнений с помощью фармакологических мер и оптимизации анестезиолого-реаниматологического обеспечения. *Obshchaya Reanimatologiya = General Reanimatology.* 2019; 15 (3): 83–101. [*Kozlov I. A., Ovezov A. M., Petrovskaya E. L.* Perioperative myocardial damage and heart failure in non-cardiac surgery Part 2. Reduction of the risk of perioperative cardiac complications by pharmacological measures and optimization of anesthetic and critical care support. (review). *General Reanimatology/Obshchaya Reanimatologya.* 2019; 15 (3): 83–101. (in Russ&Eng.)]. DOI: 10.15360/1813-9779-2019-3-83-101.
10. *Григорьев Е. В., Шукевич Д. Л., Плотников Г. П., Кудрявцев А. Н., Радивилко А. С.* Неудачи интенсивного лечения полиорганной недостаточности: патофизиология и потребность в персонификации (обзор литературы). *Вестник интенсивной терапии имени А. И. Салтанова.* 2019; (2): 48–57. [*Grigoriev E. V., Shukevich D. L., Plotnikov G. P., Kudryavtsev A. N., Radivilko A. S.* Failures of intensive treatment of multiple organ failure: pathophysiology and the need for personification (literature review). *Ann Crit Care /Vestnik Intensivnoy Terapii im AI Saltanova.* 2019; (2): 48–57. (in Russ.)]. DOI: 10.21320/18-474 X-2019–2–48–57.
11. *Deretic V., Klionsky D. J.* Autophagy and inflammation: A special review issue. *Autophagy.* 2018; 14 (2): 179–180. DOI: 10.1080/15548627.2017.1412229. PMID: 29304718.
12. *Qian M., Fang X., Wang X.* Autophagy and inflammation. *Clin Transl Med.* 2017; 6 (1): 24. DOI: 10.1186/s40169-017-0154-5. PMID: 28748360.
13. *Yamamoto H., Zhang S., Mizushima N.* Autophagy genes in biology and disease. *Nat Rev Genet.* 2023; 24 (6): 382–400. DOI: 10.1038/S41576-022-00562-W. PMID: 36635405.
14. *Vargas J. N. S., Hamasaki M., Kawabata T., Youle R. J., Yoshimori T.* The mechanisms and roles of selective autophagy in mammals. *Nat Rev Mol Cell Biol.* 2023; 24 (3): 167–185. DOI: 10.1038/s41580-022-00542-2. PMID: 36302887.
15. *Богданов Л. А., Шишкова Д. К., Кутихин А. Г.* Сравнение различных видов прогрессивных гематоксилинов при окрашивании элементов системы кровообращения и гепатолиенальной системы. *Сибирский научный медицинский журнал.* 2019; 39 (6): 46–54.[*Bogdanov L. A., Shishkova D. K., Kutikhin A. G.* Different progressive hematoxylin stains for histological examination of myocardium, blood vessels, liver and spleen. *Siberian Scientific Medical Journal/ Sibirskiy Nauchnyy Meditsinskiy Zhurnal.* 2019; 39 (6): 46–54. In Russ.)]. DOI: 10.15372/SSMJ20190606.
16. *Dergilev K. V., Makarevich P. I., Tsokolaeva Z. I., Boldyreva M. A., Beloglazova I. B., Zubkova E. S., Menshikov M. Y., et al.* Comparison of cardiac stem cell sheets detached by Versene solution and from thermoresponsive dishes reveals similar properties of constructs. *Tissue Cell.* 2017; 49 (1): 64–71. DOI: 10.1016/j.tice.2016.12.001. PMID: 28041835.
17. *Дергилев К. В., Цоколаева З. И., Рыжков И. А., Парфенова Е. В.* Трансплантация пластов мезенхималь-

ных прогениторных клеток сердца для васкуляризации миокарда после инфаркта. *Obshchaya Reanimatologiya = General Reanimatology.* 2018; 14 (6): 28–40. [*Dergilev K. V., Tsokolaeva Z. I., Ryzhkov I. A., Parfenova E. V.* Transplantation of cardiac mesenchymal progenitor cell sheets for myocardial vascularization after an infarction. *General Reanimatology/Obshchaya Reanimatologya.* 2018; 14 (6): 28–40. (in Russ&Eng.)]. DOI: 10.15360/1813-9779-2018-6-28-40.

18. *Дергилев К. В., Цоколаева З. И., Василец Ю. Д., Белоглазова И. Б., Парфенова Е. В.* Клеточные пласты на основе кардиальных прогениторных клеток продуцируют проангиогенные факторы роста и оказывают локальное стимулирующее воздействие на формирование капилляров после инфаркта миокарда. *Комплексные проблемы сердечно-сосудистых заболеваний.* 2021; 10 (3): 34–43. [*Dergilev K. V., Tsokolaeva Z. I., Vasilets Yu. D., Beloglazova I. B., Parfenova E. V.* Cardiac progenitor cell sheets secrete proangiogenic growth factors and locally activate capillarogenesis after infarction. *Complex Issues of Cardiovascular Diseases/Kompleksnye Problemy Serdechno-Sosudistykh Zabolevany.* 2021; 10 (3): 34–43. (in Russ.)]. DOI: 10.17802/2306-1278-2021-10-3-34-43.
19. *Shahid R., Jin J., Hope K., Tunuguntla H., Amdani S.* Pediatric pericarditis: update. *Curr Cardiol Rep.* 2023; 25 (3): 157–170. DOI: 10.1007/s11886-023-01839-0. PMID: 36749541.
20. *Mohan T., Tressa J. M., Ushasree P., Tharani P., Muzaffar A.* Myocarditis and pericarditis. *Innov Technol Sci Educ.* 2023; 2 (9): 1885–1896.
21. *Kosmopoulos M., Liatsou E., Theochari C., Stavropoulos A., Chatzopoulou D., Mylonas K. S., Georgiopoulos G., et al.* Updates on the global prevalence and etiology of constrictive pericarditis: a systematic review. *Cardiol Rev.* 2023. DOI: 10.1097/CRD.0000000000000529. PMID: 36883817.
22. *Li J., Takasato M., Xu Q., Bijkerk R.* Editorial: epithelial plasticity and complexity in development, disease and regeneration. *Front Cell Dev Biol.* 2023; 10: 1105402. DOI: 10.3389/fcell. 2022.1105402. PMID: 36712966.
23. *Popov S. V., Mukhomedzyanov A. V., Voronkov N. S., Derkachev I. A., Boshchenko A. A., Fu F., Sufianova G. Z., et al.* Regulation of autophagy of the heart in ischemia and reperfusion. *Apoptosis.* 2023; 28 (1–2): 55–80. DOI: 10.1007/s10495-022-01786-1.PMID: 36369366.
24. *Wang Y., Gao J., Fan B., Hu Y., Yang Y., Wu Y., Li F., et al.* Different levels of autophagy induced by transient serum starvation regulate metabolism and differentiation of porcine skeletal muscle satellite cells. *Sci Rep.* 2023; 13 (1): 13153. DOI: 10.1038/S41598-023-40350-Y. PMID: 37573414.
25. *Ruby M., Gifford C. C., Pandey R. P., Raj V. S., Sabbisetti V. S., Ajay A. K.* Autophagy as a therapeutic target for chronic kidney disease and the roles of TGF-β1 in autophagy and kidney fibrosis. *Cells.* 2023; 12 (3): 412. DOI: 10.3390/ cells12030412. PMID: 36766754.
26. *Macias-Ceja D. C., Barrachina M. D., Ortiz-Masià D.* Autophagy in intestinal fibrosis: relevance in inflammatory bowel disease. *Front Pharmacol.* 2023; 14: 1170436. DOI: 10.3389/fphar.2023. 1170436. PMID: 37397491.
27. *Su H. Y., Yang J. J., Zou R., An N., Chen X.-C., Yang C., Yang H.-J., et al.* Autophagy in peritoneal fibrosis. *Front Physiol.* 2023; 14: 1187207. DOI: 10.3389/fphys. 2023. 1187207. PMID: 37256065.
28. *Weigert A., Herhaus L.* Immune modulation through secretory autophagy. *J Cell Biochem.* Published online 2023. DOI: 10.1002/jcb.30427. PMID: 37260061.
29. *Zuo H., Chen C., Sa Y.* Therapeutic potential of autophagy in immunity and inflammation: current and future perspectives. *Pharmacol Reports.* 2023; 75 (3): 499–510. DOI: 10.1007/s43440-023-00486-0. PMID: 37119445.
30. *Dupont N., Jiang S., Pilli M., Ornatowski W., Bhattacharya D., Deretic V.* Autophagy-based unconventional secretory pathway for extracellular delivery of IL-1β. *EMBO J.* 2011; 30 (23): 4701–4711. DOI: 10.1038/emboj.2011.398. PMID: 22068051.
31. *Frangogiannis N. G.* Interleukin-1 in cardiac injury, repair, and remodeling: pathophysiologic and translational concepts. *Discoveries.* 2015; 3 (1): e41. DOI: 10.15190/d.2015.33. PMID: 26273700.
32. *Wen J.-H., Li D.-Y., Liang S., Yang C., Tang J.-X., Liu H.-F.* Macrophage autophagy in macrophage polarization, chronic inflammation and organ fibrosis. *Front Immunol.* 2022; 13: 946832. DOI: 10.3389/fimmu. 2022.946832. PMID: 36275654.
33. *Dai R., Zhang L., Jin H., Wang D., Cheng M., Sang T., Peng C., et al.* Autophagy in renal fibrosis: protection or promotion? *Front Pharmacol.* 2022; 13: 963920. DOI: 10.3389/fphar.2022. 963920. PMID: 36105212.
34. *Gupta S. S., Zeglinski M. R., Rattan S. G., Landry N. M., Ghavami S., Wigle J. T., Klonisch T., et al.* Inhibition of autophagy inhibits the conversion of cardiac fibroblasts to cardiac myofibroblasts. *Oncotarget.* 2016; 7 (48): 78516–78531. DOI: 10.18632/ONCOTARGET.12392. PMID: 27705938.
35. *Nakamura T., Yamashita M., Ikegami K., Suzuki M., Yanagita M., Kitagaki J., Kitamura M., et al.* Autophagy facilitates type I collagen synthesis in periodontal ligament cells. *Sci Rep.* 2021; 11 (1): 1291. DOI: 10.1038/ s41598-020-80275-4. PMID: 33446772.
36. *Wilson N. J., Concannon A., Malcolm J., Davidakova S., Martin W. J., Webb R., Moreland N. J.* The Treatment of acute rheumatic fever: novel use of hydroxychloroquine. *Pediatr Infect Dis J.* 2020; 39 (7): e120-e122. DOI: 10.1097/INF.000000 0000002647. PMID: 32221169.
37. *Благова О. В., Сорокин Г. Ю., Седов В. П., Коган Е. А., Саркисова Н. Д., Недоступ А. В.* Инфекционно-иммунные перикардиты: оценка клинического спектра, возможности диагностики, дифференцированная базисная терапия с применением гидроксихлорохина. *Российский кардиологический журнал.* 2020; 25 (11): 11–22. [*Blagova O. V., Sorokin G.Yu., Sedov V. P., Kogan E. A., Sarkisova N. D., Nedostup A. V.* Infectious-immune pericarditis: clinical assessment, diagnostic, and differentiated baseline therapy with hydroxychloroquine. *Russian Journal of Cardiology/ Rossiysky Kardiologichesky Zhurnal*; 25 (11): 11–22. (in Russ.)]. DOI: 10.15829/29/1560-4071-2020-3840.

Received 29.09.2023
Accepted 29.11.2023
Online first 20.12.2023

https://doi.org/10.15360/1813-9779-2024-1-2351

The Effect of High Nitric Oxide Concentrations on Oxygenators in Cardiopulmonary Bypass Machines (Experimental Study)

Alexey M. Radovskiy[1]*, Ilya V. Vorotyntsev[2], Artem A. Atlaskin[2], Anton N. Petukhov[2], Sergey S. Kryuchkov[2], Maria E. Atlaskina[2], Anna N. Stepakova[2], Alexander O. Marichev[1], Egor K. Barygin[1], Victor V. Osovskikh[1], Victor D. Selemir[3], Sergey N. Buranov[3], Vladimir V. Golovanov[3], Alexander S. Shirshin[3], Yulia V. Valueva[3], Vladimir V. Pichugin[4], Stepan E. Domnin[5], Andrey E. Bautin[1]*

[1] Almazov National Medical Research Center,
2 Akkuratova str., Saint-Petersburg 197341, Russia
[2] Mendeleev University of Chemical Technology of Russia,
9 Miusskaya sq., Moscow 125047, Russia
[3] Russian Federal Nuclear Center, All-Russian Scientific Research Institute of Experimental Physics,
37 Mira av., Sarov 607188, Russia
[4] Privolzhsky Research Medical University,
10/1, Minin and Pozharsky square, Nizhniy Novgorod 603005, Russia
[5] Research Institute «Specialized Cardiosurgical Clinical Hospital named after Academician B. A. Koroleva»,
209 Vaneeva street, Nizhny Novgorod 603950, Russia

For citation: *Alexey M. Radovskiy, Ilya V. Vorotyntsev, Artem A. Atlaskin, Anton N. Petukhov, Sergey S. Kryuchkov, Maria E. Atlaskina, Anna N. Stepakova, Alexander O. Marichev, Egor K. Barygin, Victor V. Osovskikh, Victor D. Selemir, Sergey N. Buranov, Vladimir V. Golovanov, Alexander S. Shirshin, Yulia V. Valueva, Vladimir V. Pichugin, Stepan E. Domnin, Andrey E. Bautin.* The Effect of High Nitric Oxide Concentrations on Oxygenators in Cardiopulmonary Bypass Machines. *Obshchaya Reanimatologiya = General Reanimatology.* 2024; 20 (1): 50–62. https://doi.org/10.15360/1813-9779-2024-1-2351 [In Russ. and Engl.]

***Correspondence to:** Alexey M. Radovskiy, svetlbii@mail.ru; Andrey E. Bautin, abautin@mail.ru

Summary

The aim of the study. To study the effect of high nitric oxide concentrations on hollow polypropylene fibers of oxygenators.

Materials and methods. The study was conducted in two stages. At the first stage, we evaluated the stability of oxygenator membrane made of hollow polypropylene fibers after six hours of exposure to air-oxygen mixture containing NO at 500 parts per million, or 500 pro pro mille (ppm) concentration, using mass spectrometry and infrared spectroscopy. At the second stage, an experiment with cardiopulmonary bypass (CPB) was conducted on 10 pigs. In the study group (*N*=5) animals sweep gas was supplied to the oxygenator as an air-oxygen mixture with NO at 100 ppm. In the control group animals (*N*=5) an air-oxygen mixture was used without NO. The CPB lasted for 4 hours, followed by observation for 12 hours. NO, NO_2 (at the inlet and outlet of the oxygenator), and the dynamics of methemoglobin were evaluated. After weaning of animals from CPB, the oxygenators were tested for leakproofness, and scanning electron microscopy (SEM) was performed.

Results. The oxygenator made of polypropylene hollow fibers retained its gas transfer parameters after six hours of exposure to air-oxygen mixture containing NO at 500 ppm. Based on IR-Fourier spectroscopy findings, NO did not affect structural integrity of polypropylene membranes. NO added to gas mixture at 100 ppm did not increase NO_2 to toxic level of 2 ppm in 91% of control tests during 4 hours CPB in pigs; mean value was 1.58±0.28 ppm. Methemoglobin concentration did not exceed the upper limit of permissible level (3%), and there were no statistically significant differences with the control group. All tested oxygenators have passed the leakproofness test. According to SEM findings, larger amounts of fibrin deposits were found in the control group oxygenators vs study group.

Conclusion. There were no negative effects of NO at 500 ppm concentration on the oxygenator membrane made of hollow polypropylene fibers. NO at 100 ppm in a gas-mixture supplied to oxygenators did not lead to an exceedance of safe NO_2 and methemoglobin concentrations in an animal model. Reduced fibrin deposits on hollow fibers of polypropylene oxygenator membranes were observed when with NO at a level of 100 ppm was added to a gas mixture.

Keywords: nitric oxide; cardio-pulmonary bypass; oxygenator; polypropylene hollow fibers; cardiac surgery.

Conflict of interest. The authors declare no conflict of interest.

Funding and Support. The research was carried out with the support and in cooperation with the Russian Federal Nuclear Center, All-Russian Scientific Research Institute of Experimental Physics under the contract SD-22-04-48 for performance of a constituent part of the research. Part of this research was carried out within the framework of the State task No. 123021000129-1 implementation «Development of a new device for supplying nitric oxide synthesized from ambient air to heart-lung and auxiliary blood circulation devices».

Introduction

The vast majority of cardiac surgery is performed under cardiopulmonary bypass (CPB) [1]. Despite improvements in perfusion techniques and the development of safer equipment and supplies, CPB remains a non-physiologic procedure and has adverse effects on the human body. Negative effects of CPB include systemic inflammatory response syndrome, ischemia and reperfusion injury, and blood cell damage leading to hemolysis [2–4]. Cell-free hemoglobin (cfHb) resulting from hemolysis is removed from the circulation by haptoglobin, the CD163 protein. When the intravascular mechanisms for removing cfHb are exhausted, its level in the blood rises, with adverse clinical consequences. The heme formed during the degradation of cfHb is a cytotoxic pro-oxidant that catalyzes the formation of free radicals [5]. In addition, the negative effects of cfHb are realized indirectly through the binding of endogenous nitric oxide (NO), which leads to endothelial dysfunction, impaired microcirculation, and promotes stimulation of leukocyte adhesion [6]. Arginase released during hemolysis catalyzes the synthesis of ornithine from l-arginine, a substrate for NO production, thereby reducing NO bioavailability [7].

NO can oxidize cfHb to the less toxic methemoglobin, thereby exerting organoprotective effects [8]. In addition, NO has anti-adhesive properties against leukocytes and platelets, which determines its anti-inflammatory potential [9, 10]. Through interactions with proteins such as soluble guanylate cyclase, protein kinase G, and mitochondrial K-ATP channels, NO has been shown to exert a protective effect under conditions of ischemia and reperfusion injury [11]. Given the likely deficiency and reduced bioavailability of NO in patients undergoing CPB, this may provide a rationale for adding this gas to the oxygenator to directly affect the blood and potentially improve clinical outcomes in cardiac surgery.

In recent years, the number of experimental and clinical studies investigating the properties of NO when added to an CPB oxygenator has increased significantly [12, 13]. However, the studies aimed at analyzing the interaction of NO with polypropylene, a polymer of hollow fibers of oxygenator membranes, are insufficient. For example, we are aware of only one study that examined the effect of nitric oxide on the gas exchange and structural integrity of a polypropylene membrane oxygenator. This study showed that NO and its byproduct NO_2 did not affect the structural integrity or gas exchange in a polypropylene membrane oxygenator during 6 hours of CPB *in vitro* [14].

In view of the above, the aim of this study was to investigate the effect of high concentrations of nitric oxide on polypropylene hollow fibers of oxygenators of CPB devices.

Materials and Methods

The study was conducted in two stages. In the first stage, the stability of hollow polypropylene fiber oxygenator membranes in the presence of NO in an air-oxygen mixture was evaluated. For this purpose, their mass transfer characteristics were extensively studied using an experimental unit coupled with a mass spectrometry system. The membrane material was then characterized by infrared spectroscopy. In the second step, an animal experiment was performed using a CPB machine, where an oxygen-air mixture containing NO at a concentration of 100 parts per million (ppm) was supplied.

Comprehensive stability testing of hollow polypropylene fiber membranes in the presence of air-oxygen gas mixture containing NO. The research was carried out in the world-class SMART Laboratory of Polymer Materials and Technologies of D. I. Mendeleev Russian University of Chemical Technology. We developed a unique experimental bench for testing the stability of the polypropylene hollow fiber membrane of the Inspire 8M Sorin oxygenator (LivaNova, Italy) in a gas mixture containing NO (its schematic diagram is shown in Fig. 1).

The experimental bench included a system of gas flow regulators connected to the mixing chamber, a thermostated container of distilled water, a container of 0.9% saline solution, an analytical complex represented by a mass spectrometer with two vacuum stations.

A reciprocating air compressor Remeza SB4/C-24.OLD10 (Remeza, Belarus) with built-in pressure regulator provided compressed air supply through the filtration system (mechanical filter, water separation unit) into the gas flow regulator Bronkhorst El-Flow Prestige (Bronkhorst, Netherlands), then compressed air with known flow rate was supplied to the mixing chamber. Oxygen was also delivered through a gas reducer to a similar gas flow controller, which in turn communicated with the mixing chamber. The gas mixture of N_2 and NO was injected in a similar manner. Thus, the gas mixture to be injected into the membrane contactor was prepared by dynamic flow mixing. The 0.9% NaCl solution was pumped from a glass container to the oxygenation system.

Thus, as a result of simultaneous injection of gas mixture and 0.9% NaCl solution into the oxygenation system at the membrane contactor (hollow fiber membrane of the oxygenator), the contact of two phases was implemented. The components of the gas mixture were partially dissolved in the 0.9% NaCl solution, and the undissolved part of the gas mixture was removed from the membrane contactor unit through a special nipple installed on the body of the oxygenator. The nipple was connected to a

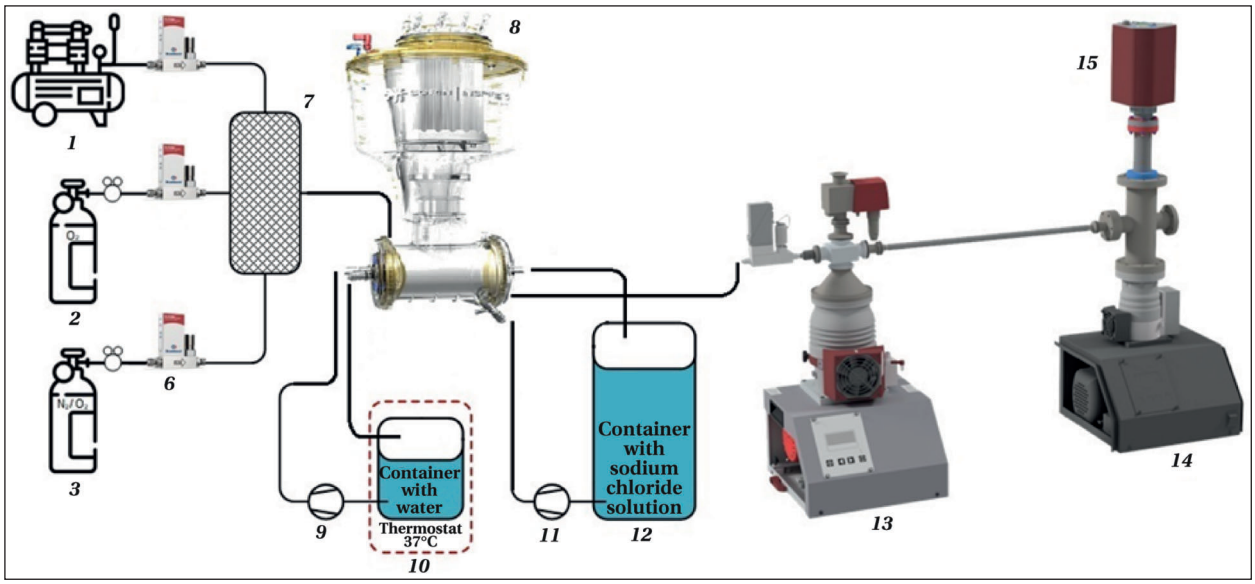

Fig. 1. Schematic diagram of the experimental bench for membrane contactor stability testing.
Note. *1* — air compressor; *2* — cylinder with O_2; *3* — cylinder with mixture of N_2 and NO; *4, 5, 6* — gas flow regulators; *7* — mixing chamber; *8* — oxygenation system; *9, 11* — pumps; *10* — thermostated container with distilled water; *12* — container with 0.9% NaCl solution; *13* — high performance vacuum station; *14* — high vacuum station; *15* — mass spectrometer.

high-precision Bronkhorst El-Flow Metal Sealed gas flow regulator (Bronkhorst, The Netherlands) through which the gas mixture leaving the membrane contactor was injected into the analytical complex. The analytical complex consisted of a Pfeiffer PrismaPro QMG 250 M2, 1-200 u mass spectrometer (Pfeiffer, Germany) coupled with a Pfeiffer HiCube 300 H Eco high vacuum station (Pfeiffer, Germany) for creating a vacuum in front of the mass spectrometer chamber and a Pfeiffer HiCube 80 Eco high vacuum station (Pfeiffer, Germany) for creating a high vacuum directly in the mass spectrometer chamber. The official software developed by the manufacturer Bronkhorst (Netherlands) was used to control the gas flow control system.

First, a simulation of the operating mode was performed, which implied the introduction of a gas mixture of N_2/O_2 = 50/50 vol.% and 0.9% NaCl solution into the oxygenation system for 6 hours. The composition of the gas mixture at the outlet of the membrane contactor of the oxygenation system was measured as a function of the duration of the experiment. Throughout the experiment, the dependence of the composition of the gas mixture at the outlet of the membrane contactor of the oxygenation system on the duration of the experiment was recorded using a mass spectrometric complex. In this way, we determined the composition of the gas mixture in the stationary mode of operation of the oxygenator, which allowed us to determine the separation factor of the system.

Furthermore, the gas mixture $N_2/O_2/NO$ in the ratio of 49.975/49.975/0.05 vol.% and 0.9% NaCl solution was fed into the system, which was preliminarily operated under the mixture N_2/O_2 of 50/50 vol.%. The rest of the experimental conditions were similar to those described above. As in the previous case, the dependence of the concentrations of the gas mixture components on the duration of the experiment was determined throughout the experiment. Since the NO concentration in the feed stream was low (0.05 vol.% (500 ppm)), this value in the gas stream leaving the oxygenator could not be representative. Under these circumstances, the change in gas transport characteristics (separation factor) was evaluated by the change in nitrogen and oxygen concentrations normalized to 100%.

To evaluate the stability of the membrane contactor (hollow fiber membrane of the oxygenator), a parameter characterizing the mass transfer in the system as a whole was used. Such a parameter was the separation factor, which was calculated from the ratio of the concentrations of the components of the mixture in two different gas streams of the system. According to the results of determining the dependence of N_2 and O_2 concentrations in the gas stream leaving the membrane contactor unit of the system, the composition of the gas mixture in the steady state (stationary) mode of operation was determined.

Based on these experimental data, the separation factor was calculated using the following formula:

$$SF = \frac{x_{N_2,r}/x_{O_2,r}}{x_{N_2,f}/x_{O_2,f}}$$

where $x_{N2,r}$ — nitrogen concentration in the retentate flow vol.%; $x_{O2,r}$ — oxygen concentration in

retentate flow, vol.%; $x_{N2,f}$ — nitrogen concentration in the feed stream, vol.%; $x_{O2,f}$ — oxygen concentration in the feed stream, vol.%. In this case, the gas stream leaving the membrane unit of the oxygenation system was the retentate stream. Thus, to determine the separation factor of the system, the ratio of N_2 to O_2 concentration in the retentate stream and feed stream was calculated.

Fourier transform infrared spectra in the range of 4000–700 cm^{-1} were recorded for additional testing of the membranes and to investigate the possible chemical interactions with NO. The analysis was performed on an IRAffinity-1 instrument (Shimadzu, Kyoto, Japan) at ambient temperature with a resolution of 4 cm^{-1} using an HATR accessory (Pike, USA). An Inspire 8M Sorin polypropylene hollow fiber oxygenator membrane (LivaNova, Italy) was used in this study. Twenty scans were signal-averaged to obtain the results.

Experimental animal study using NO-containing air-oxygen mixture delivered to the oxygenator of the heart-lung machine. This study was approved by the Bioethics Committee of the Almazov National Medical Research Center (protocol PZ_22_6_V2 dated 08.06.2022) and was conducted at the Center for Preclinical Translational Research of the Almazov National Medical Research Center.

Animals. Ten female domestic landrace pigs, aged 3 to 4.3 months, were included in the study. The mean body weight was 38.9 (37.7; 40.9) kg. The animals were divided into two groups, control and experimental. In the experimental group, 100 ppm NO was added to the air-oxygen mixture in the oxygenator during CPB. No NO was added to the oxygenator in control group animals. All animals underwent CPB for 4 hours and were observed for 12 hours. All animals were then removed from the experiment.

Anesthesia and perfusion support. Combined anesthesia was performed using general combined anesthesia and regional anesthesia (intercostal nerve block). Premedication included an intramuscular injection of zolazepam/tiletamine (Zoletil Virbac, France) 20 mg/kg. Under aseptic conditions, the peripheral vein (auricular vein) was punctured and catheterized with an 18–20 G catheter. After induction of anesthesia with propofol (Propofol-Lipuro, B. Braun, Germany) 2–3 mg/kg, direct laryngoscopy and tracheal intubation were performed. After tracheal intubation, the non-depolarizing myorelaxant rocuronium bromide was administered at a dose of 0.6–1.2 mg/kg. Anesthesia was maintained by inhalation of 1.5–2.5 vol.% isoflurane (Aerran Baxter Healthcare Corporation, USA) using a Heyer Medical AG vaporizer (Dräger, Germany). Jugular vein catheterization was performed under ultrasound guidance in all animals to ensure central venous pressure (CVP) monitoring and drug infusion. Invasive blood pressure (BP) monitoring was performed by femoral artery catheterization with a 20G B. Braun catheter (20G B. Braun) using the Seldinger technique. A 10-F Nelaton urinary catheter was inserted to control the rate and pattern of urine flow.

Vital signs were monitored using the Mindray BeneView T8 monitoring system (Mindray, PRC). Monitoring during the experiment included pulse oximetry, electrocardiography (ECG), measurement of central temperature, invasive BP and CVP, gas composition of the inhaled and exhaled mixture, and respiratory rate (RR).

Mechanical lung ventilation (MLV) was performed in normal and normocapnic modes. Mindray Wato Ex-35 anesthesia-breathing circuit (Mindray, PRC) was used for ventilation. The following parameters of intraoperative ventilatory support were used: volume-controlled ventilation (VCV) mode, tidal volume (Vt) 20–30 ml/kg/min, RR 8–14 per minute, and fraction of inspired oxygen (FiO_2) 65%. Ventilation parameters were adjusted based on the results of oximetry, capnometry and arterial blood gas analysis.

Before the main phase of the operation, the regional component of combined anesthesia was administered using nerve block with ropivacaine (Ropivacaine, Pharmzashchita, Russia) at a dose of 5 mg/kg.

Cardiopulmonary bypass during the experiment was provided by a WEL-1000B Plus device (Tianjin Welcome Medical Equipment, PRC) using an Inspire 8M Sorin oxygenator (LivaNova, Italy). Perfusion safety was ensured by monitoring the pressure in the blood lines, the blood level sensor in the cardiotomy reservoir, and the gas bubble sensor. The mandatory components of the primary filling volume (prime) of the extracorporeal circuit were gelofusin (Gelofusin, B. Braun, Germany), heparin (Heparin sodium Braun, B. Braun, Germany) at a dose of 3 U/mL prime and sodium bicarbonate for pH normalization at a dose of 3 mmol/100 mL prime. Heparin was injected at a dose of 300 U/kg prior to CPB. Activated coagulation time (ACT) was measured 5 minutes after heparin administration and CPB was started when target values were reached (ACT>480 sec). The volume perfusion rate was 3 L/min/m^2. The initial gas flow was 2 L/min and was adjusted based on blood gas analysis. Blood gas control was performed in α-stat mode. To maintain hypocoagulation, heparin was administered as needed at a dose of 100–200 units/kg, and ACT was measured every 30 minutes. Adequacy of CPB was assessed by mean blood pressure (50–80 mm Hg), blood gas analysis, and acid-base balance. Normal temperature was maintained with a heat exchanger connected to the oxygenator with a target temperature of 37.5–38°C. Heparin reversal with protamine sulfate was avoided in favor of thorough surgical hemostasis. If protamine sulfate (Protamine Sulfate, Ellara, Russia) was used, its dose was cal-

culated on the basis of a ratio of 1–1.3 mg of protamine sulfate per 100 units of heparin initially administered. The calculated dose of protamine sulfate was administered over 20 minutes.

In the postoperative period, all animals received prolonged inhalational anesthesia with isoflurane and stable hemodynamic parameters were maintained. Protective ventilation, inotropic and vasopressor support were provided as indicated. Vital signs monitoring was continued.

Surgical procedure. A left-sided thoracotomy was performed in the 3rd intercostal space. After reaching the target level of hypocoagulation, an aortic cannula was successively inserted into the ascending aorta (20 Fr aortic cannula, Medtronic, USA) and a venous cannula into the right atrial cavity through the auricle (31 Fr venous cannula, Medtronic, USA). After weaning from CPB and removal of the cannula, hemostasis was checked. After drainage into the left pleural cavity with entry into the pericardial cavity, the wound was sutured layer by layer.

NO supply to the CPB circuit. In the experimental group of animals, during the whole period of CPB, synthesized NO from the experimental sample of the plasma-chemical synthesis unit was fed into the main line of air-oxygen mixture delivery to the oxygenator at 100 ppm [15, 16]. Animals of the control group were supplied with air-oxygen mixture without NO through the CPB oxygenator. The air-oxygen mixture was delivered to the «gas in» port of the oxygenator through ¼ diameter PVC tubing. Three-way stopcocks Discofix C (B. Braun, Germany) were previously installed in the supply line: a NO supply tube was connected 10 cm before the oxygenator and a tube for monitoring NO and NO_2 concentrations was connected 5 cm after the oxygenator (Fig. 2).

To control the gas composition of the mixture supplied to the oxygenator, NO and NO_2 were monitored both before and after the oxygenator. The upper limit for NO_2 in the oxygenator circuit was set at 2 ppm. If this value was exceeded, the supply of NO was stopped. The levels of NO and NO_2 in the gas mixture supply line to the oxygenator were continuously monitored. NO and NO_2 levels at the oxygenator outlet were monitored discreetly at 30-minute intervals.

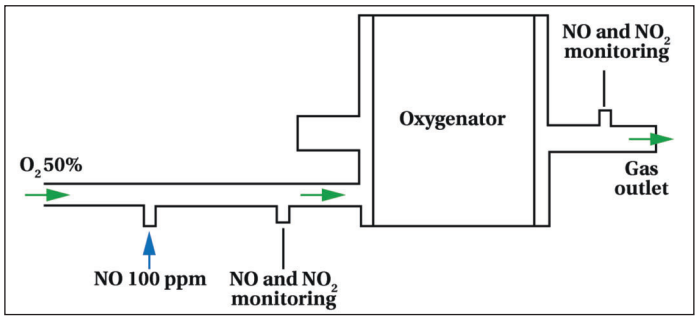

Fig. 2. Scheme of supply of air-oxygen mixture and NO to the oxygenator and monitoring of NO, NO_2.

Methemoglobin concentration determination. To assess the safety of high-dose NO delivery to the oxygenator, methemoglobin levels were analyzed. Its changes were studied at three time points: 2 hours after the start of CPB, at weaning from CPB, 6 hours after weaning.

Testing for leakage of the samples of membrane contactors of oxygenators. Samples of Inspire 8M polypropylene oxygenators (LivaNova, Italy) were leak tested to detect internal damage to the oxygenator. Simultaneous injection of compressed air and 0.9% NaCl solution into the oxygenation system in the membrane contactor simulated the working process. As part of the experiment, the gas pressure was gradually increased from 0.1 to 0.5 megapascals (MPa) in increments of 0.1 MPa. Thus, two phases such as pressurized gas and 0.9% NaCl solution contacted through the porous membrane. The gas dissolved in the 0.9% NaCl solution was desorbed in the container from which the solution was injected. 3 samples of Inspire 8M oxygenators previously used in animal studies (2 from the main group, 1 from the control group) were tested for leakage.

Scanning electron microscopy of the surface of hollow fiber samples of membrane contactors. The surface of hollow fiber samples of polypropylene oxygenator membranes used during CPB in experimental animals was analyzed by scanning electron microscopy (SEM). Three Inspire 8M oxygenator membrane samples (2 from the main group, 1 from the control group) were examined. After weaning from CPB, the oxygenators were washed with 10 liters of 0.9% NaCl solution and then filled with 2% glutaric aldehyde for fixation [13]. A JEOL 1610LV scanning electron microscope (JEOL, Japan) was used. As a result, a series of microphotographs of the hollow fiber surface were obtained at different magnifications ranging from ×45 to ×15,000.

Statistical analysis was performed using the MedCalc Statistical Software 20.218 package (MedCalc Software Ltd, Belgium). Because of the small sample size, nonparametric methods were used. The Mann–Whitney *U* criterion for independent groups and the Wilcoxon test for dependent groups were used to compare numerical parameters. Multigroup comparisons were performed using the Bonferroni correction. Data were presented as median *(Q1; Q3)*. A two-sided *P* level of significance was used. The critical level of significance was set at *P*=0.05.

Results

Extensive testing of the stability of polypropylene oxygenator membranes in the presence of an air-oxygen mixture containing NO.

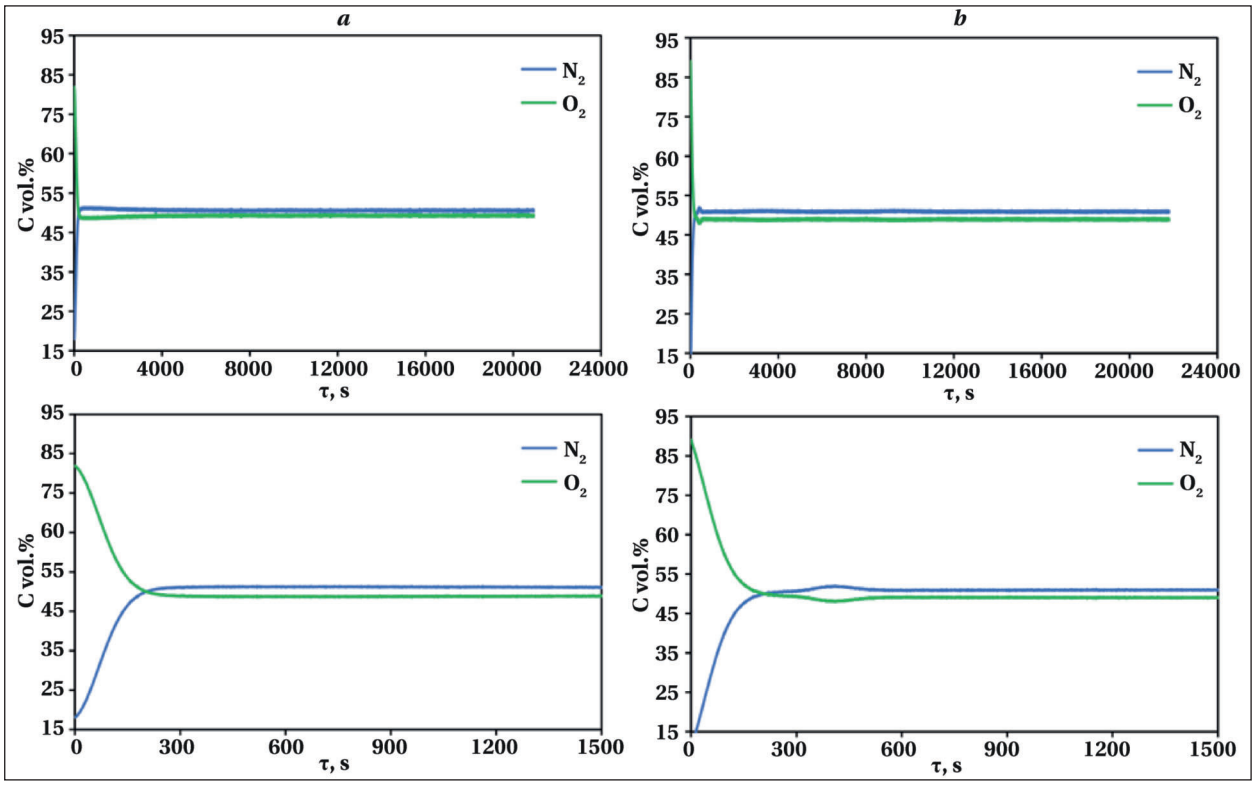

Fig. 3. Relationship between the concentration (vol.%) of N_2 and O_2 in the outlet flow of the Inspire 8M membrane unit and the time of the experiment.

Note. Simulation of the working process using 0.9% NaCl water solution with passing of gas mixture of *(a)* N_2/O_2 50/50 vol.%; *(b)* N_2/O_2/NO 49.975/49.975/0.05 vol.%.

Determination of gas transport characteristics of polypropylene oxygenator. According to the results of the analysis of the composition of the gas stream leaving the membrane unit of the oxygenator, the concentrations of N_2 and O_2 in the steady state of operation of the oxygenator were determined. The graphs of the changes in the concentrations of N_2 and O_2 in the gas stream leaving the membrane unit of the oxygenation system, depending on the duration of the experiment, are shown in Fig. 3.3. The results showed that the composition of the gas mixture leaving the membrane unit of the oxygenation system had a slight difference from the raw stream, i. e., the concentration of N_2 increased by 0.83 vol.%. When comparing the composition of gas mixtures at the outlet of the oxygenator for N_2/O_2 and N_2/O_2/NO mixtures, a minor increase in N_2 concentration (by 0.38 vol.%) was found. In addition to the graphs of the dependence of the composition of the gas mixture on the duration of the experiment, Fig. 4 shows the mass spectra of the gas mixture at the outlet of the membrane unit of the oxygenator. During the experiment with the gas mixture containing NO, a characteristic peak at m/z = 30 was detected in the mass spectra, confirming the presence of this component in the system. The averaged values of N_2 and O_2 concentrations in the gas stream leaving the membrane unit of the oxygenation system (for steady-state operation mode) and the calculated values of the separation factor are presented in Table 1.

Thus, based on the results obtained, it can be concluded that the Inspire 8M oxygenator maintains its mass transfer characteristics in the presence of 500 ppm NO in the operating gas mixture for at least 6 hours.

Analysis of IR spectra (Fourier Transform) obtained from the study. In order to determine possible

Table 1. Concentrations of N_2 and O_2 at the outlet from the membrane unit of the oxygenation system and the separation factor.

Model of oxygenation system	$x_{N_2, r}$, vol.%	$x_{O_2, r}$, vol.%	SF
N_2/O_2 gas mixture			
Inspire 8M	50.83	49.17	1.03
N_2/O_2/NO gas mixture			
Inspire 8M	51.21	48.79	1.05

Note. $x_{N_2, r}$ — concentration of nitrogen in the retentate flow, vol.%; $x_{O_2, r}$ — concentration of oxygen in the retentate flow; SF — separation factor.

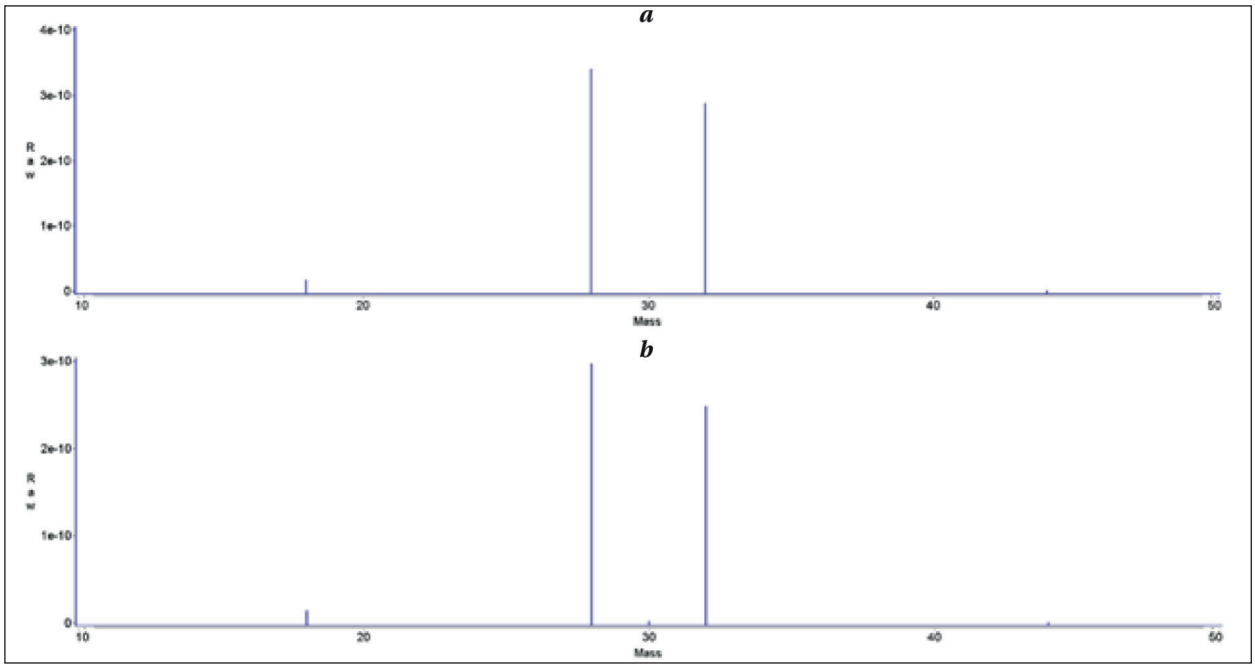

Fig. 4. Mass spectrum of the outlet flow of the Inspire 8M membrane unit.
Note. Simulation of the working process using 0.9 % NaCl water solution with passing of gas mixture of *(a)* N_2/O_2 50/50 vol. %; *(b)* N_2/O_2/NO 49.975/49.975/0.05 vol. %.

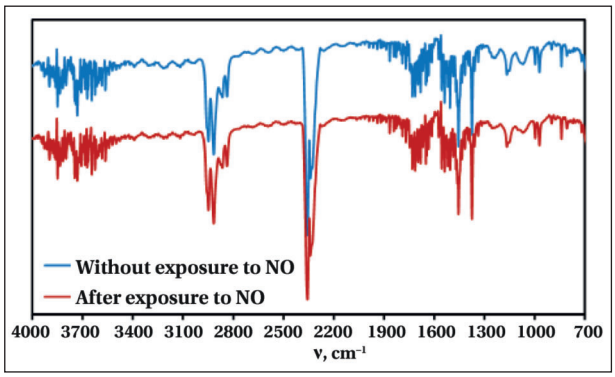

Fig. 5. IR spectra (Fourier transform) of hollow polypropylene membranes before and after exposure to a gas mixture containing NO.

chemical reactions of NO and polypropylene of the oxygenator hollow membranes, the results of IR spectroscopy were subjected to Fourier transformation (Fig. 5). The data obtained indicated that the membrane material did not undergo any changes when exposed to NO, which was confirmed by the absence of characteristic band shifts in the IR spectrum of the polypropylene of the hollow membrane reflecting NO chemisorption. There was also no evidence of physical adsorption of NO on polypropylene. According to the library of the National Institute of Standards and Technology (NIST) (USA), the peak of the IR spectrum «responsible» for bond vibrations in the NO molecule is in the range of 1830–1900 cm^{-1}. No differences were found between control samples of polypropylene membrane and samples exposed to 500 ppm NO. Thus, it can be concluded that the presence of 500 ppm NO in the air-oxygen mixture has no effect on polypropylene hollow fibers.

Results of an experimental animal study with NO supply to the oxygenators of the heart-lung machine. *Analysis of NO and NO_2 concentrations at the inlet and outlet of the oxygenator.* According to the study protocol, 5 cardiac surgeries were performed on pigs under cardiopulmonary bypass with NO supplied to the polypropylene oxygenator circuit. 100 ppm NO was delivered to the Inspire 8M oxygenator during 240 minutes of CPB. By operating the experimental device in automatic mode with a

Table 2. NO concentration at the oxygenator inlet and outlet during CPB, median *(Q1; Q3)*, *N*=5

Time from the beginning of CPB, min	NO_2 at the oxygenator inlet, ppm	NO_2 at the oxygenator outlet, ppm	*P* Mann–Whitney *U* test
10	99.5 (98.5; 103.3)	56.1 (35.3; 61.6)	*P*=0.008
40	99.4 (98.1; 100.1)	56.8 (52.3; 60.2)	*P*=0.008
70	99.8 (98; 100.6)	59 (54.8; 61.3)	*P*=0.008
100	99.1 (97.9; 100.2)	61.8 (54.2; 62.7)	*P*=0.008
130	100 (91.2; 100.3)	63.9 (53.2; 67.5)	*P*=0.032
160	99.7 (99.2; 101.4)	63.2 (61.4; 67.2)	*P*=0.008
190	100.1 (99.8; 100.5)	65.4 (63.7; 67.3)	*P*=0.029
220	99.7 (99.4; 100.4)	65.2 (64.5; 67.4)	*P*=0.008
240	100.4 (100.2; 101.2)	68.9 (67.8; 72.1)	*P*=0.009

Table 3. NO_2 concentration at the inlet and outlet of the CPB oxygenator during CPB. median *(Q1; Q3)*, *N*=5

Time from the beginning of CPB, min	NO_2 at the oxygenator inlet, ppm	NO_2 at the oxygenator outlet, ppm	*P* Mann–Whitney *U* test
10	1.45 (0.9; 1.85)	1.15 (0.7; 1.2)	*P*=0.237
40	1.75 (1.4; 1.9)	1.1 (1.1; 1.15)	*P*=0.024
70	1.7 (1.4; 1.85)	1.2 (1.1; 1.6)	*P*=0.191
100	1.1 (1.08; 1.25)	1.5 (0.7; 1.2)	*P*=0.8
130	1.8 (1.65; 1.8)	1.3 (1; 1.6)	*P*=0.045
160	1.5 (1.4; 1.65)	1.2 (1; 1.35)	*P*=0.06
190	1.65 (1.5; 1.75)	1.25 (1.1; 1.35)	*P*=0.029
220	1.45 (1.35; 1.7)	1.3 (1.15; 1.5)	*P*=0.026
240	1.6 (1.45; 1.65)	1.4 (1.38; 1.6)	*P*=0.366

target NO level of 100 ppm at the oxygenator inlet, an average NO concentration of 99.2±5.6 ppm was maintained, ranging from 95.7 to 111.3 ppm. We found significant differences in NO levels at the oxygenator inlet and outlet at all stages of measurement during CPB (Table 2). In the total sample of 45 measurements, the mean NO concentration at the outlet was 60.5±9.6 ppm, which was significantly lower than the concentration at the oxygenator inlet ($P<0.0001$). The median reduction in outlet NO concentration was 36.7 (33.7; 40.7) ppm.

There was a tendency for increased NO levels at the outlet at the time of weaning from CPB, but these differences were not statistically significant. The patterns found suggest a possible significant absorption of NO by the blood during delivery to the oxygenator, reaching 35–50%.

Data on NO_2 levels in the gas mixture supply line to the polypropylene oxygenator and in the outlet are shown in Table 3. Analyzing these parameters, we found stable values of NO_2 level during CPB, without any tendency to increase. The lower level of NO_2 in the outlet, which was statistically significant at several stages of the study, was also revealed.

In a total sample of 45 measurements of NO_2 concentration in the gas mixture supply line to the oxygenator, the mean value of the parameter was 1.58±0.28 ppm, which was significantly higher than the values obtained in the oxygenator outlet, 1.22±0.26 ppm ($P<0.001$). The median decrease in NO_2 concentration at the outlet was 0.4 (0.2; 0.7) ppm.

Four instances of NO_2 exceeding 2 ppm were noted during the study. In these situations, NO delivery was stopped and resumed after NO_2 was reduced to less than 1 ppm. There were no other instances of NO discontinuation.

Analysis of methemoglobin changes. Data on methemoglobin levels during CPB are shown in Table 4. As can be seen from the above data, 100 pm NO delivery to the polypropylene oxygenator was not associated with a significant increase in methemoglobin levels. Methemoglobin levels did not exceed the upper limit of acceptable values (3%), and no significant differences were found compared to the control group.

Table 4. Changes in methemoglobin percentage (%) during CPB-assisted cardiac surgery, median *(Q1; Q3)*, *N*=10

Stage of the study	Methemoglobin, %	
	Control group, *N*=5	NO group, *N*=5
Baseline	0.9 (0.7; 1.1)	0.9 (0.8; 1.1)
2 hours of CPB	0.8 (0.4; 0.9)	1.1 (1; 1.4)
4 hours of CPB (end of CPB)	1.9 (1.2; 1.9)	1.5 (1.1; 2.2)

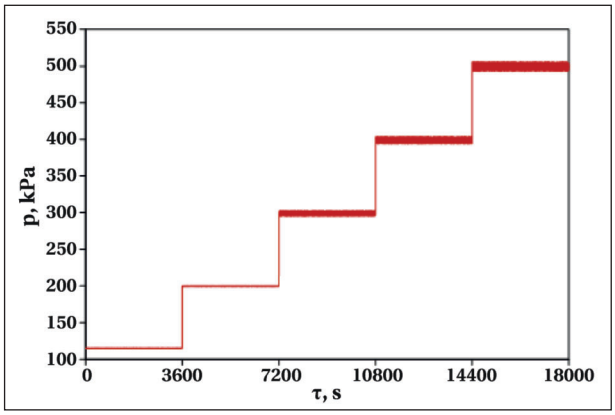

Fig. 6. Graph of the gas pressure at the outlet of the membrane contactor of the oxygenation system as a function of the duration of the experiment with incremental pressure increase in the system.

Leakage testing of oxygenator membrane contactor samples. Three Inspire 8M oxygenators previously used during animal CPB (2 from the main group, 1 from the control group) were tested. Fig. 6 shows the relationship between the pressure inside the gas-filled membrane contactor and the duration of the experiment. During this experiment, no significant differences were found in the functioning of the three samples studied and no significant variation in the gas pressure at the outlet of these samples was detected. No episodes of pressure drop were observed at any stage of the study. The data are presented as averaged gas pressure values at the outlet of the membrane contactor for the three samples studied.

Scanning electron microscopy of the surface of polypropylene hollow fiber membrane samples. Micrographs of polypropylene hollow fiber membrane samples after procedures performed on experimental animals are shown in Fig. 7.

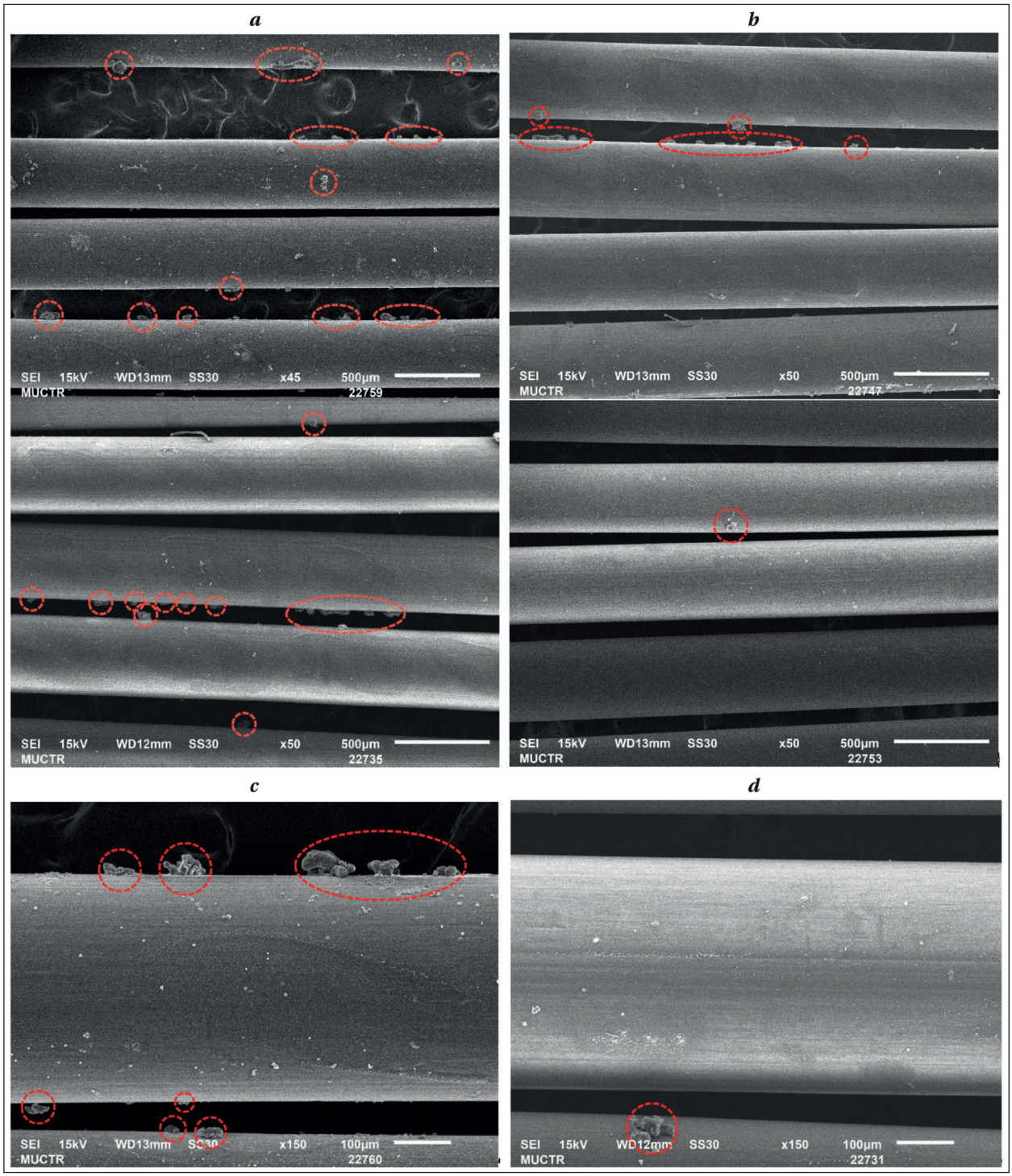

Fig. 7. Scanning electron micrographs of the surface of polypropylene hollow fiber membranes obtained by scanning electron microscopy.
Note. *a* — control group; *b* — NO supply group; *c* — control group; *d* — NO group. Magnification: *a* — ×45 and ×50; *b* — ×50; *c*, *d* — ×150. Fibrin deposits are circled in red.

The comparison of micrographs of the surface of hollow fibers of polypropylene membranes in control samples (without NO exposure) and samples after CPB with NO supply to the oxygenator showed that the surface of membranes of control samples had a significantly higher number of clots resulting from exposure to blood. For example, micrographs of the membrane surface of the control sample (Fig. 7, *a*) showed 12 (micrograph with ×45 approximation) and 10 (micrograph with ×50 approximation) groups of fibrin deposits. Micrographs of membrane samples exposed to nitric oxide showed fewer fibrin deposits (Fig. 7, *b*). The first ×50 magnification image demonstrated 5 groups of such deposits, while the second image showed 1 group.

The ×150 magnification micrographs of the samples support the above statement. On the surface of the control group specimen (Fig. 7, *c*), 7 groups of fibrin deposits were present, while only 1 group of deposits was found on the surface of the fiber of the nitric oxide-exposed specimen (Fig. 7, *d*).

Thus, examination of the surface of hollow fibers of polypropylene membranes by SEM revealed fewer fibrin clots when 100 ppm NO was supplied to the oxygenator compared to control samples.

Discussion

The polypropylene hollow fiber oxygenator was shown to retain its gas transport characteristics after six hours of exposure to an air-oxygen mixture containing 500 ppm NO. The composition of the gas mixture at the outlet of the membrane unit of the oxygenator was not significantly different from the composition of the supplied mixture. The results of the study conducted indicate that exposure to NO at such a high concentration does not affect mass transfer in the polypropylene hollow fiber oxygenator. In addition, FTIR spectroscopy was used to demonstrate for the first time that 500 ppm NO does not affect the structure of polypropylene membranes.

These findings support the results of the only study to investigate the effects of NO on polypropylene oxygenators. S.C. Body et al. investigated the effects of NO on gas exchange and structural integrity of a polypropylene membrane oxygenator. Nine membrane oxygenators were exposed to 224±10 ppm NO and 6.7±1.7 ppm NO_2 and 73% O_2 in nitrogen, and six oxygenators were exposed to 73% O_2 in nitrogen. Heparinized thrombocytopenic bovine blood was circulated in a closed circuit for 6 hours.

Comparison of O_2 or CO_2 transfer rates between groups at 0, 1, 3, and 6 hours showed no differences. No oxygenators «failed» hydraulic integrity tests or malfunctioned during the experiment. There was no evidence of degradation of the experimental material in the appearance of the oxygenators. There were also no differences in blood parameters. Pressure gradients in the oxygenators did not differ between groups at any time point and did not change over time. SEM revealed no differences in pore size, membrane structure, or loss of structural integrity, even in oxygenators subjected to further mechanical damage during structural integrity testing. However, it should be noted that potential chemical interactions between polypropylene and NO were not investigated in the above work [14].

In the second stage of our study, cardiac surgery was performed on animals under CPB with NO supplied to the circuit of the polypropylene oxygenator. We found significant differences in NO concentration at the inlet of the oxygenator and in the outlet circuit at all stages of CPB, confirming the saturation of animal blood with NO. In addition, an increase in NO concentration at the oxygenator outlet was observed during CPB, with a median of 56.1 (35.3; 61.6) at the 10^{th} minute of CPB and a median of 68.9 (67.8; 72.1) at the 240^{th} minute of CPB. The data obtained suggest that at a certain stage of CPB, the NO deposition mechanisms are exhausted, making further saturation impossible.

A review of the literature showed that most clinical studies investigating the effects of NO added to the oxygenator of a CPB machine typically use NO concentrations of 20–40 ppm [17–20]. We showed that the addition of 100 ppm NO during CPB was not associated with an increase in NO_2 concentration to the toxic level of 2 ppm in 91% of the measurements with a mean value of 1.58±0.28 ppm. In the aforementioned study, J. Body et al. showed that NO supply at a concentration of 224±10 ppm did not damage the membrane of a polypropylene oxygenator, but was associated with an increase in NO_2 concentration up to 6.7±1.7 ppm [14], which is a toxic concentration for living organisms. Therefore, it can be assumed that the NO concentration of 100 ppm may be safe for use under clinical conditions.

Analysis of methemoglobin concentrations did not reveal values exceeding the acceptable limits throughout the study. Intergroup comparisons of methemoglobin levels showed no significant differences or trends, which is not consistent with the pharmacokinetic concepts of NO therapy or the results of previous studies. For example, in the first clinical study on the effects of 100 ppm NO delivered to the oxygenator, including 47 patients, the methemoglobin concentration was significantly higher in the main group compared to the control group [21]. Our results may be due to the different susceptibility of human and animal blood to hemolysis.

All investigated oxygenators were tested for leakage and no damage to the integrity of the membrane material and the device body was found. Scanning electron microscopy of hollow polypropylene fiber oxygenators was performed for the first time after NO delivery in an in vivo experiment.

The SEM results after 4 hours of CPB demonstrated the beneficial effects of NO addition to the oxygenator. Oxygenators in the control group were characterized by more fibrin deposition than oxygenators in the main group.

Conclusion

This comprehensive study has found no negative effect of 500 ppm NO on the membranes of polypropylene hollow fiber oxygenators. In an animal study with 100 ppm NO supplied to the oxygenator, no levels of NO_2 or methemoglobin were found to exceed acceptable safe levels. A decrease in the intensity of fibrin deposition on the hollow fibers of polypropylene oxygenator membranes was observed after NO addition.

References

1. *Patel V., Unai S., Gaudino M., Bakaeen F.* Current readings on outcomes after off-pump coronary artery bypass grafting. *Semin Thorac Cardiovasc Surg.* 2019; 31 (4): 726–733. DOI: 10.1053/j.semtcvs.2019.05.012. PMID: 31125606.
2. *Bronicki R. A., Hall M.* Cardiopulmonary bypass-induced inflammatory response: pathophysiology and treatment. *Pediatr Crit Care Med.* 2016; 17 (8 Suppl 1): S272–278. DOI: 10.1097/PCC.0000000000000759. PMID: 27490610.
3. *Wetz A. J., Richardt E. M., Schotola H., Bauer M., Bräuer A.* Haptoglobin and free haemoglobin during cardiac surgery-is there a link to acute kidney injury? *Anaesth Intensive Care.* 2017; 45 (1): 58–66. DOI: 10.1177/0310057X1704500109. PMID: 28072936.
4. *Datt V., Wadhhwa R., Sharma V., Virmani S., Minhas H. S., Malik S.* Vasoplegic syndrome after cardiovascular surgery: a review of pathophysiology and outcome-oriented therapeutic management. *J Card Surg.* 2021; 36 (10): 3749–3760. DOI: 10.1111/jocs.15805. PMID: 34251716.
5. *Di Masi A., De Simone G., Ciaccio C., D'Orso S., Coletta M., Ascenzi P.* Haptoglobin: from hemoglobin scavenging to human health. *Mol Aspects Med.* 2020; 73: 100851. DOI: 10.1016/j.mam.2020.100851. PMID: 32660714.
6. *Schaer C. A., Deuel J. W., Schildknecht D., Mahmoudi L., Garcia-Rubio I., Owczarek C., Schauer S., et al.* Haptoglobin preserves vascular nitric oxide signaling during hemolysis. *Am J Respir Crit Care Med.* 2016; 193 (10): 1111–1122. DOI: 10.1164/rccm.201510-2058OC. PMID: 26694989.
7. *Steppan J., Tran H. T., Bead V. R., Oh Y. J., Sikka G., Bivalacqua T. J., Burnett A. L., et al.* Arginase inhibition reverses endothelial dysfunction, pulmonary hypertension, and vascular stiffness in transgenic sickle cell mice. *Anesth Analg.* 2016; 123 (3): 652–658. DOI: 10.1213/ANE.0000000000001378. PMID: 27537757.
8. *Spina S., Lei C., Pinciroli R., Berra L.* Hemolysis and kidney injury in cardiac surgery: the protective role of nitric oxide therapy. *Semin Nephrol.* 2019; 39 (5): 484–495. DOI: 10.1016/j.semnephrol.2019.06.008. PMID: 31514912.
9. *Galkina S. I., Golenkina E. A., Viryasova G. M., Romanova Y. M., Sud'ina G. F.* Nitric oxide in life and death of neutrophils. *Curr Med Chem.* 2019; 26 (31): 5764–5780. DOI: 10.2174/0929867326266618121309152. PMID: 30543162.
10. *Gresele P., Momi S., Guglielmini G.* Nitric oxide-enhancing or releasing agents as antithrombotic drugs. *Biochem Pharmacol.* 2019; 166: 300–312. DOI: 10.1016/j.bcp.2019.05.030. PMID: 31173724.
11. *Zhang Y. Q., Ding N., Zeng Y.-F., Xiang Y.-Y., Yang M.-W., Hong F.-F., Yang S.-L.* New progress in roles of nitric oxide during hepatic ischemia reperfusion injury. *World J Gastroenterol.* 2017; 23 (14): 2505–2510. DOI: 10.3748/wjg.v23.i14.2505. PMID: 28465634.
12. *Loughlin . M., Browne L, Hinchion J.* The impact of exogenous nitric oxide during cardiopulmonary bypass for cardiac surgery. *Perfusion.* 2022; 37 (7): 656–667. DOI: 10.1177/02676591211014821. PMID: 33983090.
13. *Пичугин В. В., Баутин А. Е., Домнин С. Е., Рязанов М. В., Сандалкин Е. В.* Доставка газообразного оксида азота в экстракорпоральный контур циркуляции: экспериментальные и клинические данные: обзор литературы. *Вестник интенсивной терапии им. А. И. Салтанова.* 2021; 3: 108–116. [*Pichugin V. V., Bautin A. E., Domnin S. E., Ryazanov M. V., Sandalkin E. V.* Delivery of gaseous nitric oxide to the extracorporeal circulation circuit: experimental and clinical data*:* a review. *Ann Crit Care /Vestnik Intensivnoy Terapii im A. I. Saltanova.* 2021; 3: 108–116. (in Russ.)]. DOI: 10.21320/1818-474X-2021-3-108-116.
14. *Body S. C., FitzGerald D., Voorhees C., Hansen E., Crowley C., Voorhees M. E., Shernan S. K.* Effect of nitric oxide upon gas transfer and structural integrity of a polypropylene membrane oxygenator. *ASAIO J.* 1999; 45 (6): 550–554. DOI: 10.1097/00002480-199911000-00008. PMID: 10593685.
15. *Баутин А. Е., Селемир В. Д., Нургалиева А. И., Морозов К. А., Никифоров В. Г., Бикташева Л. З., Афанасьева К. Ю., с соавт.* Ингаляционная терапия оксидом азота, полученным методом синтеза из атмосферного воздуха, в послеоперационном периоде кардиохирургических вмешательств у детей: одноцентровое ретроспективное когортное исследование. *Вестник интенсивной терапии им. А. И. Салтанова.* 2021; 3: 98–107. [*Bautin A. E., Selemir V. D., Nurgalieva A. I., Morozov K. A., Nikiforov V. G., Biktasheva L. Z., Afanasyeva K. Yu., et al.* Inhalation therapy with nitric oxide synthesized from atmospheric air in the postoperative period of cardiac surgery in children: single-center retrospective cohort study. *Ann Crit Care /Vestnik Intensivnoy Terapii im AI Saltanova.* 2021; 3: 98–107. (in Russ.)]. DOI: 10.21320/18-474 X-2021–3–98–107.
16. *Мазурок В. А., Нургалиева А. И., Баутин А. Е., Ржеутская Р. Е., Мазурок А. В., Оразмагомедова И. В., Груздова Д. Г., с соавт.* Объемно-компрессионная осциллометрия для оценки гемодинамики у взрослых с некорригированными врожденными пороками сердца и легочной артериальной гипертензией. *Анестезиология и реаниматология.* 2022; 6: 58–67. [*Mazurok V. A., Nurgalieva A. I., Bautin A. E., Rzheutskaya R. E., Mazurok A. V., Orazmagomedova I. V., Gruzdova D. G., et al.* Volu-

metric compression oscillometry for the assessment of hemodynamics in adults with corrected congenital heart defects and pulmonary arterial hypertension. *Anesthesiol.Reanimatol/ Anesteziologiya i Reanimatologiya*. 2022; 6: 58–67. (in Russ.)]. DOI: 10.17116/ anaesthesiology202206158.

17. *James C., Millar J., Horton S., Brizard C., Molesworth C., Butt W.* Nitric oxide administration during paediatric cardiopulmonary bypass: a randomised controlled trial. *Intensive Care Med*. 2016; 42 (11): 1744–1752. DOI: 10.1007/s00134-016-4420-6. PMID: 27686343.
18. *Kamenshchikov N. O., Anfinogenova Y. J., Kozlov B. N., Svirko Y. S., Pekarskiy S. E., Evtushenko V. V., Lugovsky V. A., et al.* Nitric oxide delivery during cardiopulmonary bypass reduces acute kidney injury: a randomized trial. *J Thorac Cardiovasc Surg*. 2022; 163 (4): 1393–1403.e9. DOI: 10.1016/j.jtcvs.2020. 03.182. PMID: 32718702.
19. *Niebler R. A., Chiang-Ching H., Daley K., Janecke R., Jobe S. M., Mitchell M. E., Varner C., et al.* Nitric oxide added to the sweep gas of the oxygenator during cardiopulmonary bypass in infants: a pilot randomized controlled trial. *Artif Organs*. 2021; 45 (1): 22–28. DOI: 10.1111/aor. 13788. PMID: 32737900.
20. *Schlapbach L. J., Gibbons K. S., Horton S. B., Johnson K., Long D. A., Buckley D. H.F., Erickson S., et al.; NITRIC Study Group, the Australian and New Zealand Intensive Care Society Clinical Trials Group (ANZICS CTG), and the ANZICS Paediatric Study Group (PSG).* Effect of nitric oxide via cardiopulmonary bypass on ventilator-free days in young children undergoing congenital heart disease surgery: The NITRIC randomized clinical trial. *JAMA*. 2022; 328 (1): 38–47. DOI: 10.1001/jama. 2022.9376. PMID: 35759691.
21. *Lowson S. M., Hassan H. M., Rich G. F.* The effect of nitric oxide on platelets when delivered to the cardiopulmonary bypass circuit. *Anesth Analg*. 1999; 89 (6): 1360–1365. DOI: 10.1097/00000539-199912000-00005. PMID: 10589608.

Received 10.06.2023
Accepted 11.12.2023
Online first 18.12.2023

https://doi.org/10.15360/1813-9779-2024-1-2367

Effect of Regional Anesthesia on Oncological Outcomes (Meta-Analysis)

Kristina K. Kadantseva[1,2], Mikhail Ya. Yadgarov[1], Valerii V. Subbotin[1,2], Levan B. Berikashvili[1,3], Roman A. Akchulpanov[2], Anastasia V. Smirnova[1], Ivan V. Kuznetsov[1], Pavel V. Ryzhkov[1], Ekaterina A. Zolotareva[4], Artem N. Kuzovlev[1], Valery V. Likhvantsev[1,4]

[1] V. A. Negovsky Research Institute of General Reanimatology, Federal Research and Clinical Center of Intensive Care Medicine and Rehabilitology, 25 Petrovka Str., Bldg. 2, 107031 Moscow, Russia
[2] A.S. Loginov Moscow Clinical Research Center, Moscow Department of Health, 86 Enthusiasts Highway, 111123 Moscow, Russia
[3] M. F. Vladimirsky Moscow Regional Research Clinical Institute 61/2 Shchepkin Str., 129110 Moscow, Russia
[4] I. M. Sechenov First Moscow State Medical University, Ministry of Health of Russia, 8 Trubetskaya Str., Bldg. 2, 119991 Moscow, Russia

For citation: *Kristina K. Kadantseva, Mikhail Ya. Yadgarov, Valerii V. Subbotin, Levan B. Berikashvili, Roman A. Akchulpanov, Anastasia V. Smirnova, Ivan V. Kuznetsov, Pavel V. Ryzhkov, Ekaterina A. Zolotareva, Artem N. Kuzovlev, Valery V. Likhvantsev.* Effect of Regional Anesthesia on Oncological Outcomes (Meta-Analysis). *Obshchaya Reanimatologiya = General Reanimatology.* 2024; 20 (1): 63–71. https://doi.org/10.15360/1813-9779-2024-1-2367 [In Russ. and Engl.]

*__Correspondence to:__ Kristina K. Kadantseva, kristina161093@gmail.com

Highlight. Regional anesthesia when used in combination with general anesthesia has no effect on oncological outcomes.

Summary

Metastatic processes remain the main cause of deaths in oncology. Methods of anesthesia, in particular regional anesthesia, are considered as potential modulators of the immune response and metastatic spread. The ambiguity of the available data on the effect of regional and general anesthesia on metastatic spread is partly due to the fact that general anesthetic in combined anesthesia is quite often not taken into account, and this, in turn, masks the possible influence of regional anesthesia.

The purpose of this meta-analysis was to make a comparative assessment of the effect of general anesthesia and general anesthesia in combination with regional anesthesia on the relapse-free and overall survival of cancer patients after surgery.

Materials and methods. We analyzed 8 randomized controlled trials involving 1822 patients and comparing the groups of cancer patients who were operated either under general anesthesia (total intravenous (TIVA) or inhalation (IA)), or general anesthesia in combination with regional anesthesia (TIVA+RA or IA+RA, respectively). Trial using combinations of inhaled and intravenous anesthetics was excluded from the analysis for a more accurate assessment of the effect of regional anesthesia. The study complies with the recommendations of the Cochrane Community and PRISMA standards. The protocol was registered on the INPLASY platform. We used PubMed, Google Scholar and CENTRAL databases. We used a subgroup analysis and GRADE tool to assess the quality of evidence.

Results. There were no statistically significant differences in relapse-free and overall survival when comparing different anesthesia methods. For a relapse-free survival, comparing TIVA vs TIVA+RA resulted in no significant difference: OR=1.20 [95% CI 0.92–1.55]; when IA vs IA+RA were compared, OR=1.10 [95% CI 0.94–1.29]. Similar results were obtained for overall survival.

Conclusion. Based on the meta-analysis results, regional anesthesia had no effect on relapse-free and overall survival in oncosurgery patients.

Keywords: regional anesthesia; oncological outcomes; general anesthesia; metastases; surgical

Conflict of interest. The authors declare no conflict of interest.

Financing. The research was supported by the grant of the Russian Science Foundation No. 23-25-00219, https://rscf.ru/project/23-25-00219/

Introduction

The increased focus on metastasis is understandable given that metastatic processes, rather than primary tumors, account for the vast majority (90%) of cancer-related mortality. Surgical stress can induce a systemic inflammatory response syndrome (SIRS), which activates the sympathetic and hypothalamic-pituitary axis and affects the progression of metastatic cancer [2]. However, in the last decade, research interest in the risk of metastasis has shifted from the traditional mechanisms of intraoperative surgical stress to the importance of perioperative immunomodulation. This factor has

become increasingly important in the assessment of tumor recurrence, highlighting the vulnerability of the perioperative period in terms of long-term outcomes in oncology [3]. Even in the early stages of tumor development, circulating tumor cells are present in various parts of the body [4], and although they are associated with a poor clinical prognosis [5], less than 0.01% of these cells develop into metastatic foci [6]. The discovery that anesthetics can modulate receptor targets on immune cells supports the hypothesis that anesthetic agents have a significant effect on long-term outcome in cancer [7, 8]. Several studies have confirmed this pattern by demonstrating that some anesthetics have a negative effect on the functional activity of natural killer cells, macrophages, and neutrophils [9, 10]. The emphasis on accelerated recovery after surgery (ERAS) protocols, which include anesthesia and post-anesthesia rehabilitation techniques, has resulted in the extraordinary popularity of regional anesthesia techniques or neuroaxial blocks due to improved postoperative pain control, reduced opioid consumption, and shorter hospital stays [11, 12]. However, during the last decade, several randomized clinical trials have been performed to test hypotheses about the effect of regional anesthesia on the metastatic potential of malignant tumors, and their results, including those included in meta-analyses, have not shown significant advantages of regional anesthesia over general anesthesia in terms of overall and recurrence-free survival [13, 14]. However, it should be noted that the comparison of mixed groups with different types of general anesthesia may have a significant impact on the final results.

The aim of this meta-analysis was to compare the effects of general anesthesia and a combination of general and regional anesthesia on recurrence-free and overall survival in cancer patients after surgical intervention.

Materials and Methods

The study was conducted according to the guidelines of the Cochrane Society and met the PRISMA (Preferred Reporting Items for Systematic Reviews and Meta-Analyses) standards for systematic reviews and meta-analyses [15]. The study protocol was registered on the International Platform for Systematic Reviews and Meta-Analyses Protocols (INPLASY) under registration number INPLASY202390088 (doi:10.37766/inplasy2023.9.0088).

Search strategy. A systematic search of PubMed, Google Scholar, and the Cochrane Central Register of Controlled Trials (CENTRAL) databases for scientific articles published between 2008 and 2023 was performed by two independent investigators. Searches were conducted in the form of queries: («anesthesia, inhalation»[MeSH] OR «anesthesia, intravenous»[MeSH] OR «anesthesia, general»[MeSH] OR «anesthesia, conduction»[MeSH] OR sevoflurane OR isoflurane OR propofol OR midazolam OR «anesthesia, regional» OR «anesthesia, epidural» OR «epidural analgesia» OR «anesthesia, mixed» OR «paravertebral block») AND («neoplasms» [MeSH] OR «cancer» OR «carcinoma» OR «neoplasm» OR «malignancy» OR «tumor» OR «NSCLC») AND («survival»[MeSH] OR «survival analysis»[mesh] OR «survival rate»[MeSH] OR «disease-free survival» OR «recurrence-free survival» OR «event-free survival» OR «overall survival» OR «recurrence-free survival»). In addition, the sources in the reference list of previously identified articles were analyzed (backward snowballing) and citations were analyzed (forward snowballing). No language restrictions were applied. MeSH (Medical Subject Headings) terms were used.

Study selection. We independently screened the studies extracted from the databases at the title and abstract analysis stage. We reviewed randomized controlled trials (RCTs) comparing groups of cancer patients who received total intravenous or inhalation anesthesia (TIVA or IA) versus general anesthesia combined with regional anesthesia (TIVA+RA or IA+RA) during surgery. Comparisons were made for recurrence-free and overall survival. After duplicate records were excluded, the final decision to include articles was based on a detailed analysis of the full-text articles by two independent reviewers. Disagreements were resolved by consensus.

The following inclusion criteria were used:

1) RCTs comparing the use of general anesthesia and regional anesthesia in combination with general anesthesia in adult patients undergoing cancer surgery;

2) the study reported recurrence-free and/or overall survival of patients.

Studies were excluded if they met at least one of the following criteria:

1) cross-comparisons (TIVA vs. IA+RA, IA vs. TIVA+RA) and other anesthesia protocols;
2) no data on survival outcomes;
3) observational or retrospective studies;
4) clinical observational studies;
5) reviews;
6) meta-analyses;
7) pediatric patients.

Data retrieval and outcome measurements. Basic study information (first author, design, sample size, type of anesthesia, patient enrollment period, inclusion criteria, patient follow-up period), subject information (age, proportion of males, TNM stage, ASA scale, tumor type, surgical procedure, and duration), and treatment outcomes were retrieved independently by two investigators and then compared for validation. The study endpoints were overall survival (OS) and relapse-free survival (RFS) at 1, 2, 3, and 5 years from diagnosis. Kaplan-Meier curve analysis, as described in the original papers [16], was used to retrieve survival data when necessary.

Assessment of risk of bias. The internal validity and risk of systematic error (bias) of the included studies were assessed by two independent reviewers using the latest version of the Cochrane Risk-of-Bias Tool 2.0 (RoB 2) [17]. Discrepancies in estimates were resolved by consensus. Systematic publication error or «publication bias», which results from a bias towards publishing studies with statistically significant results, was assessed using the Egger test and analysis of funnel plots [18].

Statistical analysis. STATA 17 (StataCorp LLC, Texas, USA) was used to perform the meta-analysis. Heterogeneity between studies was assessed using Cochran's Q criterion and I^2 heterogeneity coefficient. Significant heterogeneity was defined as $P<0.05$ and/or $I^2 \geqslant 50\%$. The odds ratio (OR) and corresponding 95% confidence interval for OS and RFS were calculated for each individual study using the inverse variance (Mantel-Haenszel) method [19]. The recommended random effects model (REML, or restricted maximum likelihood) [20] was used to pool the results and calculate an overall OR. The statistical significance (*P* value) for hypothesis testing was set at 0.05.

Subgroup analysis. Subgroup analyses were performed using several methodological approaches.

First, separate comparisons were made for two categories of studies: TIVA versus a combination of TIVA and RA (TIVA+RA), and IA versus a combination of IA and RA (IA+RA).

Second, a sequential exclusion method was used to assess the robustness of the results, in which each study was removed from the overall analysis and then reanalyzed.

In addition, separate analyses of survival at 1, 2, 3, and 5 years were performed.

Quality of evidence assessment. The Grading of Recommendations Assessment, Development and Evaluation (GRADE) systematic approach [21] was used to assess the quality of evidence for all outcomes studied. According to current guidelines, the baseline level of evidence for RCTs is considered high [21]. Two authors of this review independently assessed the quality of the evidence, and disagreements were resolved by consensus.

Results and Discussion

The primary search identified 1695 articles, of which 85 full-text articles were analyzed according to the inclusion and exclusion criteria. A flowchart illustrating the study selection process is shown in Fig. 1.

A total of 1822 patients from 8 RCTs were included in the meta-analysis [22–29].

Three of the eight included studies compared TIVA versus TIVA+RA [22–24] and five compared IA versus IA+RA [25–29]. Two studies included patients with breast cancer [23, 24], while other studies included patients with colorectal cancer, non-small cell lung cancer, and prostate cancer (Table 2). Two studies used double blinding [24, 28], four studies used single blinding [22, 23, 26, 27], and two studies used no blinding [25, 29]. Two studies used propofol for induction in the IA group [25, 27]. The proportion of patients with metastatic lesions at the time of diagnosis ranged from 0 to 23%, and the mean age of patients ranged from 51 to 70 years (Table 1). The characteristics of the included studies are summarized in Table 1.

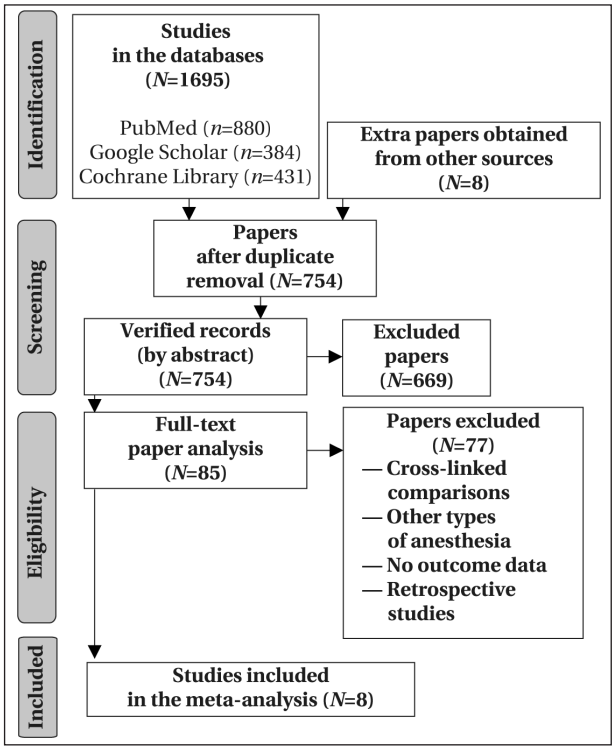

Fig. 1. Flowchart of the meta-analysis.

Recurrence-free survival. Fig. 2, a is a forest plot illustrating the results of a meta-analysis of three studies involving 819 cancer patients. These studies compared RFS with two different anesthetic techniques, TIVA and combined TIVA+RA. According to the meta-analysis, no significant differences were found between the two groups with OR=1.20 [95% CI 0.92–1.55], *P*-value for effect 0.17, *P*-value for heterogeneity 0.74, I^2=0% (Fig. 2, *a*; Table 2).

A meta-analysis reviewed data from four studies involving 826 cancer patients. These studies compared RFS using two methods of anesthesia, IA versus IA+RA. No significant differences were found with OR=1.10 [95% CI 0.94–1.29], *P*-value for effect 0.24, *P*-value for heterogeneity 0.22, I^2=0% (Fig. 2, *b*; Table 2).

Overall survival. Fig. 2, *c* shows a forest plot illustrating the results of a meta-analysis of two studies (676 patients) comparing OS of TIVA and combined TIVA+RA. No significant differences were found between the two groups with OR=1.09 [95% CI 0.70–1.70], *P*-value for effect 0.70, *P*-value for heterogeneity 0.68, I^2=0% (Fig. 2, *c*; Table 2).

Table 1. Characteristics of RCTs included in the meta-analysis.

Ref No.	Author, year of publication, country, journal	Blinding	Number of centers	Methods compared	Sample size, GA/GA+RA	Mean age, years	Percentage of men, %	BMI, kg/m²	Cancer type	Surgery	Duration of surgery, min
29	*Christopherson R.*, 2008, USA, *Anesth Analg*	No	Multicenter	IA/IA+RA	177.92/85	68.85	100	26.5	CRC	Colon resection	NA
28	*Binczak M.*, 2013, France, *Annales Ann Fr Anesth Reanim*	Double	Single-center	IA/IA+RA	132.63/69	57.5	62.9	НД	Various	Abdominal surgery	NA
27	*Tsui B. C.*, 2010, Canada, *Can J Anesth*	Single	Single-center	IA/IA+RA	99.50/49	63.45	100	28.15	Prostatic adenocarcinoma	Prostatectomy	114.5
26	*Myles P. S.*, 2011, Australia, New Zealand and other, *BMJ*	Single	Multicenter	IA/IA+RA	446.216/230	70.5	56.5	НД	Various	Abdominal surgery	NA
25	*Pi J.*, China, *J Int Med Res*	No	Single-center	IA/IA+RA	149.75/74	51	51.7	22.7	NSCLC	Resection	218.37
24	*Karmakar M. K.*, 2017, China, *Anticancer Res*	Double	Single-center	TIVA/TIVA+RA	173.58/115	51.3	0	НД	BC	Mastectomy	NA
23	*Yu L.*, 2022, China, *BMC Surgery*	Single	Single-center	TIVA/TIVA+RA	503.252/251	52.15	0	23.90	BC	Mastectomy	83.5
22	*Rangel F. P.*, 2021, Brasil, *BMJ*	Single	Single-center	TIVA/TIVA+RA	143.71/72	67	100	24.10	PC	Prostatectomy	NA

Note. GA — general anesthesia; RA — regional anesthesia; TIVA — total intravenous anesthesia; IA — inhalation anesthesia; BMI — body mass index; CRC — colorectal cancer; NSCLC — non-small cell lung cancer; BC — breast cancer; PC — prostate cancer; NA — not available.

An analysis of four studies (904 patients) comparing the OR for IA versus IA+RA showed no significant differences with OR=1.22 [95% CI 0.97–1.53], *P*-value for effect 0.09, *P*-value for heterogeneity 0.37, I^2=19% (Fig. 2, *d*; Table 2).

The lack of statistically significant differences was confirmed in all subgroup analyses, including survival at different time periods.

The assessment of study quality showed that only one study was at high risk of bias (Fig. 3).

The risk of systematic publication bias was significant for the comparison of IA vs. IA+RA in the assessment of OS (*P*=0.003), as confirmed by funnel plot analysis (Fig. 4).

The quality of evidence for the outcomes reviewed was assessed using the GRADE methodology. Factors that led to a downgrading of the level of evidence are summarized and shown in Table 3. The level of evidence for RFS and OS ranged from very low to low.

This meta-analysis was the first to evaluate the long-term outcomes of cancer patients in the context of the use of regional and general anesthesia, taking into account the differentiation of general anesthesia groups into inhalation and intravenous anesthesia groups.

Despite the high methodological reliability of the included studies, the level of evidence for recurrence-free survival and overall survival ranged from very low to low. Nevertheless, the study supports previous findings that regional anesthesia has no significant advantages over total intravenous and inhalation anesthesia in the context of long-term oncologic outcomes. The results are comparable to the conclusions of previous meta-analyses, which had an unfavorable balance between randomized clinical trials and retrospective studies [30–32]. In the largest meta-analysis, which included 25 retrospective studies and 3 randomized clinical trials with a total of 67577 patients, although there was no significant overall survival benefit when the averaged data were analyzed, a small survival benefit was found when only RCTs were considered, with weighted hazard ratios of 0.83 (HR=0.83) and 0.88 (HR=0.88) for overall and recurrence-free survival, respectively [31].

Traditional concepts of malignant recurrence and progression suggest that immune function plays a key role in tumor cell survival [33, 34]. In this context, studies have investigated the relationship between analgesics and tumor progression. For example, mu-opioid receptor agonists stimulate tumor cell migration, growth, and metastasis [35]. In contrast, local anesthetics not only block tumor cell migration mechanisms [36], inhibit tumor cell differentiation or proliferation, and have analgesic and anti-inflammatory properties [37], but also reduce perioperative opioid use. In an observational study

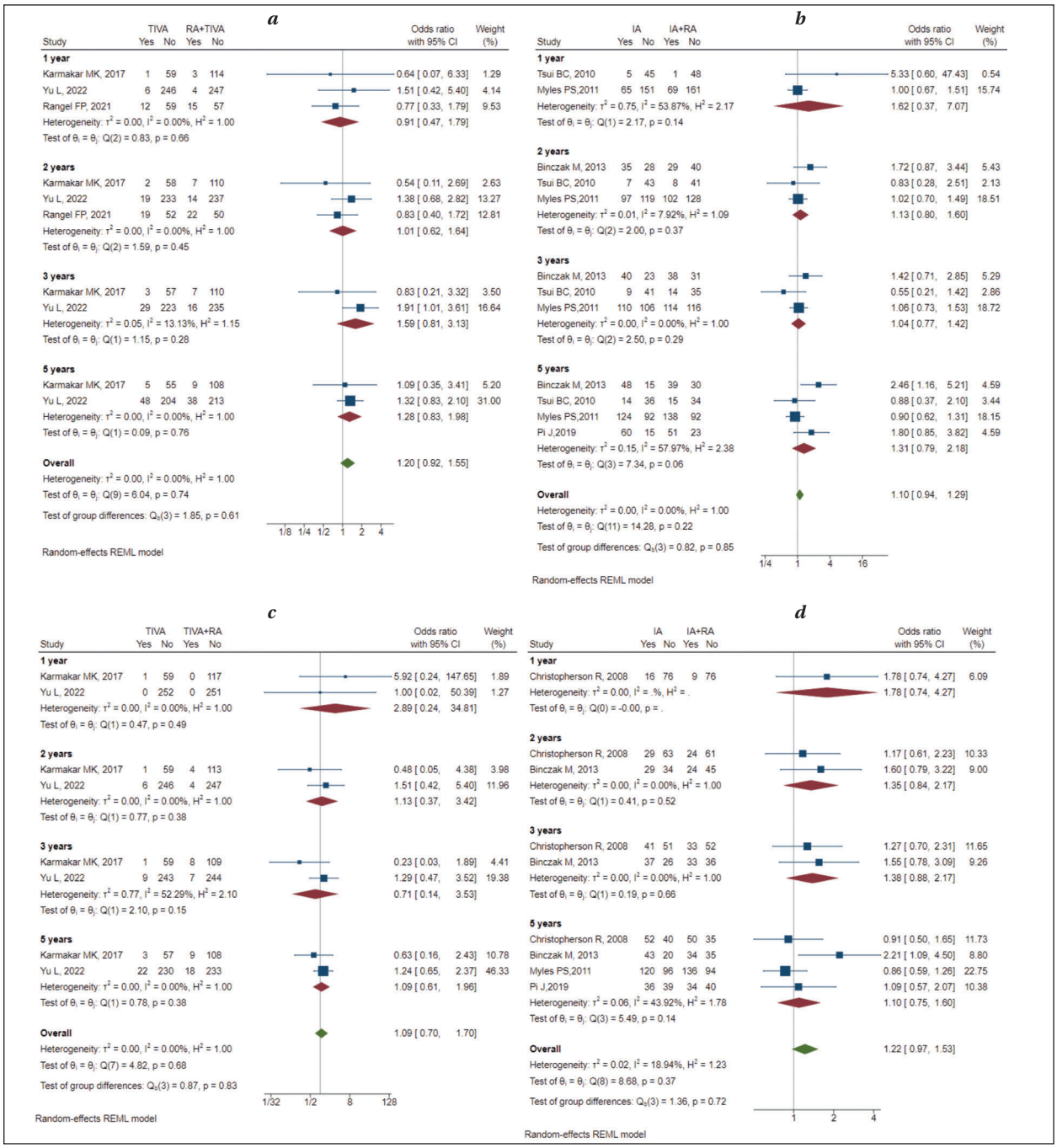

Fig. 2. Forest-plot and meta-analysis data of recurrence-free *(a, b)* and overall *(c, d)* survival in cancer patients with TIVA vs. TIVA+RA *(a, c)*, IA vs. IA+RA *(b, d)*.

Table 2. Results of the meta-analysis.

Outcome and subgroup		Papers	N, GA	N, GA+RA	OR (95% CI)	Total effect	I^2, %	Egger test
RFS	IA/IA+RA	4	404	422	1.10 (0.94–1.29)	0.27	0	*P*=0.115
	TIVA/TIVA+RA	3	381	438	1.20 (0.92–1.55)	0.17	0	*P*=0.207
OS	IA/IA+RA	4	446	458	1.22 (0.97–1.53)	0.09	19	*P*=0.003
	TIVA/TIVA+RA	2	310	366	1.09 (0.70–1.70)	0.70	0	*P*=0.577

Note. RFS — recurrence-free survival; OS — overall survival; OR — odds ratio; CI — confidence interval; GA — general anesthesia; RA — regional anesthesia; TIVA — total intravenous anesthesia; IA — inhalation anesthesia.

of 129 patients, A. K. Exadaktylos et al. showed that the control group, which received general anesthesia followed by morphine-based analgesia, had a significantly higher risk of cancer recurrence than the experimental group, which received paravertebral blockade combined with general anesthesia (*P*=0.012) [38]. However, to increase the level of evidence, additional randomized clinical trials with

Table 3. Level of evidence for the outcomes studied (GRADE approach).

Statement	D1	D2	D3	D4	D5	D6	TOTAL
The use of TIVA+RA combination in cancer patients does not lead to a change in RFS compared to TIVA	N/S (0)	Significant (–1)	Significant (–1)	Very significant (–2)	N/S (0)	No	⊕◯◯◯ Very low
The use of TIVA+RA combination in cancer patients does not lead to a change in OS, compared to TIVA	N/S (0)	N/S (0)	Выражена (–1)	Very significant (–2)	N/S (0)	No	⊕⊕◯◯ Low
The use of IA+RA combination in cancer patients does not lead to a change in RFS, compared to IA	N/S (0)	Significant (-1)	N/S (0)	Very significant (–2)	N/S (0)	No	⊕⊕◯◯ Low
The use of IA+RA combination in cancer patients does not lead to a change in OS, compared to IA	Significant (–1)	Significant (–1)	N/S (0)	Very significant (–2)	Significant (–1)	No	⊕◯◯◯ Very low

Notes. RFS — recurrence-free survival; OS — overall survival; RA — regional anesthesia; TIVA — total intravenous anesthesia; IA — inhalation anesthesia. Domains: D1 — overall risk of bias; D2 — clinical and statistical heterogeneity (inconsistency); D3 — sample inconsistency with the statement; D4 — inaccuracy; D5 — systematic publication bias; D6 — upgrading level of evidence.
0 — no downgrading of level of evidence; –1 — downgraded by 1 level; –2 — downgraded by 2 levels. N/S — not significant; N/A —not applicable. The baseline level of evidence is high.

adequate statistical power are needed to evaluate the impact of the opioid-sparing effect of regional anesthesia on long-term oncologic outcomes.

It is important to note that including trials with different types of malignancies in the analysis may distort the final results. This is because cancer survival rates can vary considerably depending on the type of tumor and the availability of radical treatment. For example, melanoma, bladder cancer, and lung cancer have 5-year survival rates of 92%, 53–77%, and 16–19%, respectively [39, 40]. Thus, M. Weng and colleagues, after performing a subgroup analysis in their study, confirmed the hypothesis of a statistically significant association between the use of neuroaxial anesthesia and improved overall survival in colorectal cancer (OR 0.653, 95% CI 0.430–0.991, *P*=0.045) [41].

Limitations. In two of the eight RCTs analyzed, the sample size reached several hundred participants, but most studies were conducted at a single medical center. The single-center nature of these studies limits their external validity, which is particularly critical in the context of intensive care, where practices may vary widely between countries. These factors could potentially bias the true effect of regional anesthesia on cancer recurrence rates.

Another significant drawback was the heterogeneity of anesthesia support in the study groups. Although the authors attempted to differentiate the groups by methods of anesthesia maintenance, such as total intravenous anesthesia and the use of inhalational anesthetics, a number of RCTs used propofol during induction in the inhalation anesthesia groups. The oncogenic potential of a tumor is known to correlate with the level of expression of hypoxia-inducible factor-1a (HIF-1a) and its subsequent effects on cell proliferation and migration, as well as the development of resistance to chemotherapy. According to some reports, propofol is able to inhibit HIF-1a activation as well as attenuate isoflurane-induced HIF-1a activation, thus partially

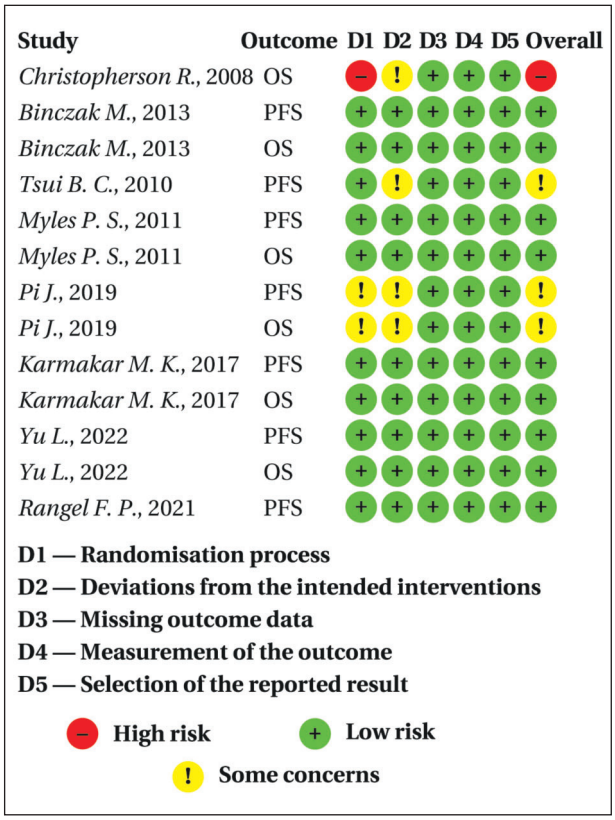

Fig. 3. Quality analysis of studies included in the meta-analysis with risk assessment of systematic bias by domain using the Cochrane RoB 2 tool.

reducing the oncogenic potential of cancer cells [42]. In addition, the postoperative analgesia regimens in each of the studies varied, ranging from the use of opioid anesthetics to no analgesia at all, which may also make it difficult to accurately assess the effects of local anesthetics.

Despite the substantial contribution of our meta-analysis to the understanding of the relationship between type of anesthesia and cancer outcomes, the current level of scientific evidence remains insufficient. New randomized trials focusing

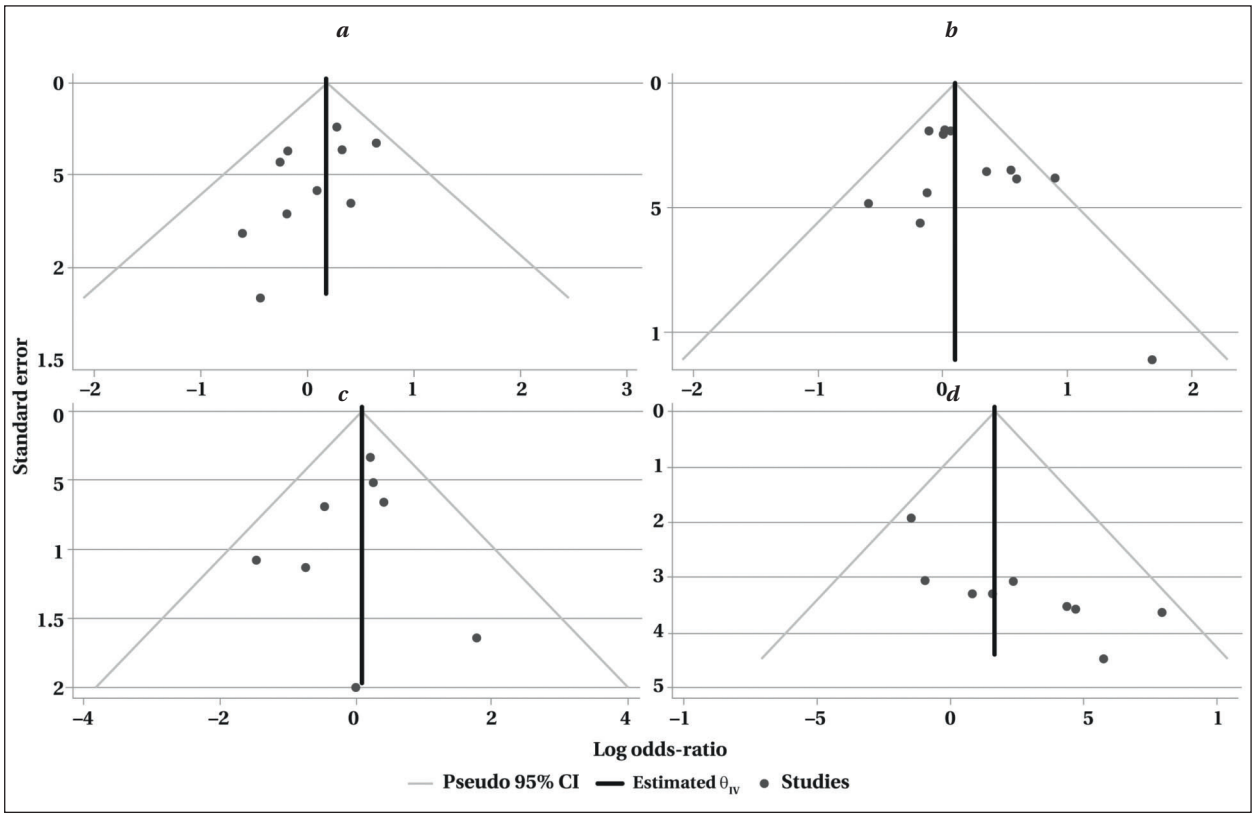

Fig. 4. Funnel plot: risk of systematic publication bias for studies comparing recurrence-free *(a, b)* and overall survival *(c, d)* for TIVA/TIVA+RA *(a, c)* and IA/IA+RA *(b, d)* in cancer

on the opioid-sparing effects of regional anesthesia are needed. Unification of anesthetic management protocols and standardization of the list of anesthetics used could greatly improve the reliability of future data. In addition, statistical survival rates may vary significantly by cancer type, necessitating a more nuanced approach in future studies.

Conclusion

A meta-analysis of 8 RCTs involving 1822 patients found no significant differences in recurrence-free and overall survival between general and combined anesthesia techniques when patient groups receiving general anesthesia were classified by the type of anesthesia used.

Thus, our findings highlight the complexity and ambiguity of the current understanding of the relationship between choice of anesthesia technique and oncologic outcomes.

References

1. *Gupta G. P., Massagué J.* Cancer metastasis: building a framework. *Cell.* 2006; 127 (4): 679–695. DOI: 10.1016/j.cell.2006.11.001. PMID: 17110329.
2. *Dubowitz J. A., Sloan E. K., Riedel B. J.* Implicating anaesthesia and the perioperative period in cancer recurrence and metastasis. *Clin Exp Metastasis.* 2018; 35 (4): 347–358. DOI: 10.1007/S10585-017-9862-X. PMID: 28894976.
3. *Colacchio T. A., Yeager M. P., Hildebrandt L. W.* Perioperative immunomodulation in cancer surgery. *Am J Surg.* 1994; 167 (1): 174–179. DOI: 10.1016/0002-9610 (94)90070–1. PMID: 8311130.
4. *Martin O. A., Anderson R. L., Narayan K., MacManus M. P.* Does the mobilization of circulating tumour cells during cancer therapy cause metastasis? *Nat Rev Clin Oncol.* 2017; 14 (1): 32–44. DOI: 10.1038/NRCLINONC.2016.128. PMID: 27550857.
5. *Hardingham J. E., Grover P., Winter M., Hewett P. J., Price T. J., Thierry B.* Detection and clinical significance of circulating tumor cells in colorectal cancer-20 years of progress. *Mol Med.* 2015; 21 Suppl 1: S25–31. DOI: 10.2119/MOLMED. 2015.00149. PMID: 26605644.
6. *Chiang S. P. H., Cabrera R. M., Segall J. E.* Tumor cell intravasation. *Am J Physiol Cell Physiol.* 2016; 311 (1): C1–14. DOI: 10.1152/AJP-CELL.00238.2015. PMID: 27076614
7. *Yuki K., Eckenhoff R. G.* Mechanisms of the immunological effects of volatile anesthetics: a review. *Anesth Analg.* 2016; 123 (2): 326–335. DOI: 10.1213/ANE.0000000000001403. PMID: 27308954.
8. *Лихванцев В. В., Ядгаров М. Я., Di Piazza M., Каданцева К. К.* Ингаляционная vs тотальная внутривенная анестезия: где маятник сейчас? (мета-анализ и обзор). *Obshchaya Reanimatologiya = General Reanimatology.* 2020; 16 (6): 91–104. [*Likhvantsev V., Yadgarov M., Di Piazza M., Kadantseva K.* Inhalation vs total intravenous anesthesia in cancer surgery: where is the «pendulum» now? (meta-analysis and review). *General Reanimatology/ Obshchaya Reanimatologya.* 2020; 16 (6): 91–104. (in Russ&Eng.)]. DOI: 10.15360/1813-9779-2020-6-91-104.
9. *Brand J. M., Kirchner H., Poppe C., Schmucker P.* The effects of general anesthesia on human peripheral immune cell distribution and cytokine production. *Clin Immunol Immunopathol.* 1997; 83 (2): 190–194. DOI: 10.1006/clin.1997. 4351. PMID: 9143381.
10. *Melamed R., Bar-Yosef S., Shakhar G., Shakhar K., Ben-Eliyahu S.* Suppression of natural killer cell activity and promotion of tumor metastasis by ketamine, thiopental, and halothane, but not by propofol: mediating mechanisms and prophylactic measures. *Anesth Analg.* 2003; 97 (5): 1331–1339. DOI: 10.1213/01.ANE.0000082995.44040.07. PMID: 14570648.
11. *Sen S., Koyyalamudi V., Smith D. D., Weis R. A., Molloy M., Spence A. L., Kaye A. J., et al.* The role of regional anesthesia in the propagation of cancer: a comprehensive review. *Best Pract Res Clin Anaesthesiol.* 2019; 33 (4): 507–522. DOI: 10.1016/J.BPA.2019.07.004. PMID: 31791567.
12. *Худяков П. А., Потапов А. Л.* Оценка эффективности общей и регионарной анестезии при дерматолипофасциоэктомии у пациенток с постмастэктомическим отеком верхней конечности. *Анестезиология и Реаниматология.* 2022; (4): 66–70. [*Khudyakov P. A., Potapov A. L.* Effectiveness of general and regional anesthesia for dermatolipofascioectomy in patients with upper limb swelling following mastectomy. *Russian Journal of Anesthesiology and Reanimatology.* 2022; (4): 66–70. (in Russ.)]. DOI: 10.17116/ANAESTHESIOLOGY202204166.
13. *Ang E., Ng K. T., Lee Z. X., Ti L. K., Chaw S. H., Wang C. Y.* Effect of regional anaesthesia only versus general anaesthesia on cancer recurrence rate: a systematic review and meta-analysis with trial sequential analysis. *J Clin Anesth.* 2020; 67: 110023. DOI: 10.1016/J.JCLINANE.2020.110023. PMID: 32805685.
14. *Li T., Meng X., Wang D., Wang Q., Ma J., Dai Z.* Regional anesthesia did not improve postoperative long-term survival of tumor patients: a systematic review and meta-analysis of randomized controlled trials. *World J Surg Oncol.* 2023; 21 (1): 68. DOI: 10.1186/S12957-023-02957-3. PMID: 36849919.
15. *Moher D., Liberati A., Tetzlaff J., Altman D. G., Antes G., Atkins D., PRISMA Group.* Preferred reporting items for systematic reviews and meta-analyses: the PRISMA statement. *PLoS Med.* 2009; 6 (7): e1000097. DOI: 10.1371/journal.pmed. 1000097. PMID: 19621072.
16. PlotDigitizer. PlotDigitizer: Extract Data from Graph Image Online 2022. https: //plotdigitizer.com/ (accessed September 15, 2023).
17. *Sterne J. A. C., Savović J., Page M. J., Elbers R. G., Blencowe N. S., Boutron I., Cates C. J., et al.* RoB 2: a revised tool for assessing risk of bias in randomised trials. *BMJ.* 2019; 366: I4898. DOI: 10.1136/bmj.l4898. PMID: 31462531.
18. *Lin L., Chu H.* Quantifying publication bias in meta-analysis. *Biometrics.* 2018; 74 (3): 785–794. DOI: 10.1111/biom.12817. PMID: 29141096.
19. *Higgins J. P. T., Green S.* Cochrane Handbook for Systematic Reviews of Interventions | Cochrane Training. Handbook. 2011: 649. https://training.cochrane.org/handbook/current%0A(accessed September 15, 2023).

20. *Seide S. E., Röver C., Friede T.* Likelihood-based random-effects meta-analysis with few studies: empirical and simulation studies. *BMC Med Res Methodol.* 2019; 19 (1): 16. DOI: 10.1186/s12874-018-0618-3. PMID: 30634920.
21. *Guyatt G. H., Oxman A. D., Vist G. E., Kunz R., Falck-Ytter Y., Alonso-Coello P., Schünemann H.J; GRADE Working Group.* GRADE: an emerging consensus on rating quality of evidence and strength of recommendations. *BMJ.* 2008; 336 (7650): 924–6. DOI: 10.1136/bmj.39489.470347.ad. PMID: 18436948.
22. *Rangel F. P., Auler J. O. C., Carmona M. J. C., Cordeiro M. D., Nahas W. C., Coelho R. F., Simões C. M.* Opioids and premature biochemical recurrence of prostate cancer: a randomised prospective clinical trial. *Br J Anaesth.* 2021; 126 (5): 931–939. DOI: 10.1016/j.bja.2021.01.031. PMID: 33712224.
23. *Yu L., Cui X., Song P., Li C., Zhao H., Chang Y.* Perioperative pectoral nerve block type II and postoperative recurrence in breast cancer: a randomized controlled trial. *BMC Surg.* 2022; 22 (1): 447. DOI: 10.1186/s12893-022-01895-3. PMID: 36585623.
24. *Karmakar M. K., Samy W., Lee A., Li. J.W., Chan W. C., Chen P. P., Tsui B. C.H.* Survival analysis of patients with breast cancer undergoing a modified radical mastectomy with or without a thoracic paravertebral block: a 5-year follow-up of a randomized controlled trial. *Anticancer Res.* 2017; 37 (10): 5813–5820. DOI: 10.21873/anticanres.12024. PMID: 28982906.
25. *Pi J., Sun Y., Zhang Z., Wan C.* Combined anesthesia shows better curative effect and less perioperative neuroendocrine disorder than general anesthesia in early stage NSCLC patients. *J Int Med Res.* 2019; 47 (10): 4743–4752. DOI: 10.1177/0300060519862102. PMID: 31510831.
26. *Myles P. S., Peyton P., Silbert B., Hunt J., Rigg J. R.A., Sessler D. I.* Perioperative epidural analgesia for major abdominal surgery for cancer and recurrence-free survival: randomised trial. *BMJ.* 2011; 342: d1491. DOI: 10.1136/bmj.d1491. PMID: 21447587.
27. *Tsui B. C. H., Rashiq S., Schopflocher D., Murtha A., Broemling S., Pillay J., Finucane B. T.* Epidural anesthesia and cancer recurrence rates after radical prostatectomy. *Can J Anesth.* 2010; 57 (2): 107–12. DOI: 10.1007/s12630-009-9214-7. PMID: 19911247.
28. *Binczak M., Tournay E., Billard V., Rey A., Jayr C.* Major abdominal surgery for cancer: does epidural analgesia have a long-term effect on recurrence-free and overall survival? *Ann Fr Anesth Reanim.* 2013; 32 (5): e81–88. DOI: 10.1016/j.annfar.2013.02.027. PMID: 23618609.
29. *Christopherson R., James K. E., Tableman M., Marshall P., Johnson F. E.* Long-term survival after colon cancer surgery: a variation associated with choice of anesthesia. *Anesth Analg.* 2008; 107 (1): 325–32. DOI: 10.1213/ane.0b013e3181770f55. PMID: 18635504.
30. *Pei L., Tan G., Wang L., Guo W, Xiao B., Gao X., Wang L., et al.* Comparison of combined general-epidural anesthesia with general anesthesia effects on survival and cancer recurrence: a meta-analysis of retrospective and prospective studies. *PLoS One.* 2014; 9 (12): e114667. DOI: 10.1371/JOURNAL. PONE.0114667. PMID: 25548913.
31. *Grandhi R. K., Lee S., Abd-Elsayed A.* The relationship between regional anesthesia and cancer: a metaanalysis. *Ochsner J.* 2017; 17 (4): 345–361. DOI: 10.1043/TOJ-16-0100.
32. *Cakmakkaya O. S., Kolodzie K., Apfel C. C., Pace N. L.* Anaesthetic techniques for risk of malignant tumour recurrence. *Cochrane Database Syst Rev.* 2014; 2014 (11): CD008877. DOI: 10.1002/14651858.CD008877.pub2. PMID: 25379840.
33. *Romagnani S.* T-cell subsets (Th1 versus Th2). *Ann Allergy Asthma Immunol.* 2000; 85 (1): 9–18. DOI: 10.1016/S1081-1206 (10)62426-X. PMID: 10923599.
34. *Friedlander R. M.* Apoptosis and caspases in neurodegenerative diseases. *N Engl J Med.* 2003; 348 (14): 1365–1375. DOI: 10.1056/NEJMRA022366. PMID: 12672865.
35. *Heaney Á., Buggy D. J.* Can anaesthetic and analgesic techniques affect cancer recurrence or metastasis? *Br J Anaesth.* 2012; 109 Suppl 1: i17-i28. DOI: 10.1093/BJA/AES421. PMID: 23242747.
36. *Piegeler T., Votta-Velis E. G., Liu G., Place A. T., Schwartz D. E., Beck-Schimmer B., Minshall R. D., et al.* Antimetastatic potential of amide-linked local anesthetics: inhibition of lung adenocarcinoma cell migration and inflammatory Src signaling independent of sodium channel blockade. *Anesthesiology.* 2012; 117 (3): 548–559. DOI: 10.1097/ALN. 0B013E3182661977. PMID: 22846676.
37. *Lucchinetti E., Awad A. E., Rahman M., Feng J., Lou P-.H., Zhang L., Ionescu L., et al.* Antiproliferative effects of local anesthetics on mesenchymal stem cells: potential implications for tumor spreading and wound healing. *Anesthesiology.* 2012; 116 (4): 841–856. DOI: 10.1097/ALN.0B013E31824BABFE. PMID: 22343474.
38. *Exadaktylos A. K., Buggy D. J., Moriarty D. C., Mascha E., Sessler D. I.* Can anesthetic technique for primary breast cancer surgery affect recurrence or metastasis? *Anesthesiology.* 2006; 105 (4): 660–664. DOI: 10.1097/00000542-200610000-00008. PMID: 17006061.
39. *Siegel R. L., Miller K. D., Jemal A.* Cancer statistics, 2020. *CA Cancer J Clin.* 2020; 70 (1): 7–30. DOI: 10.3322/CAAC.21590. PMID: 31912902.

40. Health and social care — Office for National Statistics n.d. https: //www.ons.gov.uk/peoplepopulationandcommunity/healthandsocialcare/ (accessed September 26, 2023).
41. *Weng M., Chen W., Hou W., Li L., Ding M., Miao C.* The effect of neuraxial anesthesia on cancer recurrence and survival after cancer surgery: an updated meta-analysis. *Oncotarget*. 2016; 7 (12): 15262–15273. DOI: 10.18632/ONCOTARGET.7683. PMID: 26918830.
42. *Huang H., Benzonana L. L., Zhao H., Watts H. R., Perry N. J.S., Bevan C., Brown R., et al.* Prostate cancer cell malignancy via modulation of HIF-1α pathway with isoflurane and propofol alone and in combination. *Br J Cancer*. 2014; 111 (7): 1338–1349. DOI: 10.1038/BJC.2014.426. PMID: 25072260.

Received 02.10.2023
Accepted 07.11.2023
Online first 30.11.2023

Index of Authors and Papers Published in the Journal «General Reanimatology» in 2023*

* The Number before the Bracket is the Number of the Journal; the Numbers in the Brackets are the Pages of the Paper.

Main information for the manuscript submission

PARAMETER	INSTRUCTIONS
Limitations	
Initial submission	One file in the Word format in Russian for Russian-speaking authors in English for non-Russian-speaking authors, including: — the title of the paper; — full names of all authors; — affiliations of all authors; — IDs of profiles in the scientific databases for each author; — the text of all sections of the paper; — tables, figures, photos with captions and notes; — references; — conflict of interest; — information of study funding; — acknowledgements (optional); — authors' contribution (preferably)
The length of the manuscript	Original manuscript — about 40,000 characters with spaces; Short communication — should not exceed 2,500 words; Review, meta-analysis — 25,000–40,000 characters with spaces
Front page information	
Title of the paper	Should not exceed 15 words
Information about authors	Full name (Peter A. Johnson), author profile ID in the research database(s) for each author (e-Library/RSCI (Rus), ORCID, Scopus, WoS researcher ID if available)
Affiliations	Full name and postal address of the organizations with zip code
Corresponding author	Full name, e-mail address, phone number
The paper outline and references	
Summary (abstract)	250–300 words. Sections: scope of the problem (introduction/background), aim, material and methods, results, conclusion
Highlights (main messages as text or infographics, an optional section following the summary)	1–3 messages in graphic or text form (no more than 40 words per each text message)
Key words	6–8 words listed with a semicolon (;), without a dot at the end
Body of the paper	Sections: introduction (background), material and methods, results, discussion, conclusion
Supplementary information sections	Conflict of interest, funding of the study should follow the Keywords paragraph. Acknowledgements (optional) and authors' contribution (preferably) should be placed at the end of the paper
Illustrations, including tables	Original paper — up to 8; Short communication — no more than 3; Review — up to 8
References	Dating: 70% should be published within the last 5 years, of them at least 30% within the last 3 years. Number: Original paper – 25–45; Short communication — 10–25; Review — 80–120. Format: please see the «References Formatting» section, www.reanimatology.com
Formatting	
Font	Times New Roman, 12 points. The section titles should be typed in bold
Spacing and Indentation	Line spacing — 1.5; Interval before and after the paragraph — none; Interval between sections — one extra spacing; First line indent — 1.25 cm
Fields	2.5 cm on all sides
Page numbering	In the lower right corner

Full version at www.reanimatology.com

perience
cellence
tra Care

The European Society of Paediatric and Neonatal Intensive Care

espnic
European Society of Paediatric and Neonatal Intensive Care

espnic2024.kenes.com

The European Society for Pediatric and Neonatal Intensive Care (ESPNIC) is a pan-European medical association that promotes standards in pediatric and neonatal intensive care among healthcare professionals, especially physicians and nurses.

The 33rd Annual Congress of ESPNIC will be held in Rome, Italy, June 11–14, 2024.

For more information, visit espnic2024.kenes.com.

Dear Authors!

The journal «General Reanimatology» invites you to participate in a special issue dedicated to critical conditions of neonatal and pediatric patients.

Please send relevant manuscripts in the field of anesthesiology and intensive care medicine, as well as all questions regarding the submission of articles to the special issue to the editorial office of the journal at **journal_or@mail.ru** or via an online form at the journal's website: **www.reanimatology.com**.

The submission deadline is August 01, 2024.

Editorial Team

Conox®*

Интеллектуальный Мониторинг Анестезии

Conox® – неинвазивный монитор ЭЭГ, оценивающий гипнотический и анальгетический эффекты общей анестезии.

Два мониторируемых параметра в одном устройстве

Улучшенные алгоритмы для определения глубины анестезии**

*«Монитор для контроля глубины анестезии и анальгезии Conox® QM7000-M». РЗН 2022/17297
**По сравнению с моделью «Монитор Conox для оценки глубины анестезии». РЗН 2020/11891

ООО «Фрезениус Каби»
125167, Москва, Ленинградский пр-т, д. 37, к. 9
Т.: (495) 988-4578, Ф.: (495) 988-4579
E-mail: ru-mow-info@fresenius-kabi.com
www.fresenius-kabi.ru

CON-2022-JUN-207-02 19.06.2023

FRESENIUS KABI
caring for life